The Uses of Artificial Intelligence and Virtual Reality Platforms for Developing the Next Generation of Anatomical, Medical Device, and Surgical Educational Tools

A Thesis

SUBMITTED TO THE FACULTY OF

UNIVERSITY OF MINNESOTA

BY

Alex Deakyne

IN PARTIAL FULFILLMENT OF THE REQUIREMENTS

FOR THE DEGREE OF

DOCTOR OF PHILOSOPHY

Paul Anthony Iaizzo

April 2021

Acknowledgements

The contents of this dissertation would not be possible without the help of many individuals.

I want to thank Dr. Paul Iaizzo. The example you set as a role model and mentor is invaluable. Your hard work ethic and passion for what you do is infectious and has enabled my success. Thank you for your willingness to always help me and provide feedback and advice on my work. I know I will be able to find success in the rest of my career thanks to what I learned from your mentorship over the last 5 years.

I also want to thank all the people who make the Visible Heart® Laboratories great. I'm thankful for the staff: Dr. Tinen Iles, Gary Williams, Weston Upchurch, and Monica Mahre. Your work over the years have enabled the incredible work that we do in lab. I am also thankful for the graduate students who have helped me along the way: Lars Mattison, Alex Mattson, Erik Gaasedelen, Megan Schmidt, Jorge Zhingre Sanchez, Mikalye Holm, David Ramirez, Emma Schinstock, Thomas Valenzuela, and Renee Brigham. Your friendship and help during my time in the VHL have filled the last 5 years with great memories.

Finally, I’d like to thank my family (Jeff, Stacy, and Erin) as well as Becca. Without your constant love and support I would not have achieved this amazing goal. I am forever grateful for what you have done for me.

Dedication

This thesis is dedicated first and foremost to my parents, Jeff and Stacy. Thank you both for your love and ensuring I had everything I needed to pursue my dreams. Also, to Becca; for her unending love, support, and encouragement. Lastly, I dedicate this dissertation to my grandparents, especially those who were unable to see me complete my doctorate.

Table of Contents

Contents

List of Tables

List of Figures

Thesis Summary

The primary objects of my thesis are to explore the applications of computational models for medical education and to detail how artificial intelligence (AI) technologies and virtual reality (VR) platforms can be utilized to better enable the next generation of educational tools for medical students, physicians, and medical device designers.

Computational 3D models have seen exponential increases in their uses in the medical field; as they can retain critical 3D spatial information of the given patient's anatomy of interest. Note, this is contrary to 2D images in textbooks, which are commonly in use for medical education. In general, the 3D spatial information is essential for gaining a solid understanding of human anatomy, or how a given anatomical feature may vary within a patient population. In the first section of my thesis, I overview some uses of these computational anatomical models for educational purposes; such as performing computational device deployments within various patient's anatomies. Further, these generated 3D models allow for the study of the device tissue interfaces in clinically relevant implant sites within a variety of patient anatomy.

These 3D computational models have many benefits and uses within the medical education field but can be extremely difficult and time consuming to create. For example, to create a high resolution computational model, one needs to first obtain appropriate imaging of the patient's anatomy; such as using magnetic resonance imaging (MRI) or

computed tomography (CT) scans. Then, the anatomies of interest need to be segmented within the scan to generate an accurate 3D computational model. This is a time intensive process and requires an expert knowledge of human anatomy; yet, the segmentations of the anatomies of interest within the scans often remain as the bottlenecks in this process. Segmenting a given anatomical feature such as the heart can take over a day for an anatomic - segmentation expert to generate. If a large number of computational models are needed (over 100) for a population database, it becomes logistically challenging to create such. A large group of individuals or even a company either needs to spend a considerable amount outsourcing the segmentation or dedicating a large number of internal resources to generate the dataset. For smaller companies or academic institutions with limited resources this can be impossible.

In the next section of my dossier I will provide an overview of how artificial intelligence technologies, specifically deep learning (DL), can be utilized to help generate these large computational model databases. More specifically, convolutional neural networks (CNN) can learn how to create accurate auto-segmentations of anatomical features within a scan, by first training on a dataset of fully segmented (annotated) scans. After training the CNN, it can be used to create high quality segmentation predictions on new scans. The segmentation can either be generated into a useable computational 3D model, or in some cases where it is imperfect, it can be utilized by an anatomical expert as an initial computation model, which in a reduced time, the user can make the necessary edits to generate a high quality 3D model. It will be discussed here, that even if some manual

intervention was required, the task of segmenting a human cardiac scan was reduced from over a day to under an hour in 90% of our modeling cases.

CNNs are not easy to apply to a complex novel dataset; specifically medical imaging datasets. An often-overlooked portion of generating a dataset for DL, and training and validating a CNN, is to have an understanding of the required domain knowledge of the data and medical field in general. I will discuss in one of the following chapters, on why anatomical domain knowledge is critical to successfully deploy a DL model for segmentation of medical imaging data and also suggest several avenues to how best to acquire this type of knowledge.

In the final section of my thesis, I will provide an overview how Virtual Reality platforms can be developed to take advantages of these 3D computational anatomical models with a focus on applications for enhanced medical education. Our Visible Heart® Laboratories' initial qualitative investigations into VRs efficacies as teaching tools has shown promising results. We believe this makes these platforms exceptional tool for medical education, as they preserve all 3D spatial information of critical human anatomies while offering immersive experiences for studying anatomy and/or medical device technologies.

I will begin this last section of my thesis by describing two use features to the Visible Heart® Laboratories virtual reality platforms. One includes the development of a fixed spline navigation utility that is a simpler implementation of the current movement system

which makes it easier for new users to navigate within these detailed human anatomic VR scenes. Next, I introduce instantaneous user relocation feature; which aids multiple user experiences within shared virtual environments: i.e., this allows users in the same virtual environment to instantly teleport to the location of an instructor within the scene. This in turn, allows the users to focus more on learning the given anatomy and less on trying to find other users within a complex scene. The next chapter in my thesis will detail the development of the anaglyph 3D functionality for utilization within our generated VR scenes. This feature is a cost-effective solution for allowing multi-user collaboration within the VR educational scenes. Lastly, I will demonstrate the developed abilities to perform computational device deployments within generated VR scenes. This functionality offers control of computational device deployments within an immersive setting; e.g., enabling experiments on device tissue interfaces of virtual implanted devices, in a wide range of anatomical models within a short amount of user time.

In conclusion, detailed anatomical computational models offer many benefits for medical education and enhanced virtual reality platforms can be employed as tools to amplify these benefits. Primarily through its ability to preserve the 3D spatial information of the given anatomy while creating an immersive environment to learn. Further, many of the newly developed functionalities I developed and that are described in my dissertation allow for cost-effective collaborations and the novel abilities to perform computational deployments of devices within a detailed VR anatomic scene. While VR platforms offers developing alternatives to traditional anatomical and device learning, they require

numerous detailed and verified computational anatomical models which can be difficult and time consuming to produce. As described within my thesis, recent advancements allow for AI assisted generations of anatomical computational models from medical image datasets. By combining these two technologies and platforms, our research team now has new abilities to create large anatomical computational 3D model datasets which can be used in Virtual Reality learning environments, enabling the next generation of anatomical, medical device, and surgical education tools.

.

Section 1 – Computational Anatomical Modeling and Device Deployment

The primary object of this dossier is to explore the uses of artificial intelligence (AI) and virtual reality (VR) in the medical field, and their specific applications for fueling the next generation of educational tools. In order to accomplish this, we are first going to take a step back and focus on one of the fundamental cornerstones of this field – computational anatomical modeling.

This first section will start by overviewing the current development and usage of anatomical cardiac computational models within the Visible Heart ® Laboratories, which is similar to those being performed around the world. These models are created from MRI scans of isolated human heart specimens that were donated to the lab. Once scanned, computational models can be generated for use in furthering anatomical study. Devices can be computationally implanted into these cardiac models and then 3D printed to allow for better understanding of the anatomy and the device tissue interfaces. These computational deployments allow one to study the device in a wide range of varied anatomical specimen 3D models; demonstrating how different anatomy effects the clinically relevant implant sites of devices.

Virtual prototyping: computational device placements within detailed human heart models

Published in *Applied Sciences*.

Alex J. Deakyne [1,3], Tinen L. Iles [1,3], Alexander R. Mattson [4], and Paul A. Iaizzo [1,2,3]

[1] Bioinformatics and Computational Biology, University of Minnesota, Minneapolis, MN

[2] Department of Biomedical Engineering, University of Minnesota, Minneapolis, MN

[3] Department of Surgery, University of Minnesota, Minneapolis, MN

[4] Medtronic, Minneapolis, MN

Preface

In order to fully understand the ability of AI and VR to enable and advance medical education, we need to have a solid understanding of anatomical computational modeling and some of their current uses. Here we demonstrate the process that the VHL uses to generate computational human heart 3D models from high resolution MRI scans of static, isolated human heart specimens. These anatomical specimens were deemed not-viable for transplant and have been graciously gifted to the lab through the University of Minnesota anatomy bequest program. Virtual prototyping can be performed by computational

combining patient anatomy or implanting medical devices at clinically relevant implant locations within these anatomical models. The resultant 3D models can then be 3D printed and utilized to teach/learn about the anatomy, the medical device, and the tissue device interface. Since these implants are done computationally, they can be performed in many human hearts with a wide range of pathologies and patient backgrounds.

This manuscript was published in the Applied Science Journal in December 2019. All authors assisted in the generation of the computational models of the anatomies and the medical devices. Computational implants of the devices were performed by Dr. Alex Mattson and me. All authors assisted in editing the manuscript for publication

Summary

The Visible Heart® Laboratories has a human heart library with over 500 cardiac anatomical specimens. Many of these specimens have been MRI scanned and generated into a 3D computational anatomical model. These digital models allow for further understanding of the anatomy by allowing for models to be sliced without having to damage the physical specimen. In addition, medical devices can be computationally implanted into these models to gain better understanding of the device tissue interface. Here, we performed computational device deployments of multiple medical devices into clinically relevant implant sites within four distinct cardiac models. These computational models were then 3D printed to make it easier for studying and teaching the device tissue interfaces. This methodology is important as it allows one to quickly determine how a

medical device interacts with the anatomy in a wide range of cardiac specimens; each with varied anatomy and patient history.

Synopsis

Data relative to anatomical measurements, spatial relationships, and device-tissue interaction are invaluable to medical device designers. However, obtaining these datasets from a wide range of anatomical specimens can be difficult and time consuming, forcing designers to make decisions on the requisite shapes and sizes of a device from a restricted number of specimens. The Visible Heart® Laboratories have a unique library of over 500 perfusion-fixed human cardiac specimens from organ donors whose hearts (and or lungs) were not deemed viable for transplantation. These hearts encompass a wide variety of pathologies, patient demographics, surgical repairs, and/or interventional procedures. Further, these specimens are an important resource for anatomical study, and their utility may be augmented via generation of 3D computational anatomical models, i.e., from obtained post-fixation MRI scans. In order to optimize device designs and procedural developments, computer generated models of medical devices and delivery tools can be computationally positioned within any of the generated anatomical models. The resulting co-registered 3D models can be 3D printed and analyzed to better understand relative interfaces between a specific device and cardiac tissues within a large number of diverse cardiac specimens that would be otherwise unattainable.

Introduction

The process for developing novel medical devices, procedural delivery systems, and/or next generation devices can be long, arduous, and extremely costly. For example, many steps must be taken to ensure that the device will fit correctly within a specified patient population. Typically, animal and cadaver studies are conducted to assist in determining such parameters for a device to fit into the relative anatomies [1]. While these studies offer many benefits, they are costly and time-consuming and anatomies can vary greatly from living patients. Thus, medical device innovators are seeking novel methodologies, such as computational modeling, to gain further insights on device designs [2,3]. This has initiated an increased use of computational modeling by medical device innovators to assist in the design, refinement, and/or validation of their devices [4].

Software packages from companies such as Materialise (Mimics and 3-Matic suites; Leuven, Belgium) have greatly aided in the creation (segmentation) of computational 3D models. Digital Imaging and Communications in Medicine (DICOM) files such as those obtained from computed tomography (CT) or magnetic resonance imaging (MRI) from cadaveric or clinical cases can be uploaded to these software packages for segmentation. Anatomical measurements can be abstracted from these 3D models, which is largely beneficial for improving the understanding of a wide variety of human anatomies. These measurements can also be utilized to quantify the statistical distributions of specific anatomical features within various patient populations [5,6].

In addition, medical device models can be computationally implanted into the anatomical models and subsequently 3D printed, thereby offering additional unique insights relative to the interactions between a given device and a patient's specific anatomy. Performing these implants in several anatomical models demonstrates how these devices would likely fit within varied patient anatomies. In other words, the generated 3D printed models grant further knowledge about implant site anatomies, clinical procedures, and optimal device placements, further enabling refinement of the device design to better fit an initial target population before performing expensive and time-consuming cadaver and/or animal studies. These anatomy-device models are also useful for explaining novel medical technologies to physicians. The 3D printed models help facilitate discussions between physicians and device engineers. The function of the model can be educational (explaining how the device functions) or beneficial for gaining iterative device prototype feedback (demonstrating a prototype device computationally placed in a heart and receiving feedback from physicians on how to improve the next iteration of the device).

Additionally, 3D prints of computational device placements within anatomical models offer benefits outside of medical device design. These 3D printed models can be utilized by clinical care teams to better communicate the details of a surgical procedure or as intervention amongst themselves and/or with a patient or their family. For example, investigators seeking to quantify these benefits have found that 3D printed anatomical

models significantly improved patient understanding of the planned procedure and relevant anatomy [7], thus bridging the gap of knowledge between clinical care teams and their patients.

Here we demonstrate the ability to computationally place devices within varied and detailed 3D human cardiac models. These devices were placed in a variety of locations within anatomical models, as means to study the device-tissue interface at differing implant sites. Devices were also placed in a number of different computational models with varied anatomies, allowing for the determination of ideal device placement locations as well as for the characterization of variances in anatomical delivery pathways. Finally, these models were sliced to yield views of specific internal anatomies that would not be possible on the original specimen without destroying it.

Methods

Human hearts deemed not viable for transplant were gifted to the Visible Heart® Laboratories for research through LifeSource, a regional organ procurement agency (St. Paul, MN, USA). Occasionally, these cardiac specimens were reanimated on an external perfusion apparatus utilizing Visible Heart® methodologies, allowing for capture of functional internal anatomy videos [8]. These isolated cardiac samples were perfusion fixed in an end-diastolic state and subsequently placed in agar gel, then MRI scanned utilizing a 3T MRI scanner at a resolution of 100 micrometers (Siemens Trio,

Washington DC, USA). Utilizing MRI scans of perfusion-fixed samples allows us to achieve such high anatomic resolution, which is critical to perform virtual prototyping: note, this is 10X greater resolution than can be obtained with clinical imaging since the patient heart is living and moving. The DICOM generated from these scans was segmented utilizing Mimics software (version 20.0; Materialise). The process of segmentation involved creating 2D masks by classifying pixels as to whether they represent cardiac tissue on each scan slice. The 2D masks were compiled within Mimics to create a 3D anatomical model of the cardiac specimen. The model was then imported into 3-Matic software (version 14.0; Materialise) for processing, editing, and analysis of the 3D anatomical mesh (Figure 1).

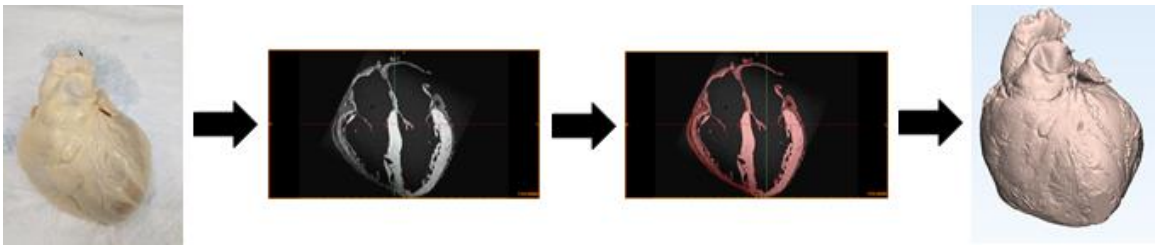

Figure 1. (Left to right) 3D model generation pipeline starting with profusion-fixed human heart, cardiac MRI scan, 2D segmentation mask of the cardiac myocardium, and resulting 3D model of the heart.

To date, the Visible Heart® Laboratories have generated over one hundred detailed 3D models of human cardiac anatomies, including a wide range of pathologies. These models can be utilized to gain critical insights on complex cardiac anatomies and alteration associated with disease states. Models of medical device prototypes can be computationally implanted in these anatomical models, allowing for analysis of device-

tissue interactions and unique understanding of spatial relationships. The 3D models can offer distinctive views of specific internal anatomies and computationally placed devices.

The Visible Heart® Laboratories have also generated 3D models of peripheral vasculatures (Figure 2). These datasets were obtained by scanning fresh cadavers that were donated through the Anatomy Bequest Program at the University of Minnesota. Large volumes of contrast dye (>2 liters) were injected through the venous and arterial systems before or while obtaining CT scans. To date, 3D models of the major vasculatures between the subclavian veins and arteries down to the femoral veins and arteries have been generated from multiple cadaver scans. These vasculature models can be computationally added to previously generated heart models to simulate possible delivery pathways for a variety of cardiac devices, e.g., those commonly delivered through the femoral and subclavian veins or arteries.

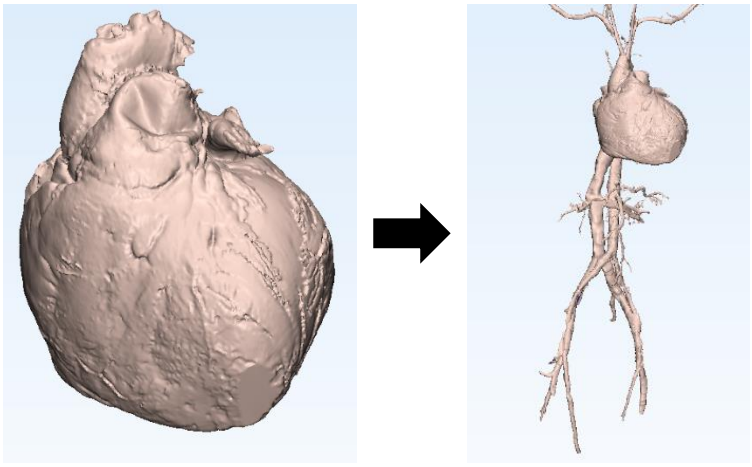

Figure 2. Example of a human heart model with computationally added vasculature.

Finally, these models can be 3D printed utilizing either Stratasys (Rehovot, Israel) GrabCAD Print version 1.30 software and uPrint SE Plus 3D printers or Ultimaker (Utrecht, Netherlands) Cura 4.1.0 software and Ultimaker 3E 3D printers. Numerous models were printed utilizing Polylactic Acid (PLA) filament for the model material and Polyvinyl Alcohol (PVA) filament for the support material. These 3D printed models clearly depict three-dimensional spatial information between various patient anatomies and computationally placed devices, thus enabling further quantitative analysis of computationally implanted devices within a wide range of anatomies.

Results and Discussion

Here we describe a set of 3D models generated from four distinct human hearts utilizing the aforementioned methodology. Relevant information about each patient is summarized in Table 1. These models are displayed in attitudinally correct anatomical orientation in Figure 3. A Micra^{TM} transcatheter pacing system (TPS)(Medtronic, Minneapolis, MN, USA) was computationally implanted into the right ventricular apex of each patient's heart model. Each heart model was then sliced along the coronal plane to offer a clear view of the anterior half of the heart and the resultant computational implant locations of these Micra^{TM} devices.

Table 1. Human heart and patient information.

Heart Number	Age	Gender	Body Weight (kg)	Body Height (cm)	Heart Weight (g)	Cardiac Medical History
102	14	F	79.8	142	333.1	None known

229	44	F	83.8	163	394	Hypertension
248	64	F	105.6	178	441.4	Hypertension
311	20	F	38.6	142	161	None known

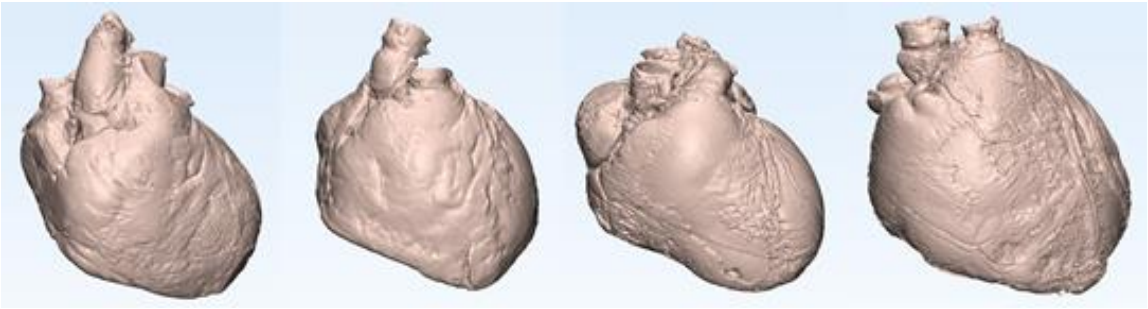

Figure 3. Computational 3D models of four MRI scanned human hearts from the Visible Heart® Laboratories (left to right: HH229, HH248, HH102, and HH311). These models were used for subsequent computational implants of cardiac devices.

Further, implanting this device in a variety of models allows for the characterization of device placement within varied human anatomy (Figure 4). Since the Micra^{TM} TPS has only one size, it was originally imperative to understand how the device fit within a range of human heart sizes.

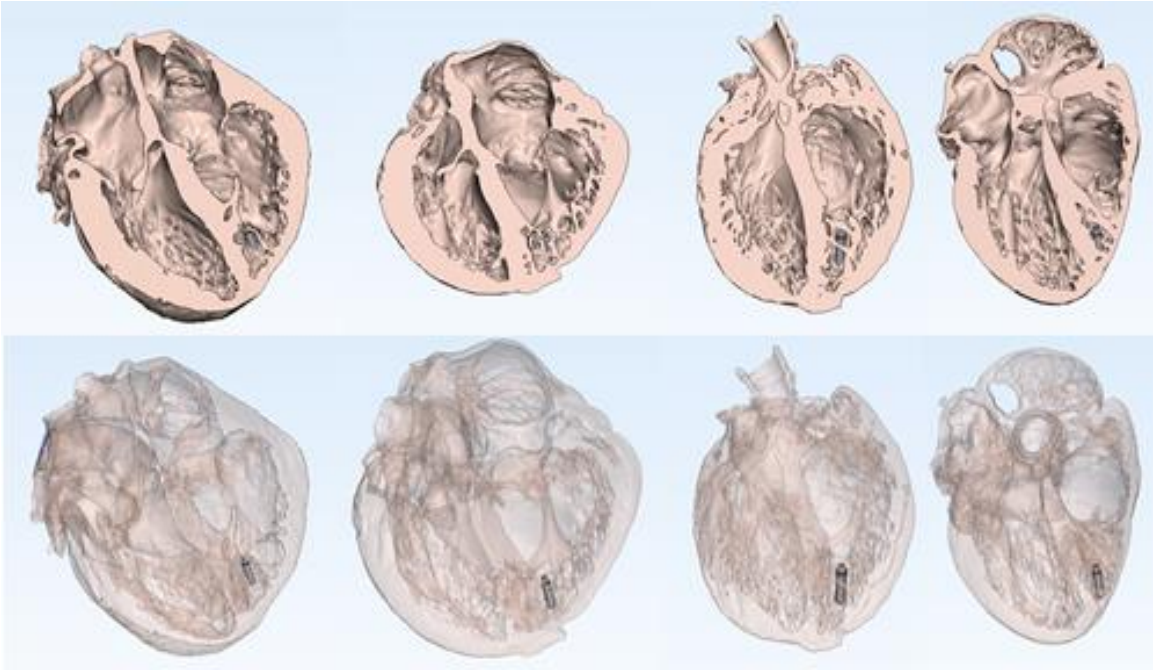

Figure 4. Anterior views of sliced human hearts depicting Micra™ transcatheter pacing system computationally implanted into each right ventricle (left to right: HH229, HH248, HH102, and HH311). Each heart model is depicted with no transparency (top) and high transparency (bottom).

Computational vasculature anatomies obtained from a cadaver CT scan were digitally added to the heart (Figure 5). This can then be utilized to model the delivery pathways, e.g., from implant into the vasculature upward from femoral veins and/or arteries up to the modeled heart. Further, we have been able to computationally add the delivery catheter for the Micra™ TPS into the modeled vascular pathway. In other words, we computationally modeled the Micra™ TPS implant along the entire delivery vascular pathway of the device, from the access point into the femoral vein, up through the inferior vena cava, right atrium, and finally into the right ventricular apex. This model, and other similar models, allow device designers to understand the anatomical constraints

that affect the delivery of the Micra™ TPS to an ideal target location—a crucial step due to this large bore delivery catheter (23F). Such insights should further enable design requirements to be established for a delivery catheter system, even before expensive animal and cadaver experiments are initiated. Additionally, these computational models can be used to help determine the constraints or boundary conditions of given anatomical sites, e.g., those that a catheter will be able to navigate and deploy a Micra™ TPS within, for patients with similar anatomy.

Figure 5. 3D human heart model (HH229) with computationally added vasculature. A Micra™ transcatheter pacing system delivery catheter and a Micra™ were computationally implanted in the right ventricular apex.

Shown in Figure 6, this model was digitally sliced along the coronal plane to reveal the posterior half of the heart and the computationally placed Micra^{TM} TPS and delivery catheter. This model was then 3D printed and hand painted to highlight the different anatomical features as well the implant system and Micra^{TM} TPS (the implanted device). This printed and painted model offers a realistic representation of a device implanted in a human patient, and its interaction with the surrounding anatomical features.

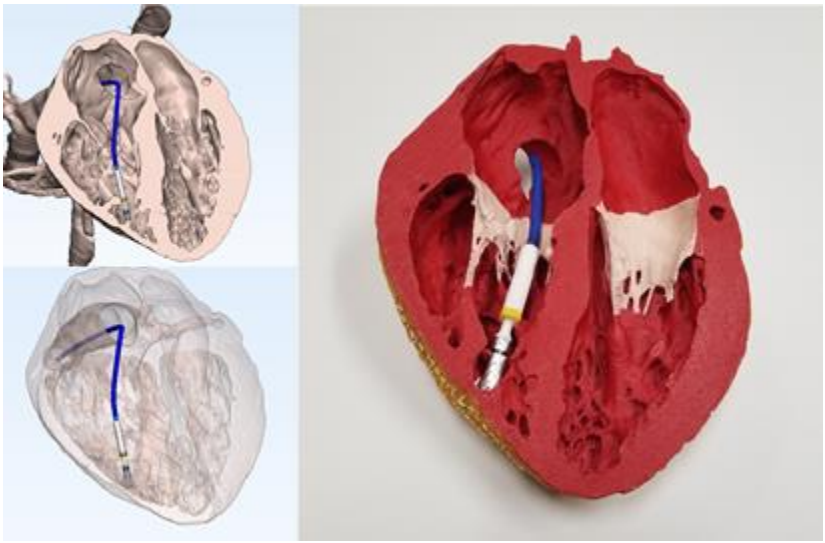

Figure 6. 3D models and 3D print of the posterior half of a human heart (HH229) with a computationally placed Micra^{TM} transcatheter pacing system (TPS) and delivery catheter. The printed heart and Micra^{TM} TPS were hand painted to highlight device-tissue interfaces.

During early Micra^{TM} TPS development and physician feedback sessions, it was questioned if more than one Micra^{TM} TPS could be implanted within a patient's heart (e.g., for end of device life replacement). Thus, designers needed to understand that the large volume of the right ventricle would allow for the placement of non-interacting concomitant Micra^{TM} TPS within the same chamber. Fresh human cadaveric studies were

performed on a small set of human hearts [9]. In Figure 7, we can visualize that a second Micra^{TM} TPS was computationally deployed within this detailed cardiac anatomy, to simulate the spatial conditions where multiple Micra^{TM} TPS were implanted within a patient's right ventricle. The heart model was sliced along the coronal plane to reveal a four-chamber view of the posterior half of the heart. The model was then 3D printed for further analyses and for educational use (Figure 7).

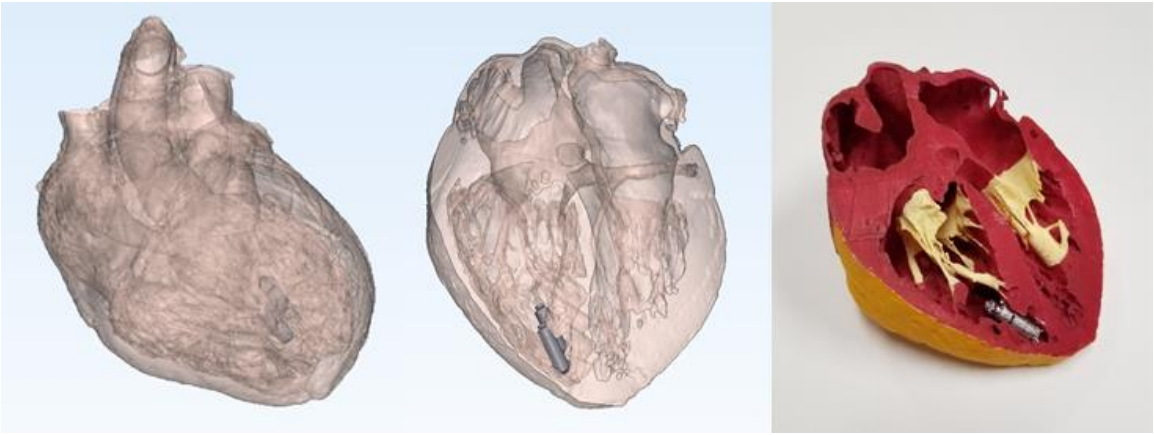

Figure 7. Multiple Micra^{TM} transcatheter pacing systems computationally implanted in the right ventricular apex of a 3D human heart model (HH229; left) and resulting 3D print which was hand painted to study device-tissue interfaces (right).

In another example of the value of computationally placed cardiac devices within these detailed human heart models, a Medtronic Arctic Front cryoballoon catheter was computationally placed within human heart model (Figure 8). This human heart model had vasculature from a cadaver computationally added to simulate the delivery pathway required to navigate the cryoballoon from the access point within the femoral vein, proximally up to the left superior pulmonary vein ostia within the left atrium. This

ablation balloon placement procedure requires an initial atrial transseptal puncture, which here was computationally placed into an anatomically accurate location on the atrial septal wall of the human heart model. The resulting computational model was 3D printed and has been utilized as an educational tool to explain the necessary steps of this complex procedure to medical students, residents, fellows, clinicians, patients, and/or medical device designers.

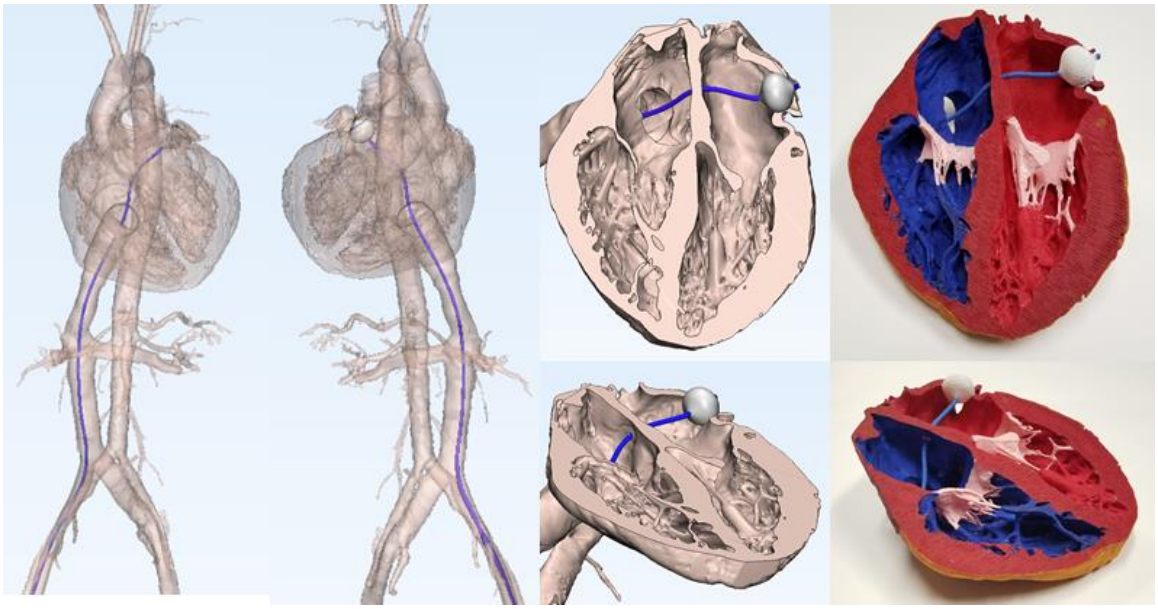

Figure 8. Human heart (HH229) and vasculature model simulating the delivery pathway for a computationally placed Arctic Front catheter and cryoballoon in the left superior pulmonary vein ostia.

Conclusion

3D printing and computational modeling are emerging tools within both clinical and medical device innovation fields, as they have incredible potential to assist and change the way medical devices are designed and/or clinically adopted and utilized. These computational modeling and printing applications offer many benefits when compared to

traditional methods of testing devices such as within human cadaver and/or animal studies. We consider that computational approaches are complementary to established preclinical and clinical device and procedure testing. The large cardiac and cadaver model database of the Visible Heart® Laboratories is an invaluable resource for such computational cardiac device placements, due to the large number and great diversity of detailed anatomical models in its human heart library. The generation of 3D printed models of these computational device placements enables further analysis and education of the procedures, device-tissue interfaces, and complex human anatomies.

Acknowledgments

Thank you to everyone at Medtronic and the Visible Heart® Laboratories that assisted with this project. We also would like to thank the organ donors and their families for providing these critical research specimens for 3D model generation.

Section 2 – Utilizing Deep Learning for Anatomical Segmentation of Medical Image Datasets: Application and Lessons Learned

In the previous section I discussed the current methodology employed by the VHL for creating computational anatomical models and performing computational device deployments. I also covered our ability to computationally combine patient anatomical models to make co-merged highly detailed anatomical 3D models. We discussed the other potential uses for these computational models and the benefits of having easy access to a large database of these anatomical models, with a wide range of pathologies, unique anatomical features, and patient backgrounds.

The current methodology for creating these computational models is a slow and arduous process. Creating a large database of these models is currently not feasible without thousands of man hours: making it an incredibly expensive process for large companies and logistically impossible for small companies or academic labs such as the VHL. We estimate it would take a PhD student at the VHL over a year of continuous work in order to fully segment all of the cardiac specimens that have been MRI scanned.

In this section I will focus on the usage of artificial to assist in the creation of large anatomical datasets. Artificial intelligence, and specifically deep learning, have made

many advancements in recent years in the process of performing semantic segmentation. Recently, there has been a focus on using these technologies to perform automatic segmentation to assist in creating new datasets. For example, Amazon Web Services has an entire department (SageMaker and specifically GroundTruth) dedicated to the usage of artificial intelligence to assist in the generation of large, annotated datasets. However, this work has not been done on medical imaging datasets.

The first portion of this section will focus on the importance of domain knowledge for applying deep learning to medical imaging datasets. While deep learning is a powerful tool, if employed without proper domain knowledge of the data it is unlikely to yield favorable results. This is especially true for medical imaging data which contains many nuances that make it difficult to successfully apply deep learning without proper understanding of the data type and the anatomical features of interest. Finally, the ability for deep learning to assist in the process of a large medical imaging dataset will be explored.

The Importance of Domain Specific Knowledge when Applying Deep Learning to Medical Data: Employing the Unique Dataset of Reanimated and Perfusion Fixed Human Hearts

This will be published as an educational blog post. These are common and popular within the deep learning community. Many of these educational posts receive thousands of views and are helpful for the growth of the medical AI community.

Alex J. Deakyne [1,2], Tinen L. Iles [1,2], and Paul A. Iaizzo [1,2]

[1] Department of Bioinformatics and Computational Biology, University of Minnesota, Minneapolis, MN

[2] Department of Surgery, University of Minnesota, Minneapolis, MN

Preface

With the recent rise in popularity of deep learning, many investigators are applying deep learning technologies to many different applications. The raw power of these algorithms has allowed for many researchers achieve state of the art results on a wide range of computer vision tasks. This has encouraged many researchers to apply deep learning to computer vision problems within the medical field, specifically the segmentation of

anatomical features within medical imaging data. This is often done without domain knowledge of the medical imaging data types or the anatomical features of interest. This can be problematic for many reasons including the fact that it is impossible for someone to correctly annotate the data, and validate the network results, if they are not knowledgeable on how this data should be correctly labeled and interpreted. In this chapter we will take a deep dive into the many pitfalls that can occur when applying deep learning to medical imaging data without the proper domain knowledge.

All authors helped in the editing and preparation of this article.

Synopsis

The utilities of deep learning and other supervised learning systems are dependent entirely on the quality of the dataset available for training; since these systems abstract information directly from the data. Deep learning has found great success in reaching state of the art performance on a wide variety of segmentation tasks. However, the datasets necessary to train such a network need to be high quality and are often difficult to produce. Further, such datasets take a long time to annotate carefully and the work is often done by many people. In this chapter we will focus on segmentation of human cardiac anatomy obtained within a unique magnetic resonance imaging dataset. Unfortunately, when dealing with the segmentation of anatomical features in medical imaging datasets, segmentation is not always straightforward, even by experts in the field. In other words, to interpret the data type and the anatomies of interest, one needs to

fully understand such, to annotate and interpret correctly. Therefore, an often-overlooked concept is the importance of domain specific knowledge when applying deep learning to medical data. Here we will be discussing why domain knowledge is crucial and address specific pitfalls when attempting to train a deep learning network to automatically segment the human heart from a highly detailed magnetic resonance imaging dataset: ones obtained from perfusion-fixed human specimens.

Introduction

Deep learning (DL) is a form of supervised learning in artificial intelligence (AI) in which a network is trained to map an input to an output. This training occurs by giving the network data pairs that consist of an input and the desired output. The network is then optimized by a loss function that measures how well it can map 'new' inputs to the correct output. Thus, the qualities and consistencies of the input and output data used to train the network are critical to the performance of the developed network, since it is directly used for optimization.

This paper will focus specifically on the task of semantic segmentation of magnetic resonance imaging (MRI) scans; note, that most of the described concepts will still apply if you are doing a similar type of AI analysis on a medical image dataset [1]. In segmentation, an image that contains a specific class (or classes) is the input to a network and it is paired with the 'ground truth' (GT) mask that represents what pixels in that input

image contain the specific class. The computational network is then tasked with generating a segmentation mask of the input image that matches the ground truth mask. This is accomplished by repeatedly sending the network these data pairs until it can successfully accomplish this task.

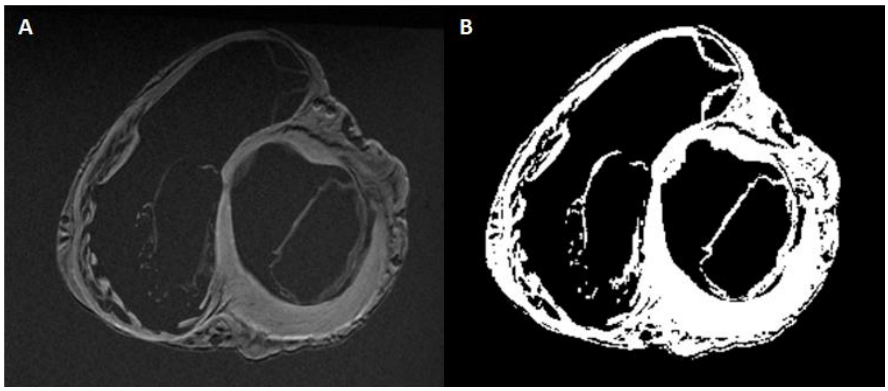

Figure 9. (A) A depiction of a training MRI scan slice (B) and the corresponding ground truth mask created by manual segmentation. Image pairs such as these will be used to train and evaluate the network.

This leads us back to a very fundamental concept from machine learning: the model you create will only be as good as the data given to it. This becomes especially true with deep learning. If the model is trained on incorrectly labeled human cardiac data, we can never expect it to produce correct results on new data. Thus, the data creation process is a critical step in the pipeline of creating a CNN to segment medical data.

For these detailed cardiac anatomical datasets, the annotation process is a time-consuming task that requires the annotator to have domain knowledge of both medical imaging and the anatomical features of focus. We will dive into the importance of domain knowledge for applying deep learning to medical imaging from two separate

fronts: mainly domain knowledge of the data type and of the details of anatomy, including human heart variabilities. While we can speak generally about the importance of domain knowledge for navigating digital imaging and communications in medicine (DICOM) data and MRI scans, this is less effective when talking about the importance of anatomical knowledge. Thus, we will demonstrate the importance of anatomical knowledge by providing specific examples of human cardiac anatomies that can be difficult for a network to automatically segment and provide considerations for how to address said difficulties.

Importance of Experience Interpreting Scans

Before we look at the importance of knowing the anatomical features of interest, we will briefly explore the DICOM data type, specifically MRI scans, and demonstrate the value in properly knowing how to interpret the data type and the anatomical features they depict. MRI scans can often be difficult to understand without previous exposure. While there are many contributing factors to this, we will focus on three of them here: they are a 2D representation of 3D data, the qualities of the scans even in our unique dataset vary greatly, and there can be the presences of artifacts: e.g., associated with the presences of cardiac device (metal).

Two Dimensional Representation of Three Dimensional Data

At first glance, the 2D images in a DICOM dataset appear like they could be treated the same as natural images in terms of data annotation; where each scan slice is segmented as a completely isolated image that has no relation to the images next to it in the dataset. However, this is not the case when it comes to MRI scans because they are actually 3D data composed of 2D image slices. Anatomical features in a scan are often registered across many scan slices. Therefore, when annotating and understanding the anatomical features on a single scan slice, one needs to take into consideration the surrounding/associated scan slices. In addition, the critical, but refined anatomical features are better captured on different axes. Therefore, in addition to utilizing surrounding scan slices, all three axes (axial, coronal, and sagittal) must be utilized to properly annotate a contiguous anatomical feature that has modulating size. This can be done by utilizing DICOM annotation software packages such as Mimics and 3Matic (Materialise, Belgium).

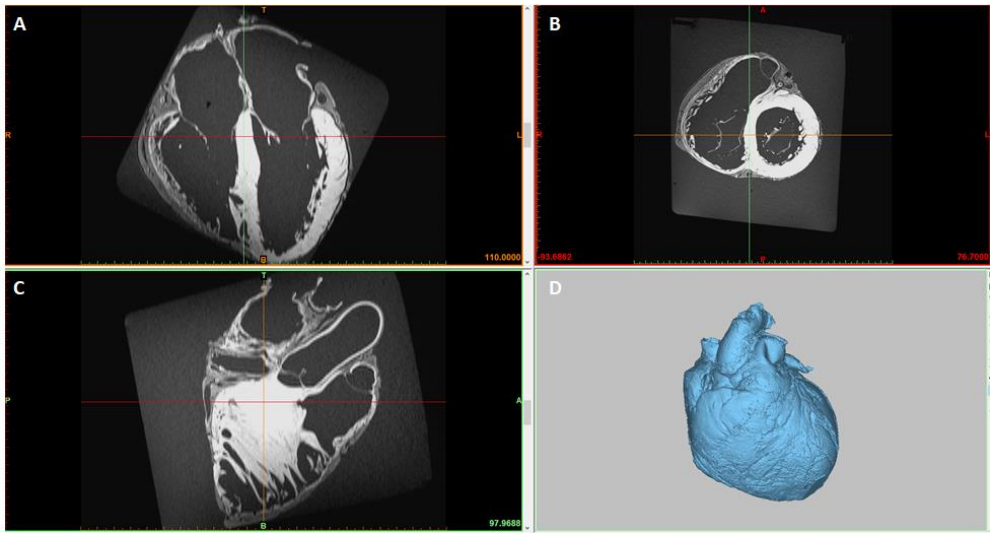

Figure 10. A picture of an MRI scan open in Mimics displaying the scan slices and segmentations on the three axes: (A) coronal, (B) axial, (C) and sagittal. In addition, (D) a 3D rendering, generated from the 2D segmentations, of the heart is displayed for context.

All these considerations should make it abundantly clear that annotating a given human anatomic MRI scan is a much more involved process when compared to annotating a set of natural images. The process of processing and understanding nuances relative to these 3D objects in terms of 2D scan slices across multiple axes is a challenging process with a steep learning curve. In addition, each scan slice should be segmented with the surrounding slices taken into consideration. The cumulation of all these considerations show that accurately annotating and evaluating MRI scans (or other DICOM datasets) is a complex and more involved process than simply annotating single 2D images.

Inconsistent Scan Quality

When obtaining a large amount of MRI scans to form a dataset, there will often be inconsistencies in the scanning parameters for each scan set studies as well as for the type of scanner used. These factors, among others, can lead to a situation where the contrast sensitivities of the scans can vary greatly. In our study here, when we had a high quality scan dataset, with good contrast sensitivity, it was quite clear as to what was the heart tissue and what was not; i.e. we often observed very bright pixel intensities for the cardiac tissues and black for background. This makes the annotations of the data simpler because there was minimal confusion about what should be segmented as the boundaries between tissue and background; these were distinct.

Unfortunately, this is not always the case with these types of datasets. It is not uncommon for the pixel intensity representation of the heart tissue and the background to be somewhat similar. In cases where the contrast sensitivities of a given scan is poor, it can be difficult to distinguish the regional boundaries between heart tissue and the background while annotating the data. In an ideal world, when the MRI acquisition leads to poor scan quality, the acquisition would be restarted to obtain a better scan. However, this is not always the case or possible, so it is important to be aware of the prospects of suboptimal scans existing in the dataset. A depiction of good and bad contrast sensitivities of MRI scans in our dataset, is shown below.

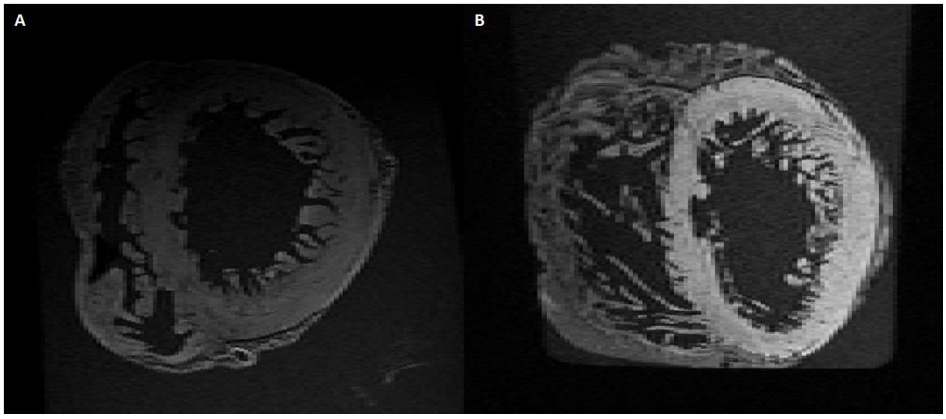

Figure 11. Example of (A) a suboptimal MRI scan of a heart and a (B) good MRI scan of a perfusion-fixed human heart.

When one needs to utilize a scan that has poor contrast sensitivity, it becomes increasingly important that the data annotator has experience with interpreting such MRI datasets and the various complex anatomical feature of interest. Thus, they will need to

trust, in part, their intuition and prior knowledge on whether a portion of the heart that should be segmented or not; when the boundary between the tissue and the background is blurred. An inexperienced annotator would be likely to make many mistakes on these sorts of scans which would greatly decrease the quality of our data. Uniquely, for the MRI dataset or the perfusion-fixed human hearts utilized here, they remain in our human heart library and thus one can physically re-examine them or utilize previously obtained internal videoscopic images to confirm a given anatomical feature.

Scan Artifacts

In a large dataset of MRI scans, it is likely that multiple scans will contain some sort of artifact: in an MRI scan these can cause errors that causes some sort of feature to show up within the scan that is not present in the actual anatomy. While we will not discuss the full extent of MRI artifacts in this paper, great resources exist that cover this topic in depth [2]. What is important to know is that artifacts are not a rarity and that they can range from having a small to a large impact on the scan quality. Below is an example of a ghosting artifact present in a scan in our dataset. Note, if a cardiac device was previously implanted into a given specimen, such will also cause significant artifacts: in some cases, these may be too significant to utilize the dataset.

Figure 12. Ghosting artifact present in and MRI scan of the heart. The ghosting artifact appears as ripples throughout the scan.

When annotating a dataset of MRI heart scans, one must be able to understand what an artifact is and properly segment the scan accordingly. In the above image with ghosting artifacts, we see that there are black lines covering portions of the 'true' heart myocardium. With proper experience in interpreting such cardiac scans, we know that these black portions across the myocardium are artifacts, and do not represent tissues that were not present in those portions of the heart. In addition, we can use our anatomical knowledge of the heart to know that the myocardium does indeed exist behind the artifact and that we should segment the artifact as tissue accordingly. An inexperienced annotator might segment this scan slice based on the pixel intensity of the heart and also look at nearby slices to see if they also present with artifacts. On the other hand, if this jejune approach were employed, large portions of the heart would be missing as the areas with ghosting artifact; which appear at the same near intensities as the background, and thus

would not be segmented. If all the scans with artifacts are incorrectly annotated in such a manner, then our model will not be robust enough to correctly segment new scans that also may contain artifacts.

Importance of Anatomical Domain Knowledge

In order to successfully employ deep learning to solve problems in the medical field per se, such as automatic segmentation of an anatomical feature, one must have a solid understanding of the associated anatomical features of interest. This knowledge is important for many reasons, but mainly in terms of creating the dataset and subsequently validating a developed network performance. Ultimately, if one does not have validations of the anatomical features of interest, then it is unlikely that they would be able to correctly label said features in their dataset. Note again for the purpose of this paper, we will specifically focus on human cardiac anatomy, but the same principles can be applied to any types of desired anatomies.

It is easiest to demonstrate the importance of anatomical domain knowledge in deep learning by walking through several of our encountered specific examples. In the following section it will be discussed, how three anatomical features of cardiac anatomies showcase the importance of anatomical domain knowledge when training a CNN on medical imaging data: i.e., the right atrial appendage, the chordae tendineae, and the

aorta. These specific examples are ones that commonly yield difficult problems for someone unfamiliar with the intricacies of human cardiac anatomy.

Right Atrial Appendage

The right atrial appendage (RAA) is located on the superior right side of the heart. It assists in pumping of blood to the right ventricle during atrial systole. Further, it is a common pathophysiological location for origins of atrial arrhythmias and is also a traditional implant site of leads needed for cardiac pacing [3, 4]. A diagram of the heart highlighting the right atrium is shown below; this image was obtained from the Atlas of Human Cardiac Anatomy [5].

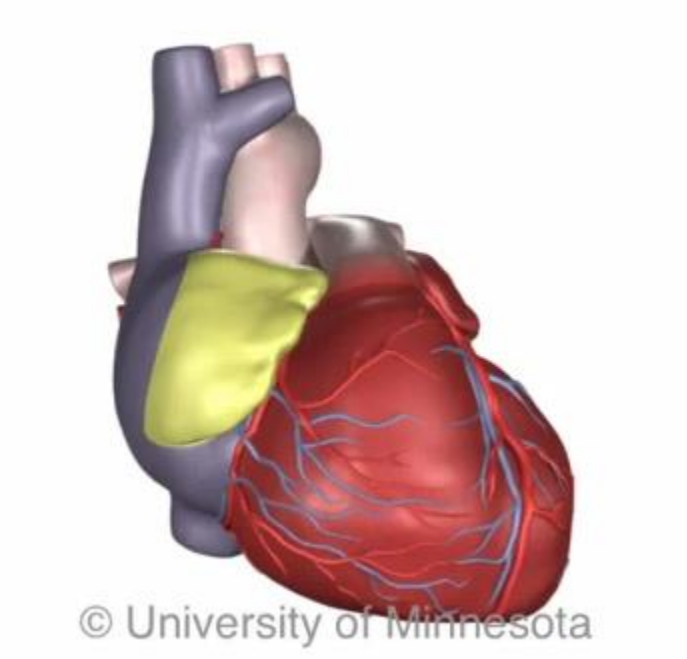

Figure 13. A diagram of a human heart highlighting the anatomic location of the right atrial appendage in yellow.

The RAA is not necessarily a small cardiac structure, and an uninformed person might think that a CNN would be able to easily segment such a structure. However, upon closer inspection of the human RAA, one can see that it is an incredibly detailed structures that poses greater challenges. The myocardial tissue of the RAA is typically so thin that one can read a business card through the structure, which is depicted below [5]. In addition, this myocardial surface is composed of bands of pectinate muscle, creating a complex surface with many ridges.

.

Figure 14. An image taken from inside the RAA of a reanimated human heart, visually depicting the thinness of this regional myocardial tissue. A business card is placed on the external surface of the RAA and one can clearly read through the tissue via a videoscope placed inside the right atrium.

With a clear understanding of the deceptively intricate anatomy of the RAA, let's visualize at how this is depicted within an MRI scan and the difficulties that these complex anatomies could pose in terms of segmentation and/or auto-segmentation. Shown below is a slice of an MRI scan showcasing the RAA. The thin portions of the

myocardial tissue are barely visible, even in this very high resolution scan: a perfusion-fixed heart, that is stationary, scanned with 1 mm slices with ~200 micron resolutions. When these tissues were registered in the scan, they are often so thin that they are in some spatial locations, only represented by single pixels. Thus, creating a high-quality 3D model from such a segmentation is incredibly difficult, since missing a single pixel in the segmentation equates to a hole in the surface of the model.

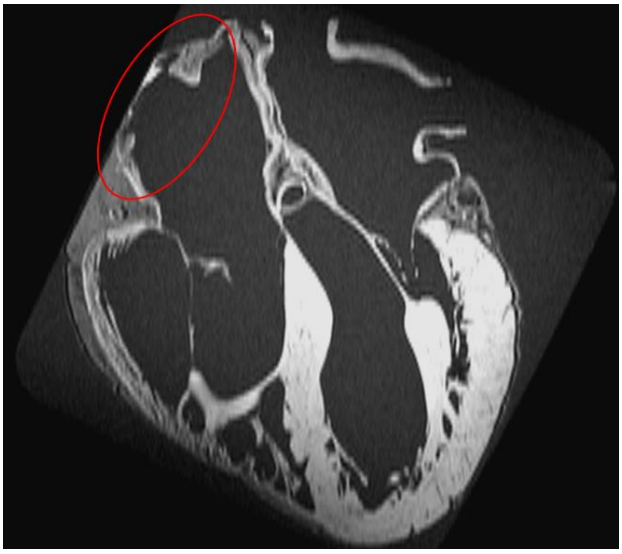

Figure 15. An MRI scan slice of a perfusion-fixed human heart. A red oval that encapsulates the RAA was added to highlight the relative RAA location within this scan.

If we adhere to strict, literal, guidelines while annotating our dataset, i.e. only segmenting tissue that clearly appears in the scan by having a high pixel intensity, the difficulty of producing a high quality 3D model of the RAA should become more understandable. An example of such a segmentation is depicted below. This initial segmentation contained many gaps in the RAA anatomy that lead to multiple holes in our masked model. In fact, most of the RAA that appears in the scan was mainly observable as pectinate muscle

bands on the interior surface of the RAA myocardial tissue. This translates to the pectinate muscle bands being segmented clearly, while much of the thin myocardial tissues in between them were not segmented correctly.

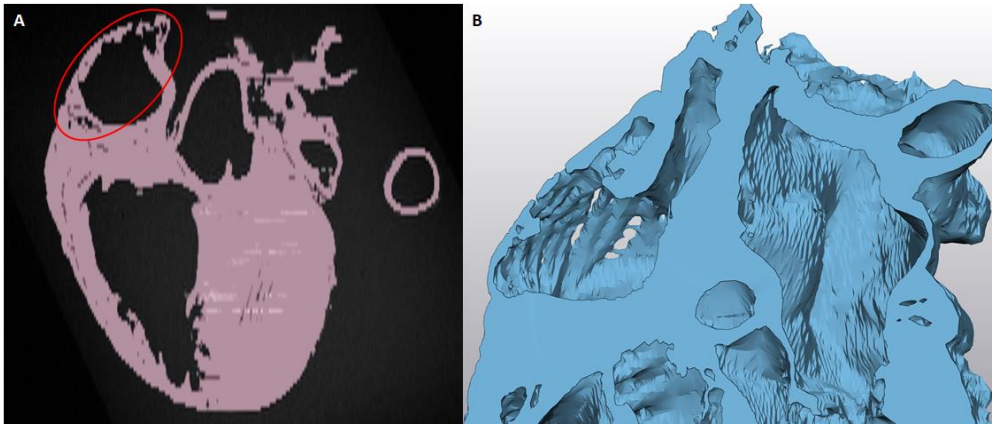

Figure 16. (A) Strict mask segmentation of the RAA and (B) resulting model. Upon close inspection, the pectinate muscles are clearly represented, while portions of the thin myocardial tissues of the RAA were missing. This model was generated by the CNN discussed in the previous section.

The important question that needs to be addressed relative to such issues are: how do we deal with these difficult and/or very thin anatomic structures when annotating and evaluating the outputs of a CNN tasked with automatic segmentation? First, to better segment these cardiac anatomies for instance, we will need to draw on our domain knowledge of the human heart structures; i.e., to predict where they may be in these scans, even if it does not show up clearly in one or more scan slices. Here we show an example of properly segmenting the right atrial appendage in an MRI scan. As you can see, there are portions that are segmented where the pixels do not show that the tissue is there. However, we know that the RAA is still there and that these MRI scans were

simply unable to capture such due to how thin the myocardium is. Again note, that these are particularly high resolution MRI scans of these static human hearts that were perfusion fixed and stationary. These issues would be even more complex for clinically obtained datasets. In this example of the RAA, it would be somewhat nonsensical to assume that there was a large abundance of holes in this anatomic region. Thus, by drawing on our anatomical domain knowledge to more properly segment the RAA, the intra-pectinate RAA regions need to be adjoined; resulting segmentation leads to a higher quality 3D model without any holes.

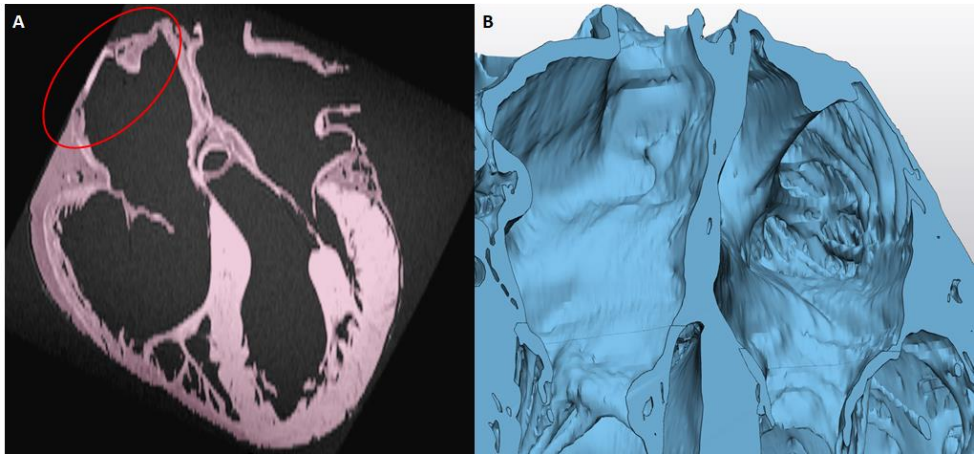

Figure 17. (A) An MRI image slice showing the proper segmentation of the right atrial appendage and (B) the resulting 3D model. Notice that all of the pectinate muscles are clearly represented and all of the thin myocardial tissue between them is fully segmented without any holes in the mode.

Only by obtaining a proper understanding of human cardiac anatomy are we able to correctly segment this dataset for use in training a CNN. Note, that we have access to these perfusion-fixed human heart specimens, so we can also physically reinvestigate the specific anatomies in question. Furthermore, this critical anatomic knowledge is also

required so to be able to carefully evaluate outputs of the developed computational networks as well. For example, we want to ensure our employed network is properly segmenting the RAA, even when these anatomies are not clearly depicted by various MRI scan slices that it is making predictions on.

Chordae Tendineae

The chordae tendinea are additional anatomic structures within the human heart that commonly proves difficult to segment, either manually or with a network. These can be very thin and complex structures, with multiple branches of all varied thicknesses that in turn will span across many slices of an MRI dataset. This commonly makes it difficult to accurately capture these anatomic features, even with a strong domain knowledge, as well as often how to interpret DICOM scans. Before we dive into this example, lets first look deeper into the anatomies of the chordae tendineae for the atrioventricular valves and their functions.

The chordae tendineae are fibrous tissue bands that connect the heart papillary muscles to either the tricuspid or mitral valves. They allow the valve leaflets to maintain the correct position throughout the cardiac cycle: importantly cooptation during systole. Damage to the chordae tendineae can lead to atrioventricular valve regurgitation and other complications within the heart [6]. Shown in the figure below is a videoscopic image of chordae tendineae visualized within a reanimated human heart: see also Atlas of Human

Heart Anatomy (http://www.vhlab.umn.edu/atlas/) [5].

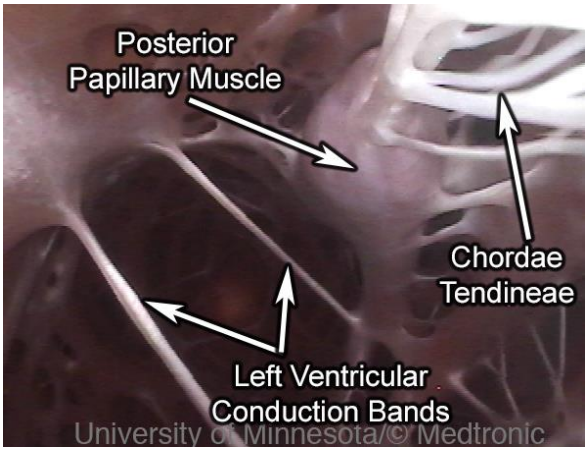

Figure 18. Chordae tendineae attached proximally to the posterior papillary muscle and distally to the mitral valve leaflet within the left ventricle of a human heart.

The above figure not only showcases the potential small dimensions of the chordae, but the complexity of their arrangements and branching structures. These features make the human chordae often very difficult to accurately segment throughout MRI scans even of these static specimens. Even in these static high resolution cardiac scans the MRI does not always register all the chordae in the scan; resulting in the same problem previously discussed with the RAA. Note as well, the chordae are typically registered across multiple different scan slices on an MRI dataset (the distance between consecutive slices in the MRI is often referred to as the resolution of the scan) and this distance can vary greatly depending on the resolution of the scan. This makes it difficult to accurately track the chordae, because even if the scan has accurately registered them, the chordae can anatomically branch multiple times between viewed scan slices. Therefore, this make it

extremely difficult to correctly segment the chordae without a thorough understanding of the anatomy.

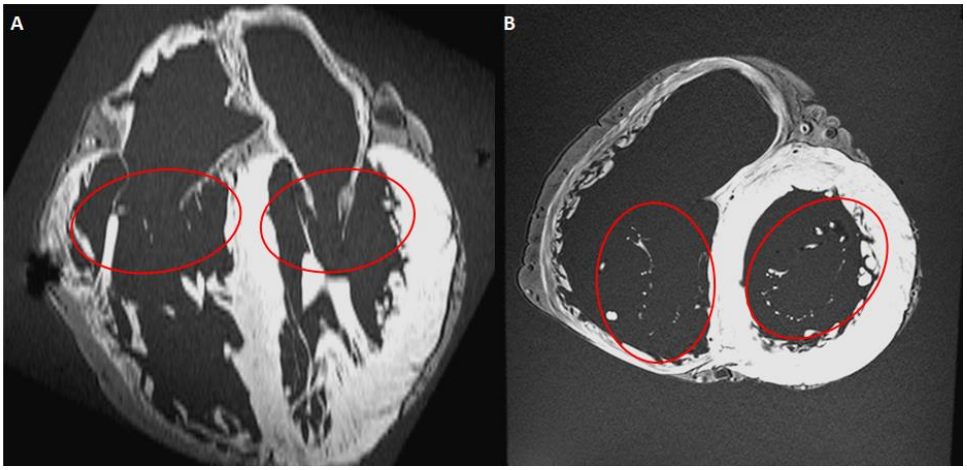

Figure 19. Two different MRI scan slices projections, depicting the chordae tendinea in the (A) coronal and (B) axial axes. The complexities of the chordae can be clearly observed by the large number of branches depicted in this figure.

It is important to reiterate these anatomical challenges can lead to several problems for a CNN to accurately segment the chordae, and thus also for the user to be able to accurately evaluate the correctness of their network. Here we see an example where our developed network was unable to accurately track the complexities of the branching nature of the chordae within the utilized MRI scan dataset. While it appears that the network did relatively ok in the 2D segmentation, we see that much of the chordae were not captured when we generated the 3D model of the heart.

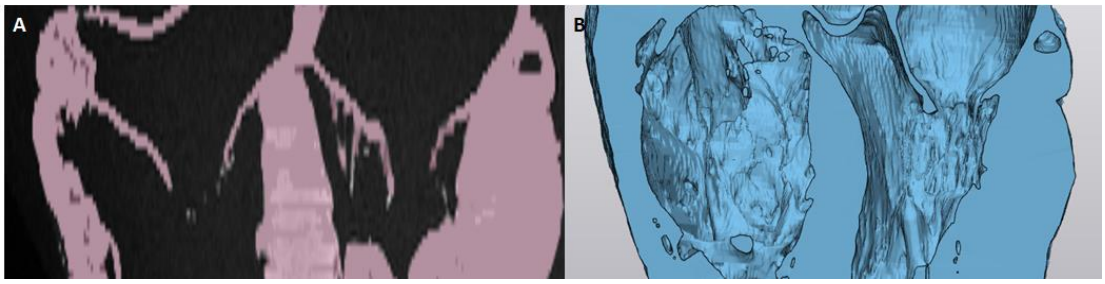

Figure 20. (A) network generated segmentation of the chordae tendinea was initially determined to be somewhat imperfect. (B) Our employed CNN failed to successfully track the chordae in the segmentation there are large gaps of missing chordae in the generated 3D model.

To address these anatomic issues, we needed to utilize our domain knowledge to understand what the chordae should appear as within a given scan. While the uniqueness of anatomy changes between every patient, having a solid understanding of the anatomy will help us deal with the variations seen within the chordae within our perfusion-fixed human heart specimens. In addition, we must be able to accurately interpret our MRI scan datasets in order to understand how to track the chordae across multiple scan slices and be able to segment the chordae when they are not registered well within a given scan. This allows us to create correct annotations of the chordae which will yield a CNN that can more accurately segment them after training is complete. Such a resultant auto segmentation is depicted in the figure below.

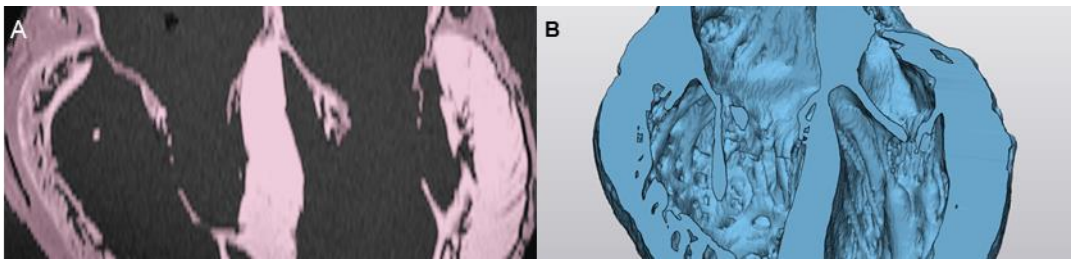

Figure 21. (A) A high quality manual chordae tendineae segmentation that captures all of the complex anatomy and the (B) resulting high quality CNN generated 3D model.

Aorta

The aortic artery is the largest artery in the human body. It is the main pathway for oxygenated blood that is pumped out of the heart and delivered to the rest of the body. As such, the aorta is also a long vessel that starts at the aortic root of the heart and traverses all the way down through the abdomen [7]. There are also multiple arteries that directly branch off the aorta in order to deliver oxygenated blood to the rest of the body. Images of the aorta are displayed in the figure below [5, 8]. As the aorta is such a central and important anatomical feature of the heart; complications related to it have severe consequences, such as aortic aneurysms [9].

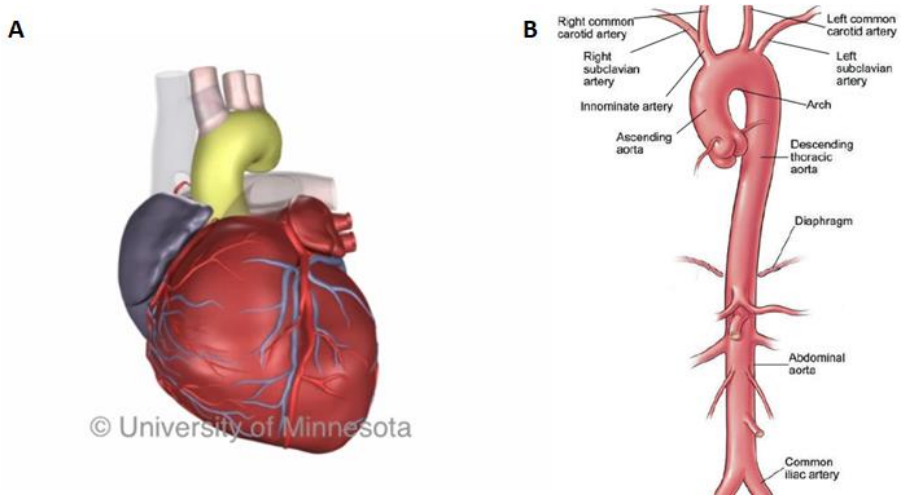

Figure 22. (A) An image of the heart with the aorta highlighted in yellow. (B) A depiction of the entirety of the aorta from the aortic root down to where it branches into the common iliac arteries.

While the aorta is not necessarily difficult to segment, it introduces an example of a concept that we will refer to here as an ‘arbitrary boundary’. Further this is an anatomical feature that can have an arbitrary boundary if it continues past a point that is necessary for our application, forcing us to decide where along the feature we should place an end boundary to stop segmenting. If we are focused specifically on the cardiac anatomy, then we likely do not need to segment the entire aorta down to the common iliac arteries. Thus, we must decide where this arbitrary boundary should be placed. Depending on the application, the boundary could be placed on the ascending aorta, after the aortic arch, or somewhere on the descending or abdominal artery.

Clearly defining the arbitrary boundary on the aorta is considered as a critical step for building a dataset for automatic segmentation. To emphasize this point, imagine a situation where you tell 10 different people to segment the heart in a scan and offer no other clarification. All 10 of these people will at some point be forced to decide where along the aorta they should place this arbitrary boundary and thus stop their segmentation. The placement of this boundary will vary greatly for each person creating a lot of inconsistencies in our database per se. This in turn could create undesired problems while training and evaluating the network.

To continue to emphasize this example, assume that 5 people stopped segmenting the aorta before the arch, and 5 people segmented the entirety of the arch and stopped the

segmentation in the descending aorta, see the figure below. While training the network, the CNN receives 5 scans in a row where the aorta is only segmented up to the ascending aorta. This informs/teaches the network that it should not segment the aorta past the ascending aorta, because every time it does it is punished by our loss function. Next, the network is sent 5 scans where the aorta is segmented all the way to the descending aorta. At first, the network stops segmenting the aorta at the ascending aorta as the previous scans suggested is correct. However, now all the scans have segmented the entirety of the aortic arch which causes our network to be greatly punished by the loss function because it failed to segment so much of the aorta. This poses a difficult problem moving forward because the network received conflicting information on how much of the aorta should be segmented, reducing its confidence in predictions; directly reducing its ability to create accurate segmentations.

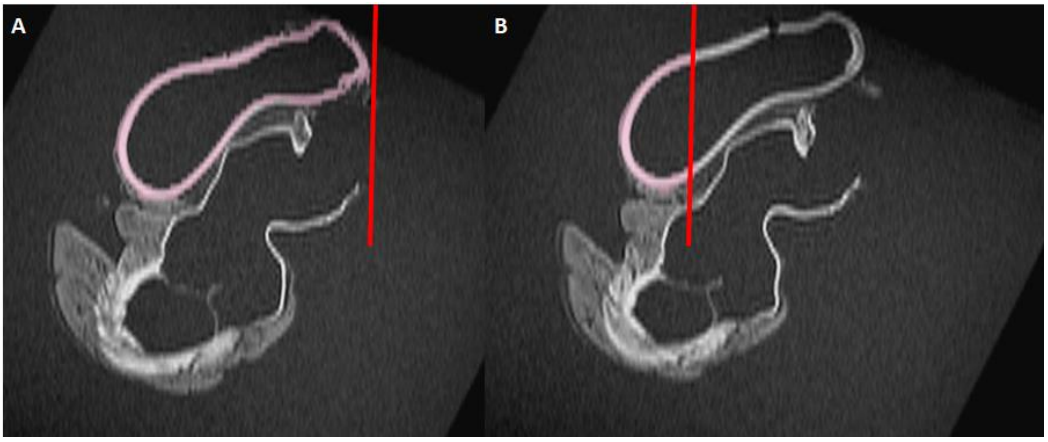

Figure 23. 2D Segmentations showing the aorta with different arbitrary boundary locations, highlighted by the red line for clarification, i.e., the boundary placed (A) after the Aortic Arch and (B) on the ascending aorta.

As you can imagine it is imperative that arbitrary boundaries for anatomical features such as the aorta be clearly defined. This will allow the annotation of the aorta to be consistent across all scans, preventing any confusion for the utilized network when training on the truth dataset. Note, when subsequently the arbitrary boundary was placed in a similar location, in all the scans that make up our dataset, the network was able to confidently locate these arbitrary boundaries in every scan, resulting in higher quality segmentations.

Discussion

Resources for Gaining Anatomical Domain Knowledge

To gain domain expertise relative to human heart anatomy, one should consider taking advanced courses, studying specimens, consulting with experts studying 3D prints of varying degrees of completeness. While all of these resources are invaluable, it is understood that they may not be readily available to everyone interested in gaining more anatomical knowledge. The Atlas of Human Cardiac Anatomy as an essential learning tool that could be used (http://www.vhlab.umn.edu/atlas/). This is a free access website with comprehensive resources for learning cardiac anatomy.

The Certainty of Errors in the Data

Even if all these considerations are taken into account and the data is labeled by experts with extensive knowledge of anatomy and MRI scans, it is inevitable that small amounts of errors will exist in a given dataset. There will be portions of the scan where the

anatomy is incorrectly labeled, and that data will be used to train the network. Since our network is unable to know which of the data has errors, one might worry if these errors will have a significant impact on the resultant CNN results. Luckily, this should not be the case, and this is one of the major strengths of a CNN. We discussed earlier how a network uses ground-truth masks and a loss function to train. If there is an error in a ground-truth mask and the network makes the correct predictions, the network gets punished for this mistake. However, this punishment pales in comparison to the numbers of times the network is rewarded for correctly segmenting similar, correctly labeled data within the dataset. Therefore, if there is not a large number of errors in the dataset, throughout training, the CNN learns to average out these errors and will continue to make correct predictions on new scans.

Impact of Errors when Interpreting Results

Until now in our discussion we have mainly focused on how errors in the dataset will affect the employed network during training. However, it also affects the results one can see when validating the network if errors are present in the validation dataset. The validation dataset consists of labeled data that is not used to train the network. This allows us to see how well the network performs on data that it has never seen before, which gives an indication of how well such a network will generalize to new data.

Nevertheless, as with training, errors in this dataset will create problems when attempting

to validate one employed network. Assume that the network makes the correct predictions on a validation scan. When we evaluate the network's prediction, we compare it to the GT mask for that validation scan. However, if there are many errors in the GT mask, there will be many differences between it and the network prediction, even if the network predictions are near perfect. These differences will cause the derived evaluation metric score to drop significantly, even though the network had made the correct predictions. This makes it critical to not take the evaluation metrics for each validated scan as idealized. It is good practice to manually inspect the predictions of your network, especially on scans where it received an associated low evaluation score. This allows one to ascertain whether there are errors present in the GT masks or if the network itself is having an especially difficult time with a certain aspect of the true image data.

Expanding the Scope

It is important to reiterate that these described approaches need not be specific to MRI scans of the heart but can be extrapolated and applied to any form of medical imaging and any complex anatomies of interest.

Yet, expanding the scope to include more anatomical features increases the challenges; as were highlighted in this paper. Most anatomical geometries have complicated and detailed features that require anatomical domain knowledge to successfully annotate and interpret the data. In this paper we only highlighted a select few of the cardiac anatomical

features, so one can imagine how long that list would be if one were to segment the entire human body anatomy present in a high resolution MRI scan dataset. In our lab we have worked on creating full computational anatomical models of fresh human cadavers which were administered high volumes of contrast agents: see is depicted in the image below [10]. It is noteworthy that an abundance of domain knowledge was required to manually create such a model, and the same knowledge would be required to create a CNN that could automate said process.

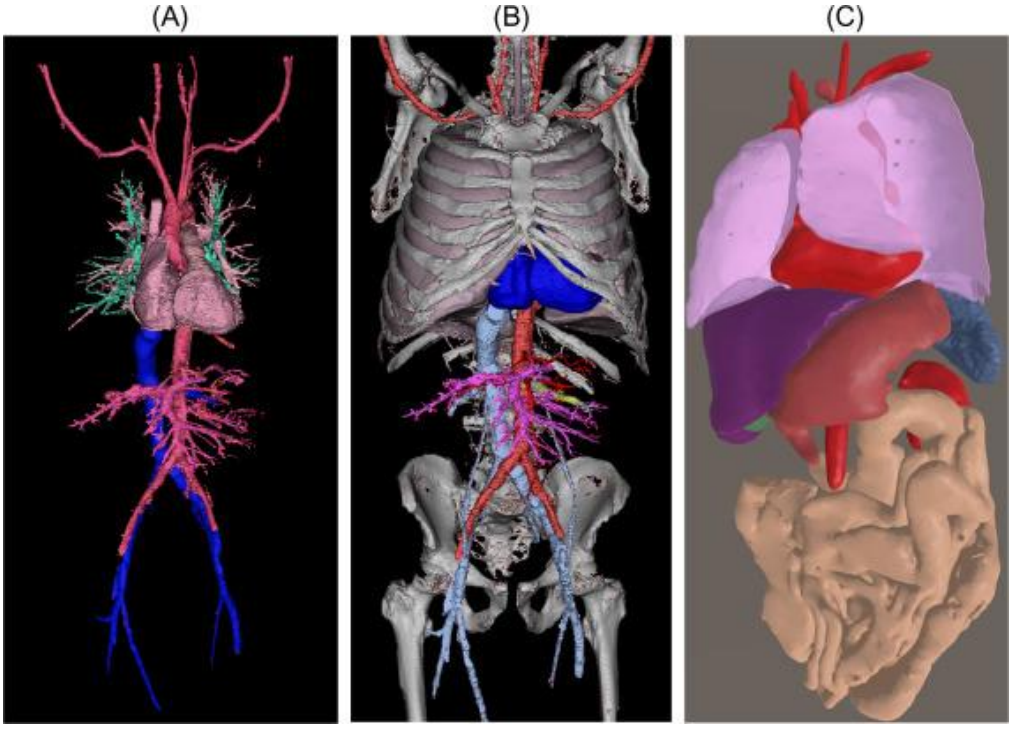

Figure 24. Computational cadaver models generated from MRI and CT scans showcasing (A) the heart and major vasculature, (B) in addition to the bones and lungs, and (C) only the major thoracic abdominal organs.

Conclusion

When using CNNs for automatic segmentation of human anatomies or other objects, the importance of the data quality cannot be overemphasized. The higher the quality of data used to train and validate our network, the higher the quality of model one can produce. Further, labeling the data in a consistent and accurate manner will help the utilized network to learn and abstract the important information within the data - which will directly lead to more confident predictions. This can be challenging when using DICOM data, such as clinical MRI scans, because there are many domain specific factors that need to be considered. It is imperative that data annotators are knowledgeable and experienced in interpreting DICOM data and the specific anatomical features of interest. As described here, even the utilization of static, high resolution MRI scans of perfusion-fixed human heart: i.e., optimized scanned to include small anatomical features and no motion artifacts.

Deep learning is a powerful tool that has near infinite potential in helping solve complex problems in the medical field in general and including imaging. Yet, an abundance of knowledge in coding and artificial intelligence is required to successfully implement a CNN on a dataset to provide a worthwhile, high quality models. However, it is often overlooked that domain knowledge for the specific application is equally important. Without substantial domain knowledge, it is incredibly difficult to correctly annotate the data utilized for both training and evaluating the network. Additionally, a lack of domain

knowledge makes it impossible to correctly interpret the predictions of the network and determine how the network is ultimately performing.

Acknowledgments

Thank you to everyone at the Visible Heart® Laboratories that assisted with this project. We also would like to thank the organ donors and their families for providing these critical research specimens for 3D model generation.

Utilizing a Deep Learning Pipeline to Assist in the Segmentation of a Large Anatomical MRI Dataset

Submitted to *IEEE: Journal of Selected Topics in Signal Processing*, in review.

Alex J. Deakyne [1,2], Tinen L. Iles [1,2], and Paul A. Iaizzo [1,2]

[1] Department of Bioinformatics and Computational Biology, University of Minnesota, Minneapolis, MN

[2] Department of Surgery, University of Minnesota, Minneapolis, MN

Preface

The previous sections of this thesis have described the need for anatomical computational models, their uses, and the difficulty in producing a large number of them. In this chapter we will explore the potential of utilizing deep learning, specifically a convolutional neural network, to assist in the generation of anatomical computational models. This network will make predictions for how to segment the cardiac anatomy in an MRI scan, and then allow an anatomical expert to rapidly review and make any necessary edits to the segmentation. After that is completed, the 3D anatomical model can be generated. Pipelines such as the one described in this chapter, will be an inevitable portion of the

process of annotating medical imaging data in the future. They offer a reduction of the time required to annotate said datasets, while still allowing anatomical experts to review and make necessary edits to the network annotations to ensure high quality computational models.

This manuscript was submitted to IEEE Journal of Selected Topics in Signal Processing and is currently in review. All authors contributed to the preparation of this manuscript for publication.

Summary

In this chapter we will detail the application of a convolutional neural network to assist in the segmentation of a large anatomical dataset consisting of high resolution cardiac MRI scans. The network was trained utilizing 51 manually segmented scans and was able to achieve a high Dice coefficient of 0.8912 +/- 0.0024 (n=11) on the validation dataset. This network was then utilized to create prediction segmentations on the remaining 128 unsegmented scans in the dataset. These predictions were made in 2 minutes each and 90% of the scans required less than 30 minutes of editing to achieve a high quality 3D model. This reduced the time needed to create a high quality 3D computational model from multiple days to under an hour in most cases. This drastic reduction in time allows a small team or individual to generate a large (over 100) anatomical computational model dataset in a matter of weeks or a large company to generate said dataset in hours.

Synopsis

Human anatomical specimens have always been a crucial part of educational training for the understanding of complex anatomies. The digitization of these samples has allowed for further analyses and study; as computational methods and software continue to be developed. Unfortunately, detailed segmenting of complex and small geometrical anatomical features and creating a valid 3D model of such can be both difficult and time-consuming processes. These methodologies are further exacerbated when organs, large anatomical regions or the whole human body anatomical datasets need to be segmented. Currently, creating 3D anatomical models from such a "big" dataset of MRI or CT scans becomes nearly not feasible, unless a large team is assembled to accomplish the required tasks. Here, we propose a deep learning pipeline that will be able to automatically create segmentations, and 3D models, from the MRI scans of perfusion-fixed human hearts. The network was able to achieve a dice score of 0.89 (n=11) on the validation dataset. The network was then used to segment the remaining 128 new MRI cardiac scans. This pipeline assists in annotating a large medical dataset by reducing the time required to segment a large MRI dataset (n > 100) from over 1000 hours to only 100 hours.

.

Introduction

3D modeling of human anatomical features has seen increased demand throughout the last decade. This has been influenced by many areas within the medical field such as education, pre-surgical planning, and the medical device industry. These 3D models

preserve all 3D spatial and relational data in the scans and present them in a way that is easier to digest than scrolling through 2D DICOM datasets. In addition, 3D anatomical models allow for further analysis and study of the anatomical specimens. Possessing computational models of these unique specimens allows for the increase in their values and educational potentials. They can be used to take accurate anatomical measurements that would have been difficult to obtain on internal structure and/or on a physical specimen; especially without damaging these specimens [1]. Investigators have used computational anatomical models and/or 3D printed models to perform computational device deployments or dissections without having to damage the original physical specimen [2]. The computational models have also fueled analyses such as statistical shape modeling or computational fluid dynamics [3,4].

Unfortunately, the task of converting a 2D scan into a 3D model is not a trivial undertaking and is often the bottleneck in these type of analyses - especially when they require numerous complex anatomical models. The generation of a computational model from a set of DICOM scans requires the numerous anatomical features of interest, to be manually segmented. This is typically done using DICOM analysis software such as Mimics (Materialise; Leuven, Belgium). Once these scans have been segmented, they are loaded into a 3D mesh editing software such as 3Matic (Materialise; Leuven, Belgium). This allows for basic editing such as wrapping, smoothing, and optimizing/fixing of the given 3D model. While these automated operations take some time, they are minimal

when compared to older approaches and the time required to create the 2D segmentations manually.

There have been and continue to be many advancements in semantic segmentation over the past few years. Some of the most crucial advances have come through the field of deep learning: which utilizes convolutional neural networks (CNNs) with millions of parameters that are automatically developed/learned during training. Since the parameters are automatically relearned by the network, this overcomes one of the main obstacles of traditional machine learning techniques; i.e., the user does not have to spend time and efforts adjusting many complex parameters in attempts to find the ideal values. CNNs are trained utilizing large datasets which allows them to learn abstract concepts about the information of interests in the images that they see. For example, in this application, the network learns what the myocardium is and how it appears in an MRI scan. Since it is trained on many well validated heart models, it learns that each heart's anatomies are unique and can then successfully segment the myocardium on hearts it has never seen prior.

CNNs learn to make accurate predictions through a training loop. During this process, image pairs consisting of the input image and the correct segmentation mask are repeatedly sent to the network. The network makes a prediction segmentation mask based on the input image. This prediction mask is then compared to the ground truth

segmentation masked provided with the input image. Since the GT mask is the ‘correct answer’ the networks performance is evaluated by how well its prediction mask matches the ground truth mask. Once this comparison is made, the CNN then updates its parameters to make more accurate prediction segmentations in the future. This training loop is repeated millions of times until the network can make accurate predictions.

The Visible Heart® Laboratories (VHL) has a unique human heart library that contains over 500 perfusion-fixed human heart specimens: in an end-diastolic state. While 210 of these hearts have been MRI scanned, only 62 have been individually segmented to create a high quality computational 3D models of each heart’s entire myocardium. This become an almost insurmountable task for the remainder of the hearts in the library after carefully scanning: i.e., each heart’s multi-plane DICOM image datasets would need to be segmented by our limited staff using traditional methods of manual segmentation, this taking approximately more than one year of manhours to do so). Therefore, we have considered that an automated process for segmenting the MRI scans is needed to maximize the benefits of these anatomical samples; by expediting the creation of computational models for each specimen.

Here, we propose a deep learning pipeline to assist in the segmentation of the remainder of unique and valuable dataset. The network was trained using the 62 high resolution human heart scans in the dataset, that were initially carefully manually segmented and

validated by multiple anatomic experts. Then, the developed CNN was employed to make predictive segmentations on the remainder of the dataset; i.e., so to assist in annotating the remainder of the previously unmodeled datasets. Since we have a high standard of quality for the computational models we produce, the network segmentations are written back onto the original DICOM scan. Importantly, this allows us to visually inspect each generated segmentation and rapidly compare it to the original scans. If any discrepancies are found between the original scan and the network prediction, it also allows us to rapidly make the necessary edits using anatomical segmentation software.

Methods

Data Preprocessing

The human hearts utilized in these investigations were considered non-viable for transplantation and were obtained fresh from the organ donor: all appropriate consents were obtained so to utilize these rare specimens for research and education. The MRI scans were all obtained after each heart specimen was perfusion fixed in an end-diastolic state: i.e., to prevent the hearts from hyper constricting or the chambers from collapsing. The anatomy of the heart is better displayed and easier to analyze when the hearts are

preserved in this manner.

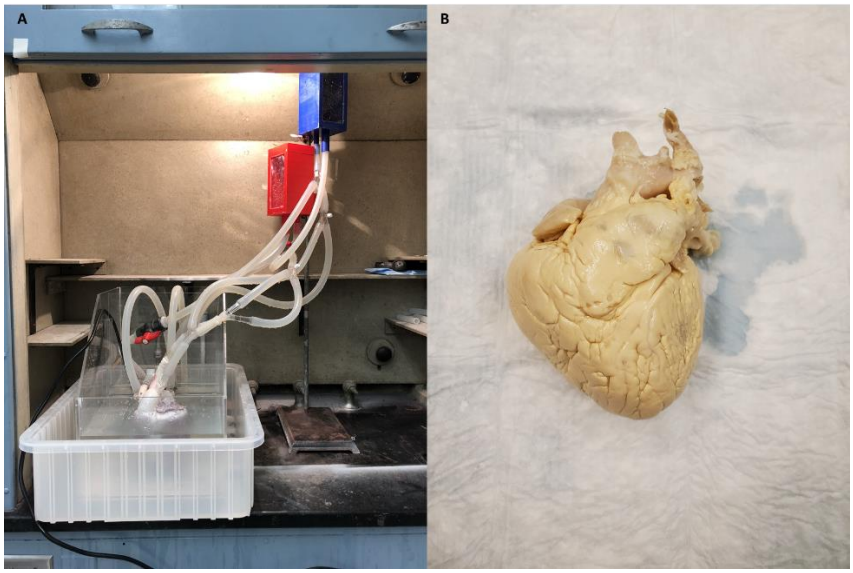

Figure 25. (A) The VHL's custom human heart perfusion fixation system. This system fixes the human heart specimens in an end-diastolic state. (B) A perfusion fixed human heart specimen ready for anatomical study.

Once perfusion fixed, the human heart specimens are prepped for scanning. To accomplish this, the hearts are isolated in agur gel and MRI scanned using 3T MRI scanners [5]. The isolated human hearts are static during the process of the MRI scan. This is advantageous when compared to clinical scans where the heart is moving because it allows us to obtain high resolution scans (1mm resolution) which is not achievable in a clinical setting. Accordingly, the detail of the anatomy captured in these scans is superior to that of clinical datasets. The myocardium of the hearts was then segmented using the same methodology found here to create the "ground truth" (GT) masks for training [6].

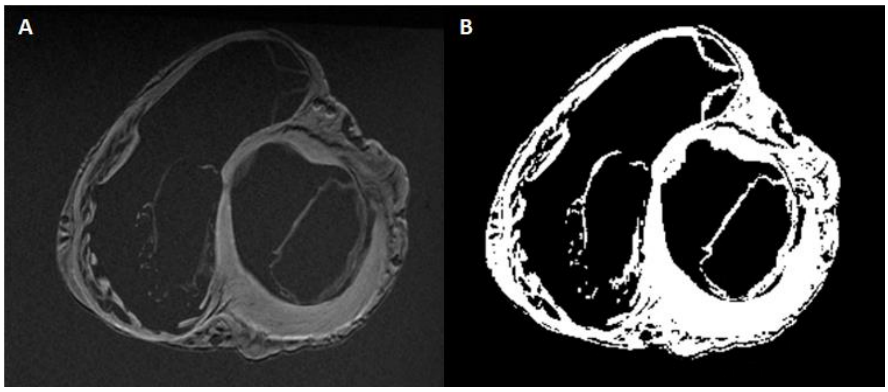

Figure 26. A depiction of a training scan slice (A) and the corresponding ground truth mask created by manual segmentation (B) obtained from human heart HH0311 in our database.

Network Architecture

The base architecture used for the network in this project was a U-Net designed for 2D images [7]. However, the encoder of the U-Net was replaced by a pre-trained ResNet34 [8]. The ResNet architecture is a deeper and better network than what is traditionally used as the encoder for a U-Net, granting a larger number of convolutional filters for our network to learn. Secondly, we incorporate the pretrained weights for this network; that was trained on millions of natural images [9]. These pretrained weights offer a better starting place than random initializations and allowed us to take advantage of some of the great filters responsible for detecting simple things in the images such as edges and basic shapes.

CNN Training and Evaluation

The network was trained using 51 of the fully annotated scans. An additionally 11 fully annotated scans were used to validate the network. A series of transformations were

applied to the images before they were sent to the network during training. The images were sent to the network at native resolution (512x512 pixels). The images were also subject to flips and rotations. Images were sent to the network in batches of 48 images. The network was trained using one cycle policy and cyclical learning rates [10].

The network model results were analyzed using the Dice coefficient. This equation allows us to determine how similar the segmented hearts were by whether they labeled the same pixels as the heart tissue or background. The heart scans were evaluated by this metric in their totality so that we had an accurate assessment of how the network and user generated heart models compare.

$$dice = \frac{2 \times TP}{(TP + FP) + (TP + FN)}$$

Figure 27. The Dice coefficient is defined by two times the true positive (TP) values over the sum of the true positives with the false positives (FP) and the true positives with the false negatives (FN). This equation provides a relative understanding of the similarities of two segmentations.

Analysis of New Scan Predictions

The new scans that the network predicted on, had no ground truth annotations to calculate a dice score. Therefore, we needed to manually grade the network segmentation outcomes. To do this efficiently the predicted segmentations for each scan were written back onto the original scan. The segmentations were saved as a high pixel value to stand out from the rest of the scan. This enables the network predictions to be visually validated since the segmentations could be compared to the original scan. Additionally, the scan

could be opened in a segmentation tool such as Mimics where the predicted mask can be manually edited to improve the mask if it was not considered by the anatomical expert to be a perfect segmentation. While this does introduce some manual intervention if the generated mask was not up to par, importantly it drastically reduces the time required to segment the cardiac structures from days to minutes.

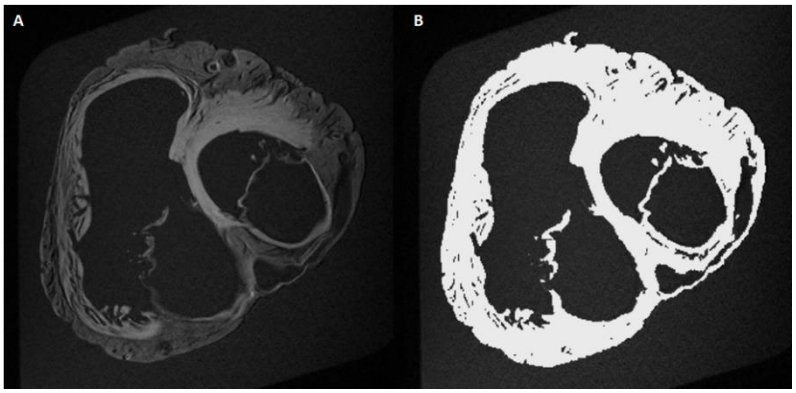

Figure 28. An image showcasing (A) the original scan slice from HH0092 used as an input to the network and (B) the network predictions overlaid on top of the original scan for easy validation of the network segmentation quality.

The generated segmentations were split up into three distinct categories: high quality, acceptable, and needing revision. The ‘high quality’ segmentations were the ones that need minimal or no manual editing - such as wrapping or smoothing the mesh. The ‘acceptable’ segmentations were noted as the ones that meet the minimal requirements of quality that we need for our dataset; but likely would require less than 30 minutes of manual editing the segmentation in order to have a high quality 3D model. Note, commonly these ‘acceptable’ models included minor flaws such as small holes in the mesh or rough surfaces; all of which could be fixed with minor edits to the mask. The

models in the ‘needs revision’ category were ones that the network had a difficult time segmenting and it would take over an additional 30 minutes of manual editing in order to create a high quality model.

The entirety of this pipeline for assisted segmentation using AI is described in the diagram below. A new scan is sent to the CNN where a prediction segmentation mask is created. An anatomical expert then reviews the prediction mask and compares it to the original scan to determine the quality of the segmentation. If the segmentation is deemed high quality then the computational 3D model of the heart segmentation is generated and saved. If the network generated segmentation mask has too many errors to be considered high quality, then the anatomical expert makes the necessary corrections to the errors in the mask. Once these errors have been corrected, the anatomical expert will then review the segmentation again to ensure it is high quality before generating and saving the computational model. If needed, the anatomical expert can inspect the physical heart specimen (in the VHL Human Heart Library) to gain a better understanding of a certain anatomical feature within the cardiac scan. This iterative process can be repeated until the 3D model generated from the segmentation mask is deemed high quality.

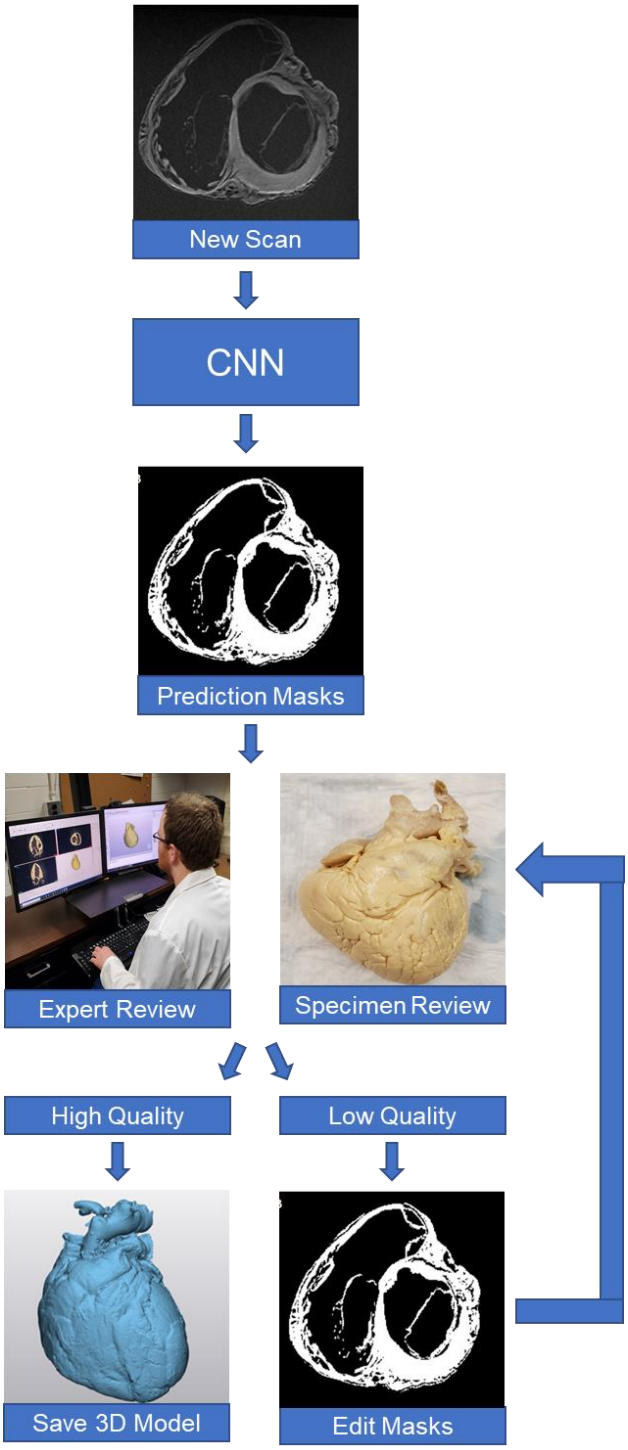

Figure 29. Diagram depicting the workflow of our CNN assisted segmentation pipeline.

Results

Training Results

The employed pipeline utilized for this project, could generate its predictions for an entire human heart scan within 2 minutes; i.e., using a modest 2080 graphics card. The mean dice score for the scans in the validation dataset was 0.8912 +/- 0.0024 (n=11). In comparison, other investigators have reported similar validation dice scores when performing myocardium segmentation on clinical MRI scans [11]. This gives us confidence that we have a well-trained model capable of performing quality segmentations on new scans of our perfusion-fixed human hearts. Additionally, visual inspection of the predictions revealed the trained network could make high quality cardiac models and accurately segment the cardiac structures within the MRI scan. Examples of the network segmented hearts compared to the original are shown below. The relative qualities of the generated models could be improved quickly by performing simple 3D mesh edits such as wraps or smoothing functions in 3Matic.

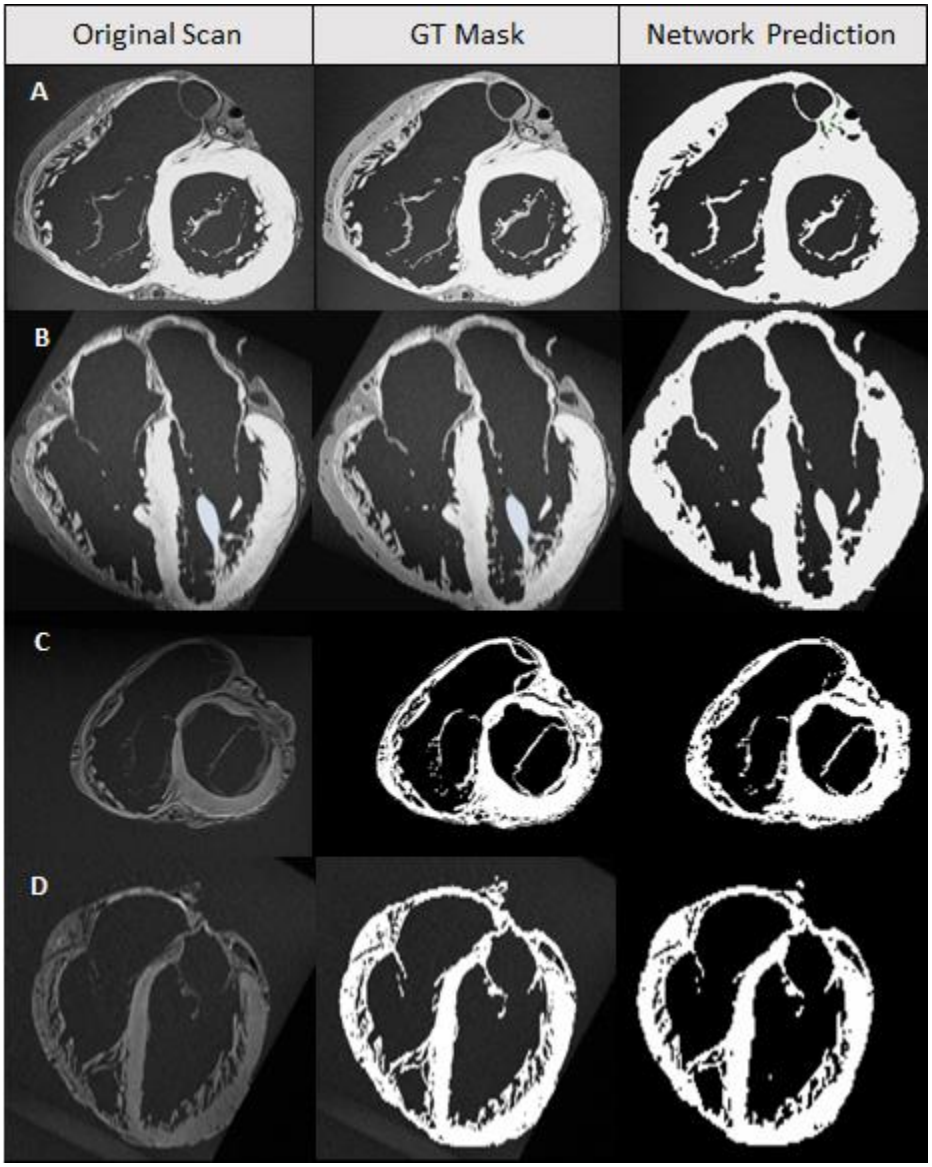

Figure 30. A collage showcasing the original scan slice, the ground truth mask, and the network prediction for HH0229 (A) showcasing the axial and (B) coronal axis. In addition, the same is depicted for the (C) axial and (D) coronal axes for HH0311.

New Scan Results

The network generated models for the remaining 128 cardiac MRI scans in the dataset; those that had not been annotated yet. Seventy-four of these automatic segmentations were deemed ‘high quality’ in that they required no manual editing to be considered consistent with the qualities of the segmentations produced by manual segmenters. Examples of some high quality models are pictured below.

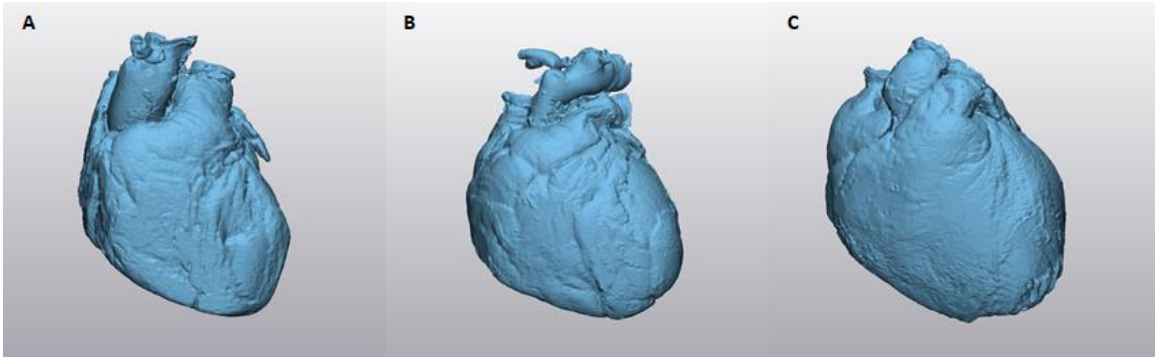

Figure 31. 3D models created from the network segmentations for hearts (A) HH0177, (B) HH0128, and (C) HH0161. These three hearts were classified as ‘high quality’ segmentations and reflect the qualities of other segmentations within the our laboratory’s ‘high quality’ category.

41 of the automatic segmentations were defined to be within the ‘acceptable’ category. Generally, these segmentations were great, but small portions of the resultant 3D computational models contained one or more holes, a rough surface, or an over segmentation. While these errors prevent the segmentations from being considered high quality, they in turn took little effort and time (less than 30 minutes) to rectify. Note, after these edits were made, these models would be considered ‘high quality’. While this does require some manual intervention, it still drastically reduces the time required to produce

a ‘high quality’ segmentation from days to under an hour when compared to our current employed methodology.

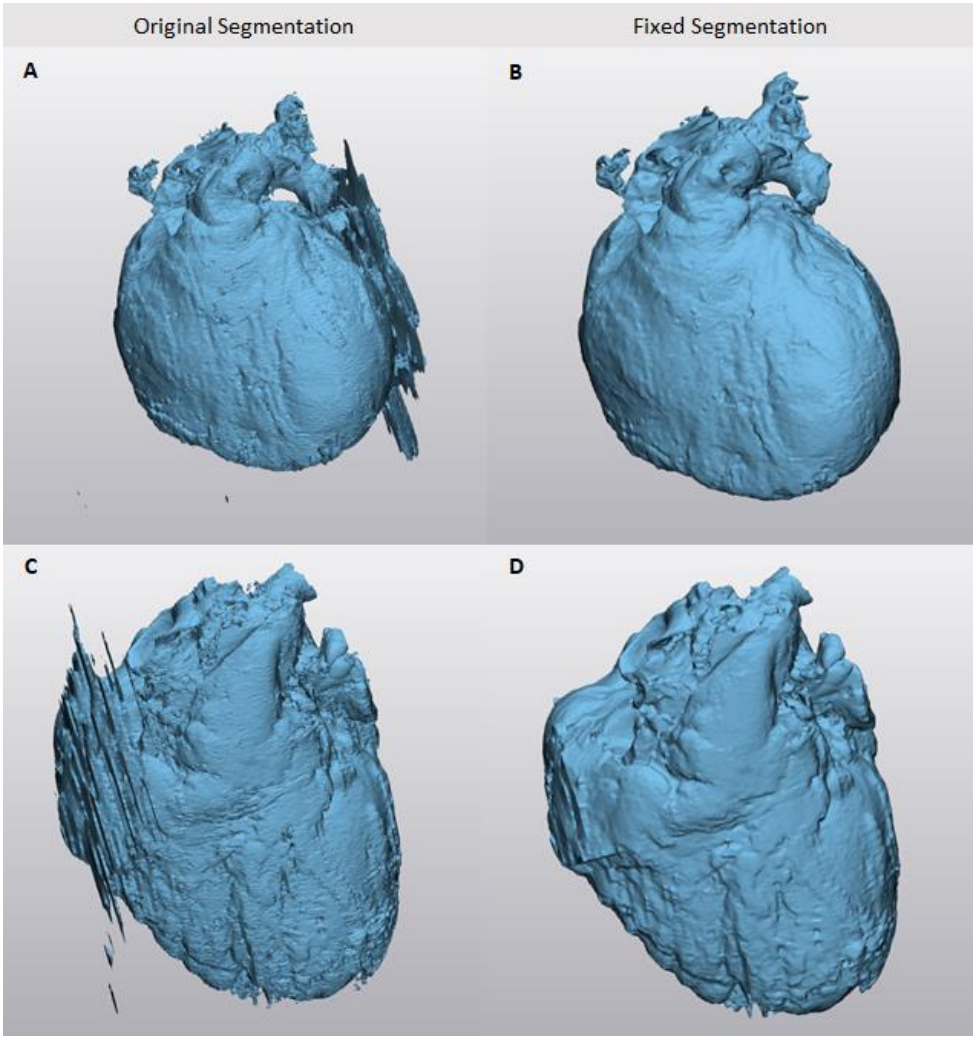

Figure 32. Examples of 3D models created from the employed CNN segmentations deemed as ‘acceptable.’ The models depicted show the original segmentation with some errors, and the manually fixed computational models. Importantly, these types of error in segmentations can even look drastically wrong, but only take a few minutes to correct using Mimics. The models depicted are the (A) original and (B) fixed model for HH0175 and the (C) original and (D) fixed models for HH0086.

Of the CNN generated 3D models, only 13 of the 128 were placed into the ‘needs revision’ category. These segmentations were considered as somewhat problematic and would require a anatomic expert significant time investment, of typically over 30 minutes, to manually revise the mask until with would qualify to be placed into a ‘high quality’ segmentation category. These initial computational heart models typically contained many holes within the cardiac surfaces; i.e., the under segmentation of a critical anatomical feature that resulted in a missing portion of the heart. While this latter category of auto-segmentations requires a non-trivial amount of human intervention to fix, they are still considered as better starting points than typical methodologies one would currently employ: like a simple threshold of pixel intensity. Importantly, this CNN approach still reduces the time required to generate a high quality segmentations from days to hours. Regardless, these segmentations encompassed only 10% of the total segmentations generated by the network for our unique dataset of high resolution MRI scans or perfusion-fixed human hearts.

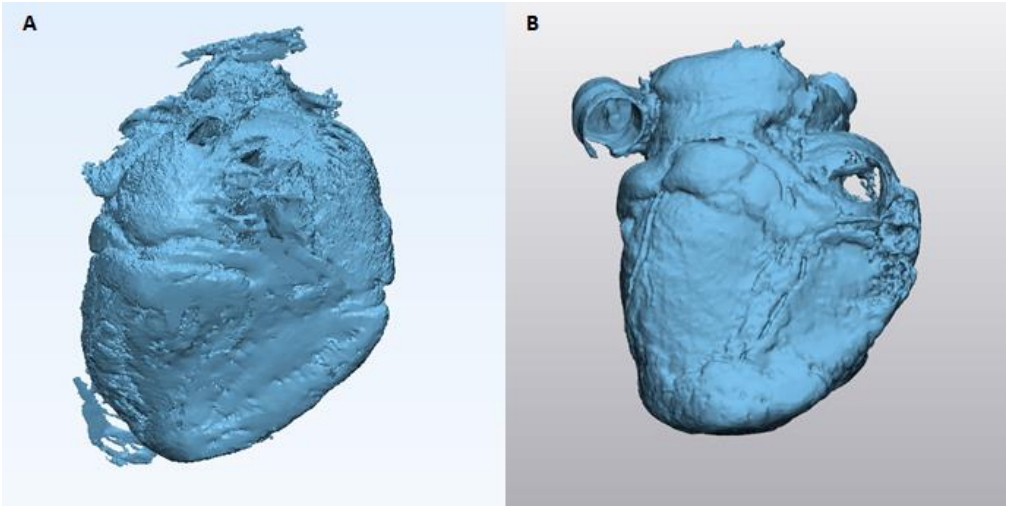

Figure 33. Shown here are resultant computational 3D models that were placed in the 'Needs Revision' category. These CNN segmentations often contained many small holes or a few large holes in the models. These often required > than 30 minutes for a trained anatomical expert, experienced with Mimic to modify appropriately. The models show here are of (A) HH0115 and (B) HH0153.

A table the total number of scans utilized in this study and the relative performance by our employed CNN; this table also breaks down the distribution of how the network generated segmentations were classified. It is important to note that in over 50% of the CNN 3D models generated for our input dataset, the resultant segmentations were classified by an anatomical expert as 'high quality'; meaning they need little to no manual segmentation editing. In addition, only 10% of the generated model were classified as 'needs revision' meaning that the network was unable to produce accurate 3D segmentations. This yields confidence that our employed and trained network was able to generalize well to new data; as it was able to produce an acceptable or high quality segmentation on 90% of the new scans that it had not seen while training.

Table 2. Breakdown of how the network produced segmentations were classified.

Total Scans Segmented	High Quality	Acceptable	Needs Revision
128	74	41	13

Discussion

In our application of a CNN for the generation of 3D computational models of human hearts, in most cases the resultant models require no to little editing before being sent to 3Matic for normal postprocessing. We imputed high resolution MRI scan datasets

uniquely obtained from perfusion-fixed human hearts; this was static imaging. Thus, demonstrating that the employed network can successfully generate high quality human heart models of the cardiac tissues imaged within the multiplanar MRI scans. It is important to note, that while 41 resultant CNN generated models were placed in the acceptable category, the subsequent required manual intervention by the experience user was typically less than 30 minutes. In contrast, those placed with the major revisions category, often consists of scans with a large number of artifacts that confused the network. While these latter generated 3D models were considered far from an ideal segmentation, using them as a starting point still reduces the overall segmentation times from days to hours to generate high quality models.

Automatic segmentation pipelines such as the one discussed here will become invaluable to medical device designers in the future. Segmentation of patient anatomical datasets are considered as a necessity for understanding the pathophysiogical anatomies of a wide range of patient populations. Nevertheless, currently the input sample sizes used for such studies are often limited, due primarily by the time-consuming process of manual segmentation. With the automations of these processes, experts working in these fields will be able to significantly reduce the times required for segmentations of complex anatomies; which in turn allows them to use larger datasets that offer a better understanding of the patient population.

It should be noted here that the MRI human heart scans used for generating our computational 3D models were perhaps of higher qualities than one can obtain today in clinical settings: e.g., due to issue of cardiac cycle gating and other motion artifacts. This introduces new challenges for segmentation as the scans are able to accurately register incredibly thin anatomical structures, such as the chordae tendineae, that would not be registered in clinical scans of the same anatomy. Yet, the perfusion-fixation process itself may have induced anatomical alterations; such needs further investigations.

The generated 3D models from these scans can be utilized for a wide range of applications. They can be used for further anatomical inspection of anatomies (such as the chordae tendinea) that would not be possible without dissecting and damaging the physical specimen. They can also be utilized to perform computational fluid dynamics (CFD) simulations to gain better understanding of cardiac anatomy and function. Additionally, these models can be placed on the Atlas of Cardiac Anatomy to allow people to learn more about cardiac anatomy on the free access website.

The current iteration of the CNN model used has relatively low complexity. Future steps of this research would be to utilize models of higher complexity in an attempt to achieve better segmentation results. The new data generated by the network could also be used to further train the current version of the network, introducing an active learning loop. In such a loop, high quality segmentations generated by the network on new scans can be

added to the training data set to further fine-tune the training of the network in hopes to achieve better segmentation results in the future.

Conclusion

Segmentation of human anatomical features can be a very time-consuming task requiring both expertise in the given anatomical area and segmentation software. In the computational process of producing 3D models of such anatomies, the detailed segmentation is often the bottleneck; in many clinical applications this can make the needed processes logistically impossible, due to the required manhours time investment. Here, we have demonstrated a pipeline that is able to automatically segment cardiac tissue from high resolution MRI datasets. While such tasks are much more challenging that a blood volume segmentations, the employed CNN still performs the required tasks admirably. This employed pipeline drastically reduces the time required to generate high quality segmentations of these scanned human heart, and therefore 3D models, which enables the creation of large fully annotated datasets of 3D anatomical models which are an invaluable resource.

Acknowledgments

Thank you to everyone at Medtronic and the Visible Heart® Laboratories that assisted with this project. We also would like to thank the organ donors and their families for providing these critical research specimens for 3D model generation.

Section 3 – Developing Virtual Reality as a Next Generation Anatomical Teaching Tool

The final section will focus on utilizing virtual reality for anatomical education. In the past the VHL has utilized virtual reality to create immersive VR scenes that showcase both anatomy and medical devices. This functionality has been tested by world leaders in anatomical education and expert physicians. While they believe that this can be utilized to advance anatomical education, they provide feedback on new functionality to improve our software's potential. These new functionalities will be discussed throughout this section. It is important to note that this qualitative feedback from expert educators has us confident in the educational efficacy of our platform and the next steps of this research is to perform quantitative studies into such.

In this section we will outline four new functionalities that were developed based on feedback from anatomical educators. First, we will outline a new form of locomotion in VR that we have defined as 'fixed spline navigation' that simplifies a user's movement in VR, allowing them to focus more on learning anatomy. Second, we will take a look at user relocation functionality in shared virtual reality environments that makes it easier for instructors to teach in VR. Next, we will outline anaglyph 3D functionality that is a cost effective alternative for teaching many people anatomy while using VR. Lastly, we will

describe new functionality that allows users to perform computational device deployments within VR, allowing for computational deployments to be done quicker and with more precise control.

Fixed Spline Navigation in Anatomical Virtual Reality Scenes: Applications for Learning Delivery Pathways for Medical Devices

Submitted to *IEEE Engineering in Medicine and Biology*, in review.

Alex J. Deakyne [1,2], Tinen L. Iles [1,2], and Paul A. Iaizzo [1,2]

[1] Department of Bioinformatics and Computational Biology, University of Minnesota, Minneapolis, MN

[2] Department of Surgery, University of Minnesota, Minneapolis, MN

Preface

The current navigational system in VR allows for a user to freely navigate throughout a scene. However, it can be difficult to master for new users. At educational outreach and conferences, users are given only a few minutes to test out the VR system. Unfortunately, sometimes users spend their entire allotted time determining how to navigate in VR and spend no time learning about the anatomy. Here, we present a simplified VR navigational

system that allows users to only move forward and backward along a fixed spline within the scene. This allows users to spend much of their time in VR focused on learning anatomy and not learning how to navigate through the scene.

This functionality was suggested by anatomical educators and physicians who used our VR platform. They believed adding this functionality would increase the potential of this platform to teach anatomy. I am responsible for developing this functionality with some assistance from Nick Karlovich. All authors helped in the preparation of this manuscript for publication.

Summary

The current navigation system of the VHL VR platform can be difficult for new users to learn – especially in a limited amount of time. We sought to simplify the navigation by allowing users to travel only along a fixed spline within the VR scene. This allows users to focus their time on learning the anatomy within the scene. We will explore this functionality by looking at an example of it within an anatomical scene showcasing a patient aorta for considerations of a transcatheter aortic valve replacement (TAVR) delivery.

Synopsis

Virtual reality is seeing wide uses in many facets of industry, medicine, and education. The medical field in particular has made advancements in visualization technologies

thanks to employing virtual reality. In conjunction with advances in computational 3D modeling, virtual reality has allowed for anatomical structures to be rendered in high details and viewed and studied in immersive 3D virtual spaces: which can make for more interactive and effective teaching tools. The Visible Heart® Laboratories has created various suites of virtual reality scenes which can be used to assist in the design of medical devices, training of future professionals, and educate users relative to human anatomical features. Yet, a current obstacle in many of these platforms are the user's lack of experiences in effectively navigating through complex virtual environments; e.g., causing them to spend more time learning how to move through the scene instead of learning the complex anatomy itself. Here, we present new functionalities for such a platform that allows for the implementation of fixed spline navigation: i.e., which restricts the user's movement to a spline, while still allowing a 360-viewing experience. This functionality drastically reduces the learning curve for navigating in virtual reality, enabling new users to focus on learning the given anatomy within the generated scene. Specifically, the technologies created are presented here for the case for enhancing the study models of a patient's aorta; e.g, to learn about the delivery pathway for a transcatheter aortic valve replacement procedure. The employment of these novel VR technologies may enhance the education experience in the training of both medical professionals and medical device innovators.

Introduction

Locomotion in Virtual Reality

Virtual reality (VR) can be employed as an effective educational tool due to the immersion and unique perspective it provides. To date, the Visible Heart ® Laboratories (VHL) has generated hundreds of virtual reality scenes of anatomical models for educational purposes [1]. While these educational tools have been described to have many benefits, use testing of them has also revealed multiple shortcomings; especially for first time users with little or no experience navigating in VR. Further, when we demonstrated our VR platform at conferences and educational outreach opportunities, typically each user only has a few minutes to utilize the system. Therefore, when an inexperienced user gets their turn in VR, sometimes it can take more than their allotted time just to learn how to navigate within the anatomical scenes. In other words, this is unfortunate because they spent the whole time trying to learn how to navigate in VR, instead of experiencing and learning about the high-quality anatomical models.

In most cases, the process of moving throughout a VR system incorporates artificial locomotion, since the user moves throughout the virtual space without physically moving; this is completed by using a button on the controller to initiate these movements. The method of using a handheld controller to control the movements of a user in VR is defined as avatar movement [2]. In the case of our developed VR platform, a user moves towards a given object in a given direction wherever the controller is pointing. Our use testing has determined this is the easiest way for most individuals to navigate throughout a virtual environment within our developed platform - even though it can take some users

several minutes to learn how to navigate well. For some time, it has been discussed that further reducing the complexities of navigation within our system would come at the price of restricting the user's freedom to navigate wherever they desire in these anatomical models. As a compromise, while this is not a best solution for all situations or generated anatomical scenes, introducing these functionalities for certain scenes (e.g., at conferences or educational outreach opportunities) would allow users with limited time, to better focus their attentions on solely the anatomies and less on learning how to move within VR.

In earlier developmental attempts, we had attempted to use scripted movements to completely control the user's interactions with a given scene. In scripted movement, the user moves throughout the scene along a predefined pathway, at a predefined speed, while having no control over their movement themselves [2]. While this removed the needs for the user to learn how to navigate, some users experienced induced motion sickness in VR; i.e., when they have no control over their own movements [3]. Multiple users who tested scripted navigation in our platform, noted experiencing motion sickness even when they hadn't before when using VR, so we decided to no longer use this approach and felt it was best to pursue a different solution.

Therefore, we decided the best way to simplify the navigation while reducing user exposure to episodes of motion sickness, was to constrain their self-initiated movements

to a generated spline; giving the user the ability to control the speed of their movements along the spline. For example, they can use the controller to move forward or backwards on the generated spline: note the splines are constructed to still allow for study to critical anatomical features. This greatly simplifies the required user experience for navigating in VR – allowing the users to focus more of their attention on the study of the anatomical models. Further, since the user decides how they move along the spline, they are now able to stop at a specific site along the spline to spend more time studying a specific portion of the anatomical model and not worry about how to proceed next. This has been identified by users as another huge advantage when compared to fully scripted locomotion where a user is unable to control their movement; often flying past anatomical features they would like to or should have spent more time exploring.

In addition to simplifying the navigation for new users, this functionality benefits scenes which can be especially difficult to successfully navigate through even for the experienced VR gamer. Scenes that require traversal through an artery or vein for a prolonged period have proved challenging for even experienced individuals who know such anatomies to navigate through. Without such spline technologies, often users were unable to stay within the given vessel for the entirety of the generated scene. It should be noted that when such happens, it is not always easy for the user to correctly find their way back within the vessel at any specific location. This leads to confusion and wastes a lot of valuable time, decreasing the educational opportunity of the VR platform. In this

paper we will utilize and explore an example of such developed detailed anatomical scene: i.e., utilizing developed fixed spline navigation in VR to explore a patient's aorta which is associated with the delivery pathway for a transcatheter aortic valve replacement (TAVR).

Transcatheter Aortic Valve Replacement

Transcatheter aortic valve replacement is a procedure for replacing the aortic valve of the functioning heart in a minimally invasive manner, using a delivery catheter with typical access through the femoral artery [4]. Today, these procedures require very large catheter sizes (some over 20 French) which can be clinically problematic for navigating all the way from the patient's femoral access up to their aortic root. In fact, described for the recent PARTNER clinical trial, around 15% of TAVR procedures had complications due to the patient's inherent vasculature [5]. These complications are often caused by irregularities in the patient's vascular anatomies such as excess tortuosity or an irregularly small diameter of the femoral or aortic arteries [6]. In such a case, alternative access sites can be explored [7]. In order to determine whether a patient has a suitable delivery pathway for a TAVR, in many cases 3D models of the patient aorta are created and analyzed [6]. Here, we will implement fixed spline navigation in virtual reality (VR) to explore one such patient's complex aortic anatomies. The generated fixed spline within the scene mimics the delivery pathway up to the aortic root and thus allows a given VR user to easily navigate through the aorta and study the nuances of this patient's anatomy.

Methods

The anatomical 3D models were generated using Mimics and 3Matic software from Materialise (Materialise, Belgium) after which the 3D models were then imported into Unity (Unity Technologies, San Francisco, CA, USA) to create the detailed VR environments for each 3D model, using previously described methodologies [1]. Next, we first needed to determine a methodology for creating a scripted path throughout the anatomical model in the VR environment; one that the user will be able to navigate bi-directionally along and allowing for 360 degrees of visualizations at each defined spline location. The easiest way to accomplish this is by utilizing a Bézier system. This system uses a chain of quadratic Bézier curves to create a path. Thus, our path was mathematically defined below; which was used to compute the locations of an object between any two anchor points defined within the scene.

$$B(t) = (1-t)^2 * P_o + 2t(1-t) * P_1 + t^2 * P_2, 0 \leq t \leq 1$$

Figure 34. Quadratic Bézier Path Equation.

To create the path in our scenes we utilized an existing Bézier path creator which helped abstract away some of the code for generating these paths within Unity [8]. This software package allows paths to be created consisting of anchor points and control points. Anchor points are defined as points along the path where the user will travel. Each anchor point has a corresponding control point that defines the curvature of the path passing through that point. Depicted below is a simple generated Bézier path in unity, defined by two anchor and control points.

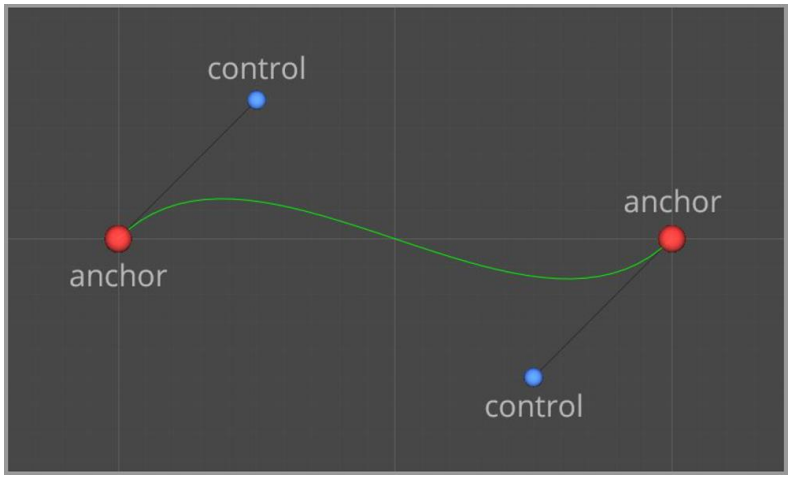

Figure 35. Example of a Bézier path in Unity depicting the anchor and control points required to generate said path.

Custom scripts were next developed that enabled the user to move along these paths in the virtual scenes. Upon entering a given scene, a script generates the equation that defines the path within a scene. Once this task was accomplished, another script spawns the user at the starting anchor point of the path. More custom scripts were then needed to allow the user to move along the path within the scene. In the normal navigation functionality of our system a user presses forward on the touchpad and they move forward in the direction the controller is facing. Simplifying that functionality here, when a user presses the top of the touchpad they move forward along the path and if they touch the bottom of the touchpad they will move backward along the defined path. This was managed by a script that defines a 'step' that we set. The step determines how far along the given path a user will move when they press on the touchpad. Naturally, the step was set to be relatively low, so that the user could smoothly traverse the path through the anatomical models.

Results

The developed code made it significantly easier to implement the new functionalities for fixed spline navigation within new or existing anatomical virtual reality scenes. As such a given path was created within a virtual reality scene containing an aorta model from an obtained patient CT scan. The path within the generated scene was defined to mimic the delivery pathways for the deployment of a TAVR valve within that patient; i.e. starting at the abdominal aorta and going superiorly to the aortic root. This allows users the unique experiences of traveling along the delivery pathway while have the abilities to critically assess and analyze this complex anatomy.

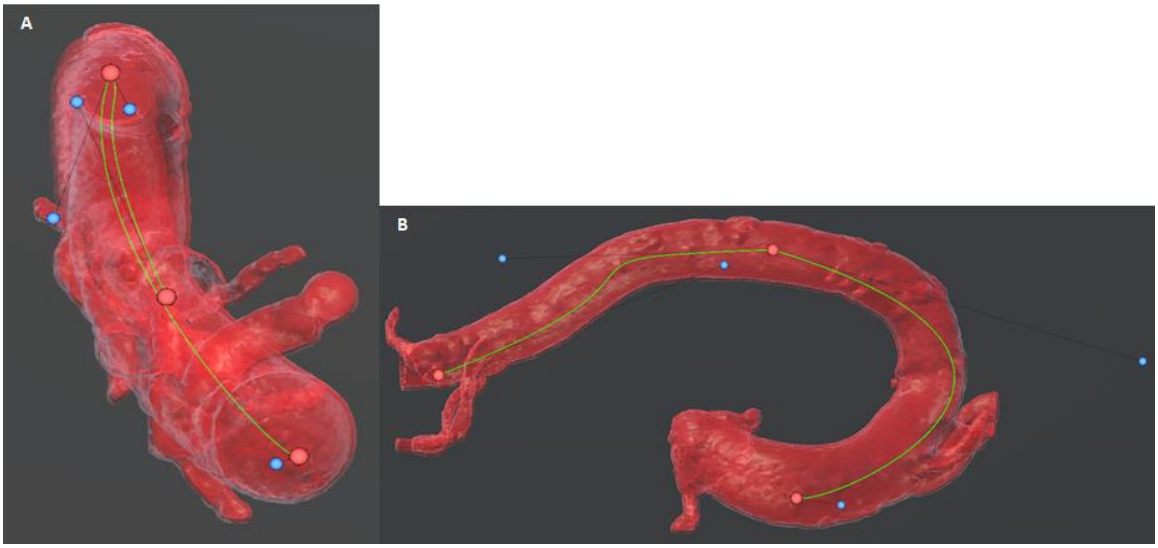

Figure 36. A 3D model of an Aorta with the user defined Bézier path shown in the (A) cranial and (B) lateral view within Unity.

When any user enters the scene, they start at the abdominal aorta and can navigate along the fixed spline defined by the Bézier curve. Since this implementation allows the user

control of how they move along the spline, they are free to stop and study the anatomy at a certain location or to go back to a previous landmark, which was not readily possible in fully scripted locomotion. Note, visually the computational spine path does not appear for the user when they are within the scene in VR, as to not to distract or obstruct their view of their anatomic study.

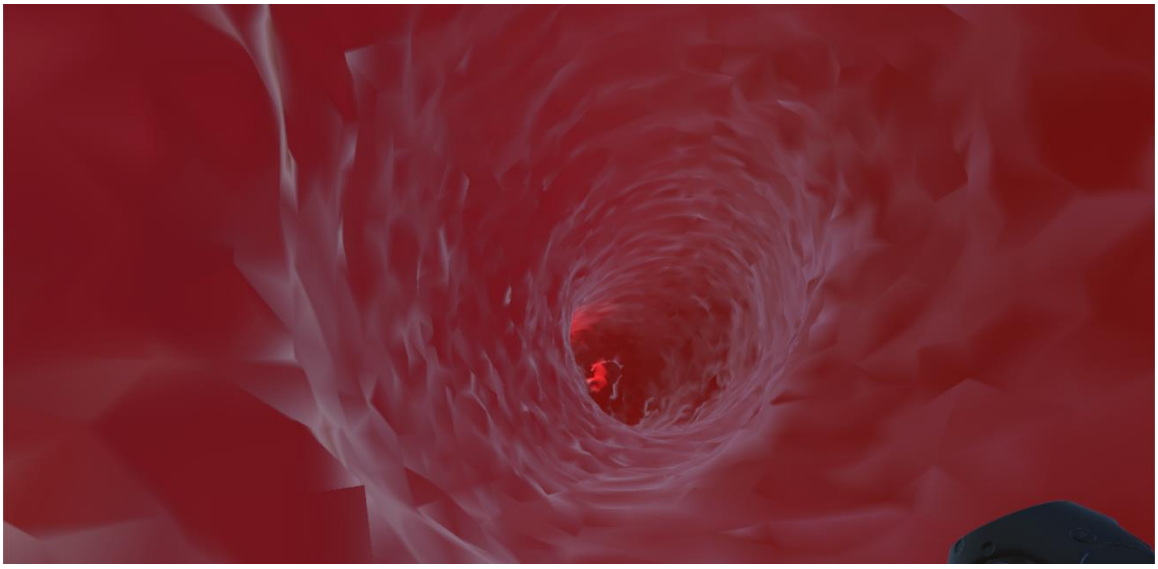

Figure 37. A VR user's view of the aorta model while navigating along the fixed spline. The VR user is currently in the abdominal aorta and moving towards the aortic arch and then the aortic root.

Discussion

Here we have demonstrated the abilities for fixed spline navigation to simplify the problem of locomotion in complex anatomical VR scenes. These generated navigation technologies allow for new users to focus their attention on learning complex human anatomies instead of how to move within complex VR scenes. Yet, since this approach allows the user to be in control of how they move along the spline in VR, they can in turn

stop at any defined spline location and focus on specific portions of the anatomy that interest them with a 360 degree vantage point. We consider here that this VR navigation approach offers numerous benefits, especially when users have limited time to experience VR; e.g., when utilized at a scientific conference or an educational outreach event for any age learner.

This VR navigation platform also assists in moving through complex or difficult to navigate anatomical models; such as shown here from the descending aorta to the aortic arch. Further, based on user feedback, tools such as this could be utilized to teach medical school students or surgical residents about the critical differences seen in real patient vascular anatomies. For the example discussed here, it offers the possibilities to critically learn the required delivery pathway for a clinical TAVR procedure within real patient anatomies, while being within an engaging VR immersive environment. In future studies, a given patient's vascular anatomies that were deemed not appropriate for a TAVR procedure could be modeled and explored with this platform to offer a unique and immersive experiences for learning more about clinically problematic anatomic features such as excessive vessel tortuosity. While for the case presented here, the patient anatomy was used to demonstrate the functionality of fixed spline navigation, no surgical decisions were made from such an experience as it was not the focus of the paper. Future work could involve using VR to study a generated patient's anatomic VR scene as a decision-making tool for pre-surgical planning.

It is important to note that fixed spline navigation functionality can be readily implemented into any of the anatomical VR scenes that our research team has created. The anatomical models of said scenes can vary anywhere from a normal heart model, heart models with congenital defects, a full cadaver model, or even include a myriad of medical devices such as coronary stents, pacemaker devices, or replacement valves. Many of these scenes have been detailed and showcased in our previous work [1].

Conclusion

Our generated software scripts allow for more precise controls for navigation with a complex, perhaps unfamiliar, virtual reality learning environment. Importantly, by restricting a given user's movements to a predetermined navigation line within a given anatomical scene, educators can create more precise, and potentially engaging learning tools. This allows any type of user, experienced or inexperienced, to focus on studying the anatomy without the challenges of navigating in VR, hopefully leading to increased educational outcomes. This navigation platform also allows the anatomical educators the abilities to help students focus on the most important anatomical features within the scene by creating custom splines that will direct the user to what they predetermined to be the important anatomical locations.

Acknowledgments

Thank you to everyone at Medtronic and the Visible Heart® Laboratories that assisted with this project. We also would like to thank the organ donors and their families for providing these critical research specimens for 3D model generation. Thank you to Nick Karvolich for his help with developing some of this functionality.

A Relocation Function for Augmenting Teaching in a Multiple User Shared Virtual Environment

Alex J. Deakyne [1,2], Tinen L. Iles [1,2], and Paul A. Iaizzo [1,2]

[1] Department of Bioinformatics and Computational Biology, University of Minnesota, Minneapolis, MN

[2] Department of Surgery, University of Minnesota, Minneapolis, MN

Preface

Since VR fully occludes the user's vision, it can make collaboration difficult amongst multiple users. Therefore, the VHL developed networking functionality to allow users to occupy the same virtual environment. While this functionality allowed for collaboration, it made it difficult for instruction as users were often unable to find the teacher within a VR environment. Here we introduced user relocation functionality that allows users to instantly teleport to the teachers position within the shared VR environment.

This functionality was developed by me and all authors assisted in the preparation of this manuscript for publication.

Summary

User relocation functionality assists anatomical educators while using this tool to teach anatomy. When the instructor wants the other users in the scene to look at something, the users can instantly relocate to the instructor's position within the shared virtual environment. This removed the large amount of time that was wasted waiting for users to find the instructor instead of learning the anatomy. In this chapter we will demonstrate this functionality within virtual reality scenes showcasing multiple users studying a human heart model and a full cadaver model.

Synopsis

Virtual reality platforms have dramatically both grown in popularity and uses over the past few years. Their critical uses as a teaching tool are currently being investigated; with promising preliminary results. While VR allows users to enter a virtual environment with unparalleled levels of immersion, there are some apparent limitations that arise when it is used as a teaching tool; primarily that it is difficult to achieve high levels of collaboration during utilization. As such, research has been done to develop shared virtual environments that allow multiple users to enter the same virtual space, represented by avatars, and interact with one another. However, these systems have additional drawbacks, i.e. it is difficult to find other users in a virtual environment. This becomes especially true in most teaching scenarios; for example, where an instructor desires to show students multiple noteworthy locations within the same anatomical environment. Here we propose a solution, an update to our current shared virtual reality anatomy

environments, that allows users to instantly relocate to the position of the instructor/proctor. This solution reduces the time needed in the virtual environment to direct students to critical anatomic features: i.e., when users are attempting to locate the instructor. In other words, this feature aids to maximize the time spent instructing and learning critical aspects of the immersive virtual reality environments: here we will focus on scenes utilized for teaching human anatomy.

Introduction

Virtual Reality (VR) requires a headset that completely obstructs the user's view of the outside environment and replaces it with a simulated one. This allows for the user to experience immersive virtual scenes. These technologies as they are applied to medical training have been used to immerse users in highly detailed anatomical models as tools to anatomic learning [1]. However, since the user's vision is completely obscured, it makes collaboration between multiple individuals within the same environment/system very difficult. To address such issues, we introduced previously networking capabilities which allow multiple users to share and study within the same virtual environments [2]. While this work in part addressed the problem of collaborating and providing anatomic lessons in the virtual space, user testing of the functionality by anatomical educators and physicians revealed that there were still needs for additional improvements.

One of the main benefits of this technologic platform, are the abilities for a teacher/proctor to instruct multiple students within a shared virtual space. Standing within an anatomical structure model, such as a heart, and pointing out the critical details of multiple anatomical features is truly unique and enriched immersive experience. Nevertheless, in large complex anatomical scenes where there are sectioned locations (e.g., chambers of a heart) it can be often difficult to keep numerous students together, when the instructor desires to move to a different location within the virtual space, so to highlight a different anatomical structure. The instructor is often very familiar with navigating in such a scene, but additional user are not: i.e., this can be a hard process for the novice students to navigate to a location in a virtual space they are unfamiliar with. In the scenario where a teacher is instructing students with little knowledge of the anatomy within the scene, this problem becomes exacerbated as all navigational landmarks within the scenes are parts of the complex and unfamiliar anatomy to the students. Early applications of anatomic scenes with multiple users was tested within our laboratory by both anatomical educators and physicians to gain feedback about their relative effectiveness, specifically as teaching tools. After hours of testing these initial functionalities, we received important feedback that it was often too difficult for users to find each other within these complex anatomical virtual spaces. For example, often, the given instructor wanted to show the students a specific part of the anatomical model, but the students had difficulty even finding the instructor; i.e., this wasted important educational time, that could have been spent learning human anatomy. In their opinions,

to improve the effectiveness of this technologic platform as a teaching tool, novel functionality needed to be added that made it easier for students to find their instructor in seconds within the shared virtual environments.

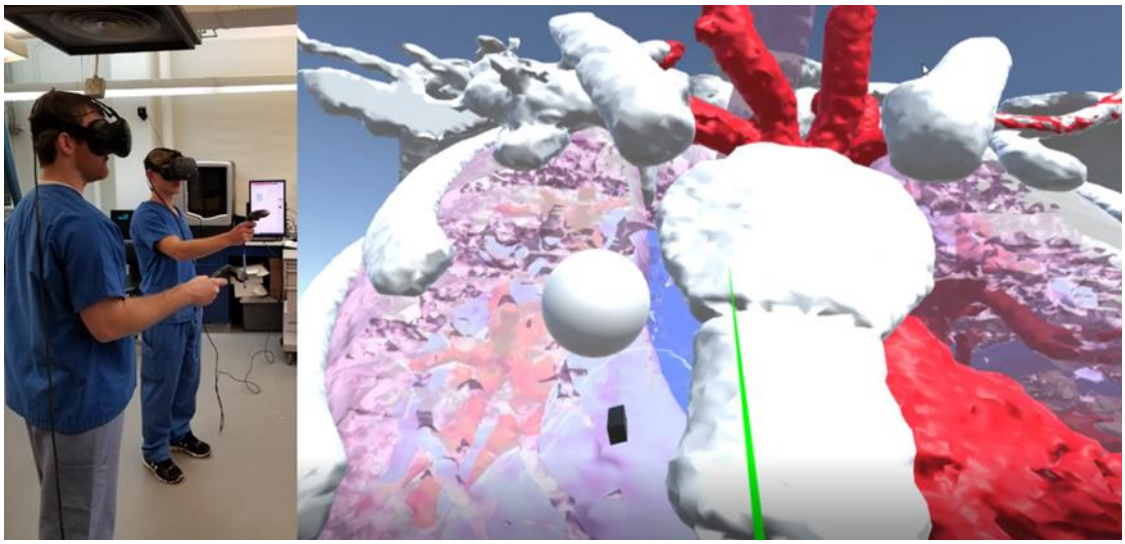

Figure 38. An example of an instructor and one student user navigating within the same shared virtual reality environment; studying an anatomical model depicting a fully modeled thoracic cavity and its contents. While the users are in the same room, all the necessary information is processed over the network. The VR image shown is from the perspective of the student and the instructor's avatar can be clearly seen in their line of sight.

A novel and yet very simple solution to this problem was to allow the instructor to control the movements of all users within the scene. The instructor could navigate freely around the virtual environment, and all the students would see the exact same thing that the instructor is seeing. While this would prevent students from getting lost in the scene, it would also restrict one of the major benefits of these anatomical virtual environments: the abilities for students to explore the models to learn more about the anatomy becomes

limited. Therefore, we needed a solution that helped students navigate and find the instructor in a virtual environment without restricting their abilities to independently navigate the environment; yielding an enhanced experience as they described such.

Upon our initial design of the system, we utilized an avatar feature so to represent each user in the virtual space; these were made relatively small so to not obstruct anatomic features of a scene. In other words, this ensured that at no point would a user be in a position where their view of an anatomical model would be obstructed by the avatar of another user. This design worked great when users were standing next to each other in the virtual environment or independently exploring the anatomical models. However, this introduced a new user problem that severely impacted the abilities to collaborate and instruct others. If users were not next to each other it was incredibly difficult for users to find each other within the complex anatomical models. While increasing the size of the avatars would make it easier for users to find each other within the virtual environment, once they were close together the large size of the avatars would obstruct the views that all users had of the given anatomy.

The size of the user’s avatars also makes it difficult to keep track of other users while moving. If an instructor is utilizing this tool to teach anatomy to students, they will likely move to many different locations within the anatomical model. Initially we had the users attempt to follow the instructor's avatar as they navigated to a new anatomical site. This

often resulted in one or more students losing track of the instructor and it often took a long time before the user was able to find the instructor; wasting precious time which could have been used to learn anatomy. The students were chasing the instructor and not learning or taking time to inspect anatomic features. Further with this VR approach, since the syncing of all user locations occurs over the internet, an unstable internet connection can also reduce the fluidity of an individual user's movements. It was concluded that in general it was a nearly impossible task to follow a instructor in the scene, if their own movements were choppy due to a taxed internet connection.

Therefor in order to facilitate the instructor's ability to teach students in these types of complex anatomic virtual environments, while also addressing the problems previously discussed, we developed code that allows users to immediately relocate to the current location of the instructor within the shared virtual environment. After, many iterations of technological solutions, we deemed this to be the most elegant solution to the aforementioned problems; i.e., for several reasons. First with this feature, the user's avatars can remain small since users will not need to track the instructor from great virtual distances. Additionally, when the instructor desires to navigate to a new location within the scene, they no longer need to help or wait for all the students navigate to the desired location. Instead, the instructor can quickly navigate to the desired location (critical anatomical feature) and then have all the students immediately teleport to the instructor's location by the simple press of a button. This allows more time spent within

the shared virtual environment to be focused on learning the anatomic lesson instead of being lost in the virtual reality.

Methods

The virtual reality environments with the base networking functionality was created using the same methodology as previously reported [2]. Incorporating functionality that enables a user to relocate to the instructor's location sounds like a deceptively simple problem to solve. Yet, the complexity of this task becomes great because the feature needs to happen over a network server. Yet, adding the functionality of one user teleporting to the location of another object locally (one user in one environment), can be a rather straightforward task for anyone who does VR development within Unity (Unity Technologies, San Francisco, CA, USA). We are going to first explore how this is accomplished before moving onto the complex step of performing these tasks over a network with multiple users.

Every object in a generated local virtual environment, including the user, has a transform (the current location of an object and the direction it is facing within the environment) associated with it. Using custom scripts, we can create a method that looks up the transform information of the object that we want the user to relocate to. Since this is in a given local environment, one can do this when the scene is created, and the transform information is then saved as a variable within our script. One can then use another script that will set the user’s transformation to be the exact same as the transform information

of the object. By doing so the user instantly relocates to the same location of the object. For scene applications, one can tie this relocate method/feature to be executed when the user presses, for example, the back-trigger button on the VR controller. This allows the user to freely navigate through the scene and then easily relocate to the object's location whenever they desire.

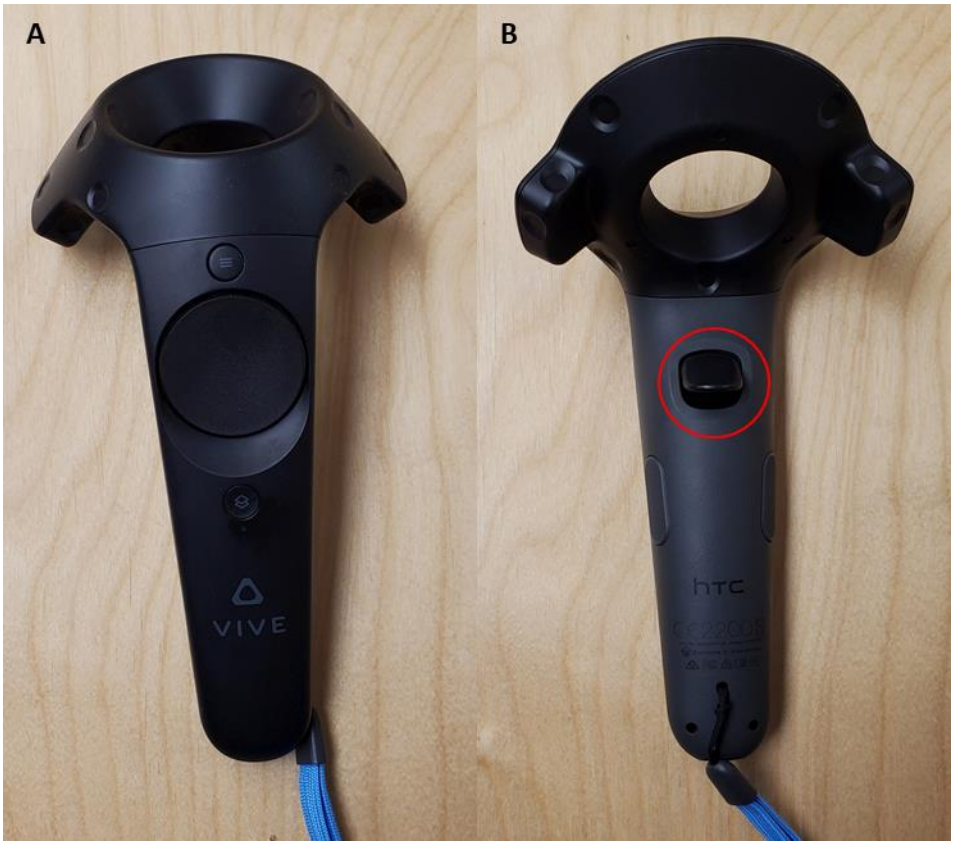

Figure 39. A picture of the (A) front and (B) back side of the utilized VR controller. The back trigger on the controller has been highlighted with a red circle.

Unfortunately, the use of this solution becomes much more complex when one wishes to accomplish this over a network connection with multiple users within a shared virtual scene. For example, when we were syncing multiple users over a network, we were no

longer able to reference objects directly. Therefore, the complexity of our final solution was more significant for two main reasons: we are teleporting to another user's location (which can be constantly changing) and we are performing these actions over network(s) and not locally within a given program.

In a shared virtual environment, every object that we want to be referenceable to the users on the network must be instantiated (created/updated) onto the network server itself. This is because one wants to ensure that anytime any of these objects are changed or manipulated, this happens for all users in the shared virtual environment. Otherwise, things would change for some users and not for others, defeating the purpose of a shared virtual environment since the environment will look different to each user. Whenever a user joins the server, or a new object is created that is interactable, one must instantiate that object onto the server and set up its network state properties as previously described [1]. This ensures that this object will be synced across the server for all users.

The server is created as the first user enters the shared virtual environment. The network state of the first user to join the environment is updated to be the server user. Every user that joins the environment after that, is then referenced as a client and given a unique ID token. This is incredibly convenient for us because we can always directly reference the instructor’s avatar by looking up the server object, since the instructor will always set up the virtual environment for their students. When we instantiate the instructor’s avatar

onto the server, we now need to create another state that contains their transform information within the virtual environment. This network state is constantly updated to match where the instructor is and, since this transform state is instantiated on the network, it is now something that can be referenced by all other users who are in the shared virtual environment. If we did not create the transform as a network state, then the other users in the shared virtual environment would not be able to access this information on the network.

After this hook was placed on the instructor's transform information, and that state is permeated onto the network, we needed to then create a method for the other users/clients/students to obtain this information from the network. When a student joins the virtual environment and is instantiated on the network as a client, one then attaches a new network state to that user that contains the necessary scripts required to get the current transform information of the instructor. For example, this method can be executed by any client in the environment by pressing the back-trigger button on the controller. When this operation is called by a student, it looks up the state information of the server/instructor user. Once it has access to the state information of the server user, it returns the current transform information of the instructor. This information is then sent back to the student across the network. Once the student receives this transform information from the network, its own transform network state is updated to be equal to the server's network state. Since in this approach we are accessing and updating each

user's network transform state information, the updates for any server or client are synced for all users in the shared virtual environment. A diagram showing the execution sequence for a student relocating to the instructor's location in a shared virtual environment is shown below.

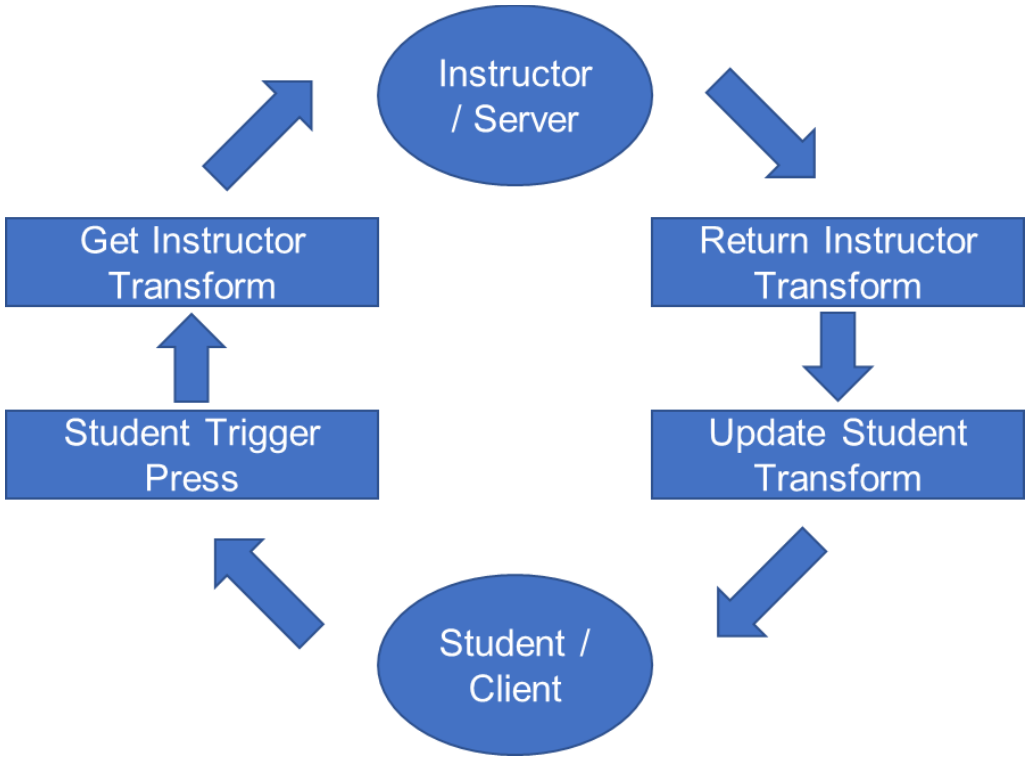

Figure 40. A diagram depicting the needed steps that occur within the network when the student presses the trigger button to relocate to the instructor's location. As stated earlier, a given student is representative of a network client and the instructor as the network server.

Results

Many unique, but detailed scenes were created for anatomical instruction with the capability of shared virtual environments with user relocation functionality. First, we will look at a simple approach where an instructor and a student are both in a computational model of a human heart; with their intentions of reviewing anatomical features. The instructor and student begin the lesson in the left atrium and were interested in first reviewing the mitral valve anatomy. The mitral valve is a bicuspid atrioventricular valve that separates the left atrium and the left ventricle. More functional anatomical information about the mitral valve has been covered in detail elsewhere [3, 4]. In this case, the instructor began by pointing out the locations and then explaining the anatomic features of the mitral valve annulus and the structure of the valve leaflets. To further explore the anatomy, the instructor then navigated down to the left ventricular apex and view the mitral valve from that perspective. Typically, it is considered that the student is unfamiliar with cardiac anatomy and with navigating in VR. Therefore, the instructor navigated to the left ventricular apex, and notified the student once they are in place. The student was then able to simply press the back-trigger button on their VR controller to immediately relocate to the current position of the instructor. From here, the instructor was able to discuss with the student more about the complexities of the mitral valve anatomy, highlighting the papillary muscles and the chordae tendineae.

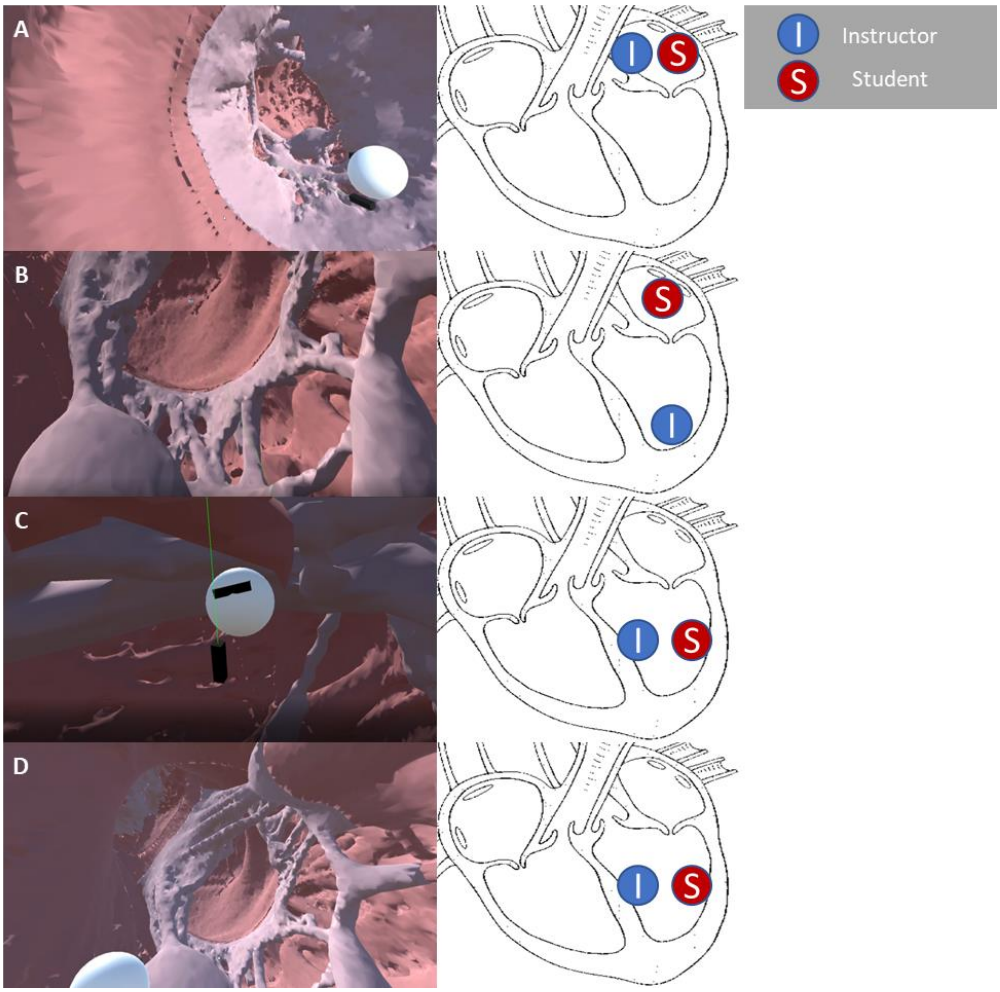

Figure 41. An example of the user relocation functionality in a VR scene of a human heart. For each step of the process, we depict the VR user's view along with a simplified graphic showcasing where each user is located within the heart. (A) VR view of an instructor and student that were standing in the left atrium studying the mitral valve anatomy. Next, (B) the instructor navigated to the left ventricular apex while the student remained in the left atrium. (C) The student presses the back trigger on their controller and instantly relocates to the instructor's position in the left ventricle. (D) Now, both the instructor and student are in the left ventricle where they continue studying the mitral valve anatomies from the new location.

While relocation functionalities can be clearly described and helpful in the previous example, in such there were not many obstacles or complex anatomies to traverse from one location to another, which is typically not the case if detailed anatomical representations are utilized. In the next example, we have incorporated the relocation functionalities into a shared virtual environment containing a partially modeled human cadaver generated from MRI and CT scans; even is this partial model the anatomical knowledge needed to navigate within is exponentially greater.

To begin within this more complex VR scene, the instructor and student start at the head of the cadaver model and were next analyzing the spinal column as well as the carotid arteries and jugular veins. Next, the instructor wanted to teach the students in the virtual environment, about the locations and anatomies of the liver and hepatic vasculature. While not discussed here, the anatomies and functions of the hepatic organ system has been covered extensively elsewhere [5]. If a given students had little anatomical knowledges of these internal organ systems, it would be challenging to instruct them how to navigate to the liver from the spinal cord for example. Further, it would be even more difficult for someone to follow along tortuous pathways for in and out of organ structures while in such a shared virtual environment (as discussed previously). Hence, in these situations, the relocation functionality can be incredibly useful due to the large sizes and complexities of a multi-organ anatomical model; i.e., within this shared 3D virtual environments. In another approach, the instructor can tell the students to follow them to

the liver, and if any of the students get lost along the way, they can simply press the back trigger on their controller and instantly relocate to the location of the instructor. In this example, the students relocated to the instructor's position within the liver where they can now learn about the hepatic vasculature in an immersive and collaborative environment.

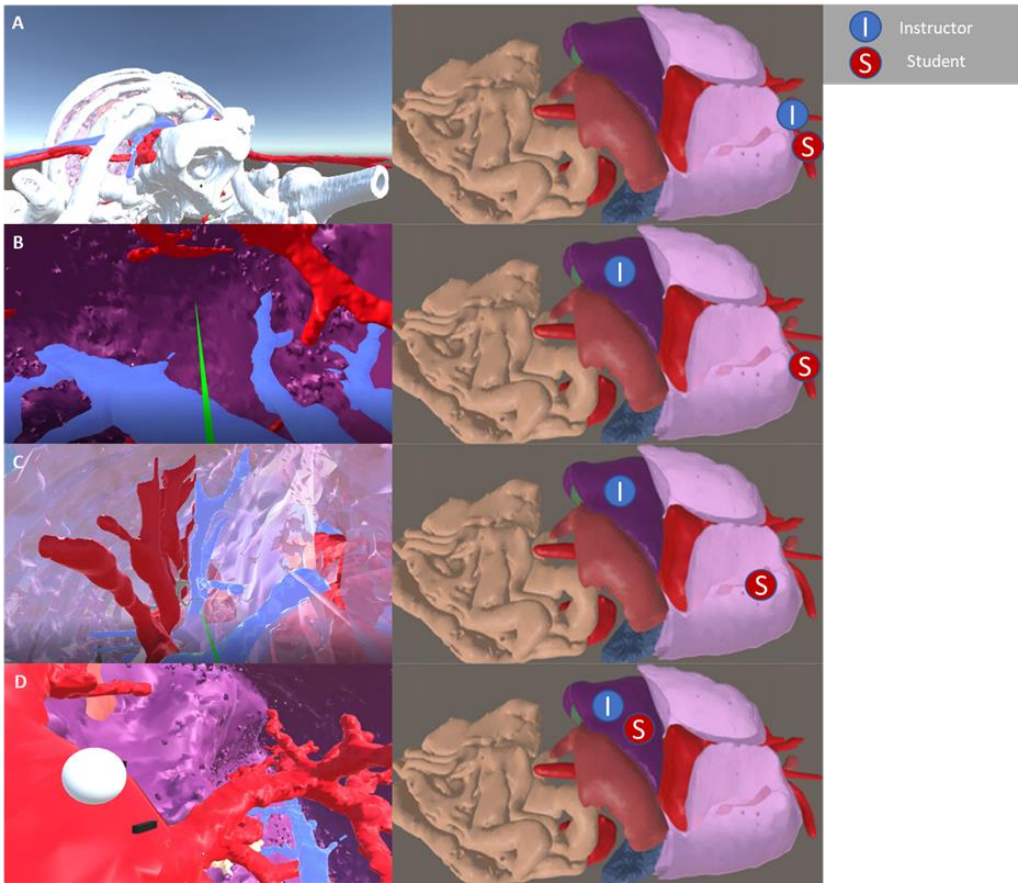

Figure 42. An example of the user relocation functionality in a VR scene of a human cadaver model. For each step of the process, we depict the VR user's view along with a simplified graphic showcasing where each user is located within the scene. (A) The instructor and student were studying the carotid arteries and jugular veins. (B) The instructor then moved quickly, due to her or his understanding of 3D human anatomy, to inside the liver. (C) The student attempted to follow the instructor to the liver but, due to their unfamiliarity of 3D human anatomy, got lost inside the lung and were unable to find the liver. (D) Instead

of wasting time attempting to find the instructor inside the liver, the student was able to instantly relocate to the instructor's position. The instructor and students can now readily begin to study the hepatic vasculature from this new location.

Discussion

In this chapter, we discussed the development of a VR relocation feature to quickly link individuals within a complex anatomical VR scene to a given location. This allows the instructor to have some control of their student's location in a complex VR environment, hopefully making the process of teaching anatomy easier, while still giving students the freedom to explore these scenes and study anatomy independently. In the examples provided here, it was illustrated that even though the implementations of our solutions requires complex networking code, the execution of the functionalities from the user standpoint is as easy as pressing a single button of the VR controller. In addition, the students only need to access the transform location of the instructor when they want to relocate to their position, reducing the amount of information streamed through the network in our application, allowing for smoother experiences for all users. As with the rest of the functionalities added in the Visible Heart ® Laboratories VR platform, this relocation feature can be added to any scene displaying any anatomical model within our VR database; which currently is in the hundreds [1].

Here we only highlighted two anatomical examples since the focus here was to specifically describe the nuances of the user relocation functionality. Nevertheless, there

are many or endless possibilities for the applications in which this technologic approach can be applied. This approach could be used by an anatomical expert (anatomist or physician) to help teach the complex anatomical features of heart defects. Further, this approach could have applications in pre-surgical planning, where a given physician and their clinical care team can walk through the detailed anatomies together. Additionally, this can be used by a team of medical device designers, to navigate through the device tissue interfaces utilizing computational models in virtual reality. All of these scenarios have been discussed in more depth in previous work [1,2].

The current implementation of the relocation methods teleports a student to the location of their instructor, in the virtual environment. This was developed - by request of the anatomical educators and physicians who have been utilizing and testing our ongoing system developments; i.e., to improve networking functionalities of our developed anatomical teaching tools, since too much time was often wasted trying to get a group of students to the same locations, within our previous iteration. As a solution, it is now possible that the users can all teleport to the location of their instructor as desired. Note, since all users who join the network are assigned a unique ID, we can reference that ID in our code to find the transforms of a given user instead of looking at the server user's transform.

These developed VR implementations can accommodate many, all, users within the same shared virtual environment. While there is currently no limit to the number of users that can join the scene, it should be noted that the overall performance of such a system can have an inverse relationship to the number of users. For example, every user added into the system increases the amount of information that needs to be transferred across the network to continuously synchronize the locations of every user in a complex geometric shared virtual space. As such, multiple users can decrease the smoothness of the experiences for all users, as desynchronization can be more common.

Conclusion

Here we have demonstrated a computational approach that simplifies the processes of teaching complex human anatomies in a shared virtual environment, by allowing students the abilities to instantly relocate to the location of their designated instructor. The complex networking code required to enable this has been consolidated into a simple and elegant solution for the end users. These processes reduce the times spent waiting for all users to navigate to a given VR location, which can be especially difficult when users are unfamiliar with the complex anatomies within a generated scene or on the other hand with how to navigate in VR. Therefore, this in turn maximizes the time spent by a group of individuals in teaching/learning complex human anatomy. This ultimately yields more control of the experience to the instructor, without hindering the student's abilities to independently navigate the virtual anatomical scenes, if desired, on their own.

Acknowledgments

Thank you to everyone at Medtronic and the Visible Heart® Laboratories that assisted with this project. We also would like to thank the organ donors and their families for providing these critical research specimens for 3D model generation.

Development of Anaglyph 3D Functionality for Cost-Effective Virtual Reality Anatomical Education

Accepted to *Computing Conference 2021*, awaiting publication.

Alex J. Deakyne [1,2], Thomas Valenzuela [2,3], and Paul A. Iaizzo [1,2,3]

[1] Department of Bioinformatics and Computational Biology, University of Minnesota, Minneapolis, MN

[2] Department of Biomedical Engineering, University of Minnesota, Minneapolis, MN

[3] Department of Surgery, University of Minnesota, Minneapolis, MN

Preface

The previous chapter of this thesis focused on using multiple VR setups to allow users to enter the same virtual environment. However, this is an expensive solution and is often not logistically possible. This is especially true in an academic setting where there is not

enough money in the budget to buy multiple VR headsets and computers, or in large lecture scenarios where hundreds of students are gathered to learn about anatomy. Here we present a cost-effective solution for teaching anatomy using anaglyph 3D functionality.

This functionality was developed by me. The computational models and VR scenes were developed by Thomas Valenzuela and me. All authors contributed to the preparation of this paper for publication.

Summary

In this chapter we detail the development of anaglyph 3D as a cost-effective virtual reality anatomical teaching tool. In academic settings where it is not feasible for every user to have their own VR headset and computer, a cost-effective solution was required. The anaglyph 3D functionality allows the VR user's view within an anatomical scene to be broadcast on an external display with anaglyph 3D shading. This shading allows other users to wear cheap anaglyph 3D red/blue glasses to gain a 3D effect of the VR user's view. This functionality preserves the 3D relational information that is crucial for a proper understanding of anatomy.

Synopsis

Virtual reality (VR) is rapidly becoming more widely available and accessible as a technology due to the affordability of cheap computing power. This has made it possible for virtual reality systems to capture audiences in industry and education, as well as for

personal use. Currently, a major limitation of VR headsets is that the user's vision is completely occluded, making it difficult for them to interact with others. While this can be solved by having a VR headset and VR capable computer for each user, this becomes much more expensive and, often, an unrealistic solution. This becomes even more problematic in an educational setting since it is difficult for the given instructor and large groups of students to have a shared learning experience. Here, we have developed anaglyph 3D functionalities into our Visible Heart® Laboratories' anatomical virtual reality platform. These functionalities augment what is viewed by the virtual reality user with a custom anaglyph shader which in turn projects it to an external display. This allows a multitude of users to wear anaglyph "red/blue 3D glasses" and view the same anatomies the VR instructor is viewing in VR, while preserving the important 3D anatomical spatial relationships.

Introduction

3D modeling of human anatomical features and subsequently, virtual reality (VR), are seeing increased use in the medical field. These 3D anatomical models have provided increased educational outcomes when learning anatomy [1]. Additionally, they have been deemed beneficial when used for pre-surgical planning and/or clinical teaching [2]. In addition to this, various forms of virtual reality have been shown to help with medical education [3]. The Visible Heart® Laboratories (VHLs) has also developed a virtual reality platform to take advantage of these technologies so to create an effective combined anatomical and medical device teaching tool [4].

Within our Visible Heart® Laboratories virtual reality platform, the camera view is seen by the virtual reality user while it is also outputted to an external display. This is a distorted 2D viewpoint of the immersive 3D environment seen by the VR user. While this allows bystanders to get a glimpse at what the VR user is seeing, it is considered suboptimal, because it removes them from the rich 3D anatomical information that is retained within the VR environment; which is considered critical for optimizing ones understanding of complex anatomical features. Therefore, we highly recommend/encourage all our users to experience these device/tissue scenes within virtual reality.

Unfortunately, there are few scenarios where it is possible for large numbers of users to engage with our VR platform. For example, when this educational approach has been used at many conferences and outreach opportunities, one user is in VR at a time for several minutes and many bystanders are watching the external display (see figure below). Yet, even when a crowd watches someone use the VR system, it often stimulates innovation and collaborative ideas, due to the uniqueness of the anatomical and medical device models displayed. Nonetheless, we as educators want functionality in our platform that enhances the experiences of the bystanders; to fuel even more beneficial understanding and collaboration.

Figure 43. The standard setup of our VR platform demonstrations at conferences. One attendee uses the VR system to explore anatomical models and what they are seeing is projected as a distorted 2D view on an external display. Meanwhile, other attendees watch and discuss what they are seeing on the external display.

While work has been done to create shared virtual environments with multiple users within our VHLs' platform, it is not always an ideal solution [5]. Typically to do such, each user in the VR space requires their own VR Headset and their own VR capable computer. Thus, the entry cost is upwards of $2,000 for each user. While this price could be acceptable for small teams in an industry setting, it loses its feasibility when we shift into academic settings - especially when attempting to instruct larger groups such as at a conference or undergraduate students in anatomy classes.

To address this problem, we developed low cost functionalities that offers bystanders not using the VR headset an experience that still preserves some of the crucial 3D anatomical

information available in VR. Here we present the utilization of anaglyph 3D functionalities within our VR platform. Anaglyph 3D is the '3D effect' that encodes each eye's image with different colors, traditionally red and blue, allowing for a 3D perspective to be obtained from 2D images; i.e., by utilizing standard red/blue 3D glasses. We applied a custom anaglyph 3D filter to augment what the VR user is viewing. This anaglyph view is outputted from Unity to an external display; allowing bystanders to wear inexpensive anaglyph red/blue 3D glasses and concurrently experience 3D representations of what the VR user is seeing.

Figure 44. Traditional red/blue anaglyph 3D glasses.

In this manuscript we will discuss the methodology we employed for creating these Anaglyph 3D virtual reality scenes. In addition, we describe the types of scenes created and the various ways in which they have been used for anatomical education. Finally, we note our planned next steps for this research which includes conducting user surveys to obtain quantitative data about the values of these methodologies for teaching anatomy when compared to traditional methods.

Methods

The base version of Unity (Unity Technologies, San Francisco, CA, USA), which is used to develop our VR platform, currently does not allow a filter such as anaglyph to be applied directly to a camera; this made it essential for us to develop our own custom anaglyph filter. This was completed by developing custom anaglyph shaders to be used within our virtual environments. A Unity shader is a custom function that determines how each pixel of an image or surface is rendered. Since anaglyph functionality requires the image from one eye to be rendered in red and the other to be rendered in blue, we created a script that contains two shaders. One shader renders the right eye view with a red tint and the second shader renders the left eye view with a blue tint.

Unity only allows us to output a single camera view in Unity to our external display. Traditionally - in our VR platform - the camera view output to the external monitor is the VR camera that captures what the VR user is continually looking at. The VR camera is a representation of what is seen in the right and left eye of the VR headset. This presents a challenge because it prohibits us from applying our anaglyph filters directly to the VR camera views. If we did this, the VR user would have a highly distorted view because the image going into their right eye would be tinted red while the image going into their left eye would be tinted blue. This required us to add two additional cameras within Unity that mimics exactly what the VR camera within Unity is seeing. We attached a right eye and left eye camera as ‘children’ of the VR camera (with a slight offset between them to

account for the offset between the right and left eye). Since these cameras are children of the VR camera, they will always show exactly what the VR user is looking at.

Two camera views cannot be exported from Unity to an external display. Consequently, we had to develop a way to merge the views from the two anaglyph cameras within Unity. This was accomplished by placing a quad (a 2D rectangular object in Unity) in the virtual environment, but outside the rendering distance of the VR camera; ensuring the VR user would never see it. We set the two anaglyph cameras to render their view, with their respective anaglyph shader, onto this quad. This results in the quad successfully rendering an anaglyph representation of the VR user's view; which is what we desire as the output to our external monitor.

Thus, we need a camera to capture the live rendering of the anaglyph view on the quad. A final camera, the output camera, was added to the virtual environment to capture the live anaglyph rendering on the quad. The output camera is exported to the external display. This solution allows the view of the VR user to be output to an external monitor with an anaglyph filter, offering a 3D representation of the VR user's view to any bystander utilizing anaglyph 3D glasses. A Unity workspace of one of our anaglyph scenes depicting this setup is displayed in the figure below.

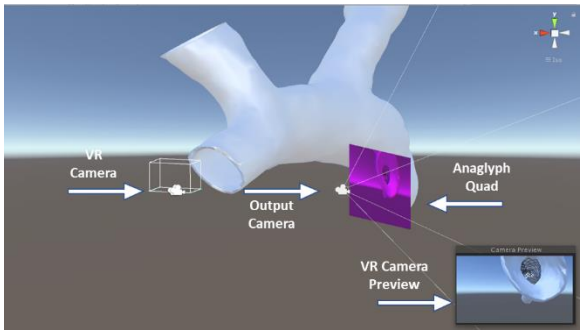

Figure 45. Unity workspace showing the anaglyph quad which displays the anaglyph rendering of the VR user's view. The output camera, which will be displayed on the external display, captures the anaglyph rendering on the anaglyph quad. The view of the VR user, displayed in the bottom right corner of the figure, shows that the VR user's view is not affected by the anaglyph filters.

Functionality to have the external display switch between showing the normal view of the VR user and the augmented anaglyph view was also developed. This was accomplished through a custom script that toggles whether the anaglyph shaders should render the corresponding pixels in anaglyph filters or not. Within the VR environment these two modes can be seamlessly toggled on and off by simply pressing the interface computer's spacebar.

Results

Anatomy and Medical Devices Anaglyph Scenes

The VHLs has added anaglyph functionalities to a wide range of anatomical and medical device virtual reality environments - scenes. Presented here is a human heart 3D model created from a magnetic resonance imaging (MRI) scan of the heart. The heart has been enlarged in size to allow the user to fly throughout the heart to better understand the

nuisances of the internal anatomies. This allows users to gain a new perspective of the detailed human heart anatomy as well as gain a better understanding of the 3D spatial relationships between anatomical features; since the anaglyph functionality preserves the 3D information viewed within VR. To date, this scene has been a staple of our educational platform for teaching the complex anatomies within the human heart.

We have also created many anaglyph scenes that showcase both anatomical features and incorporated medical devices. One such example is of a Medtronic Micra™ transcatheter pacing system (TPS) (Medtronic, Minneapolis, MN, USA) in the process of deployment within a human heart model. In this scene the Micra was prepped for deployment in the apex of the right ventricle. These anaglyph scenes help users understand the complexities of the various device tissue interfaces. In addition, users can study the details of the delivery catheter and delivery pathways of such systems within unique and complex human anatomies.

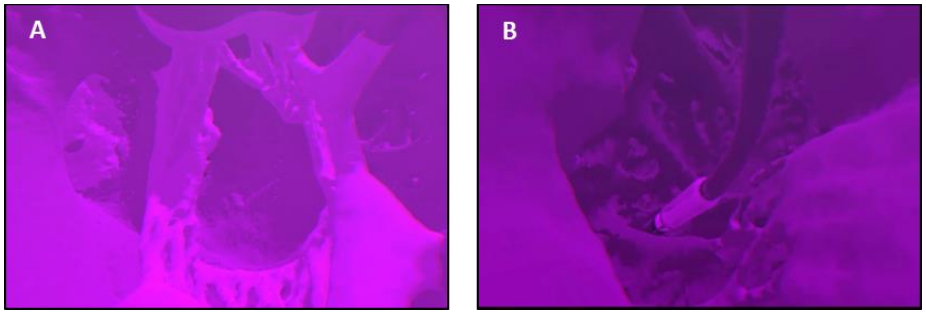

Figure 46. (A) An anaglyph view of a VR user moving inside an enlarged human heart model. The VR user is standing in the left ventricular apex of the heart and looking up at the aortic and mitral valves. (B) An anaglyph view of a VR user standing in the tricuspid valve annulus within a human heart model. The user

is looking toward the right ventricular apex where a Medtronic Micra is set to be deployed. If you view these images with 3D glasses, you will gain a 3D perspective.

Our lab continues to work closely with many physicians who are subject matter experts on many cardiac device placements, including bifurcation coronary stenting. Further, many of these physicians have visited the Visible Heart® Laboratories where they have performed device placements: e.g., bifurcation stenting procedures within reanimated swine hearts [6]. Further, these hearts and the deployed stents were later microCT scanned and computationally 3D modeled. These bifurcation stent models were then placed into virtual VR environments with anaglyph functionalities. Many videos of these anaglyph virtual reality scenes can be viewed for free on the "Atlas of Human Cardiac Anatomy" (http://www.vhlab.umn.edu/atlas/) [7].

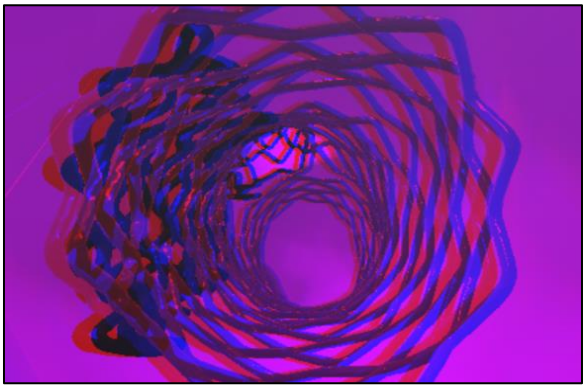

Figure 47. Anaglyph view of a VR user inside a coronary artery where a crush bifurcation stenting technique was performed. Again, if you view this image with 3D glasses, you will gain a 3D perspective.

Education and Conferences

This anaglyph VR functionality has been utilized by the VHLs to teach anatomy in the undergraduate physiology lab courses at the University of Minnesota. For such, an

instructor using virtual reality navigated through multiple anatomical scenes to showcase the complexities of human cardiac anatomy. As the instructor showcased the anatomy, over 90 students at a time watched the anaglyph rendering of the instructor's educational journey, allowing them to learn with a 3D representation of the anatomy.

Figure 48. Instructor utilizing VR with anaglyph functionality to simultaneously teach 90 undergraduate students anatomy at the University of Minnesota.

This anaglyph functionality approach has also been used at many conferences. As with our original VR platform, it is common for one conference attendee to use the VR system at a time. Often, a crowd of bystanders gather to watch what the VR user is doing and to await their turn to use the system. Now, we encourage the bystanders to grab and wear the anaglyph glasses to gain the 3D perspectives of the anatomical scenes; so to gain better understandings of these unique 3D models before they enter them themselves within virtual reality. This unique and immersive experience has helped us fuel discussion and collaboration between conference attendees.

This anaglyph functionality has also been used during the recent SBHCI Bifucation Summit conference hosted from San Paulo, Brazil. While this conference was entirely virtual, we were still able to use this as a teaching tool. Conference attendees were mailed a pair of anaglyph 3D glasses prior to the start of the conference. Virtual reality scenes were created that showcase 3D models of bifurcation stenting techniques. These models were obtained by reconstructing micro-CT scans of hearts with bifurcation stents deployed in them. During a conference session, the anaglyph rendering of the VR user was broadcast to the conference attendees. As the instructor analyzed the bifurcation stenting models and their interaction with the coronary artery model, users across the world were able to wear their anaglyph glasses and view a 3D representation of the device tissue interfaces between the various coronary anatomies and the stent 3D models.

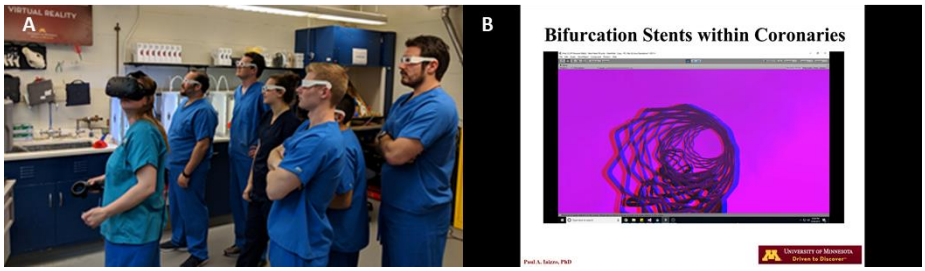

Figure 49. (A) A VR user explores anatomical scenes while bystanders wear anaglyph 3D glasses to get a 3D representation of the anatomical VR models displayed on the external monitor. (B) Conference slide showing anaglyph videos to conference attendees. In this video we have a VR user navigating through the coronary arteries where a bifurcation stent has been deployed within a coronary artery.

To date, we have not conducted formal quantitative assessments of the relative educational effectiveness of these methodologies. However, we have obtained a plethora

of positive qualitative data: i.e., the anatomical educators and expert clinicians worldwide that have used this system believe it to be a superior method of teaching anatomy when compared to traditional methods. This, along with the evidence of the benefit of VR for medical education shown by other investigators gives us confidence that these are superior teaching methodologies when compared to traditional means for anatomical education [3].

Conclusion

This work continues to build on the increasing use of virtual reality by our VHLs for medical education; which has been shown to increase educational outcomes primarily due to the preservation of the 3D spatial information of complex anatomical features. Our work aims to increase the breadth of VR tools for educational purposes by enabling more users to simultaneously have increased benefit while observing a user in VR. While multi-user VR environments have been created, it is often not a realistic solution because of the expensive entry cost.

Here, we have proposed a unique solution to this problem which enables cost-effective functionalities for allowing multiple users to take advantage of the benefits of virtual reality for teaching human anatomy through unique 3D anatomical models. The employments of anaglyph functionalities allow for the output displays to render anaglyph 3D representations of the complex anatomical models including device/tissue interfaces. This offers richer experiences to viewers/students; i.e., while preserving the critical 3D

anatomical information. Such an anaglyph output can be utilized on any 2D display, including large screen TVs and projectors, allowing for easy integration into any classroom or even using within virtual conferences.

Future work involves creating a study to gain a better, quantitative understanding of the effectiveness of these newly developed teaching tools.

Acknowledgments

Thank you to everyone at Medtronic and the Visible Heart® Laboratories that assisted with this project. We also would like to thank the organ donors and their families for providing these critical research specimens for 3D model generation.

Interactive Computational Medical Device Deployments Within Virtual Reality

Submitted to *Journal of Medical Internet Research*, in review.

Alex J. Deakyne [1,2] and Paul A. Iaizzo [1,2]

[1] Department of Bioinformatics and Computational Biology, University of Minnesota, Minneapolis, MN

[2] Department of Surgery, University of Minnesota, Minneapolis, MN

Preface

In the first chapter of this dossier we detailed a methodology for performing computational deployments of medical devices within anatomical models. While these computational deployments offer many benefits, they are time consuming to perform and difficult to correctly place a device within the anatomy. Here we present new functionality that allows for these computational deployments to be performed within virtual reality. This yields more control to a user in performing the computational

deployments of a device, while also decreasing the time required to do such.

This work was performed by me and all authors helped in the preparation of this manuscript for publication.

Summary

This chapter details the developed functionality for performing computational device deployments within VR. This allows a user to interact with medical devices in a virtual environment within an anatomical model. The user can attach a medical device to their VR controller which allows for precision control of the medical device. The user can then navigate to clinically relevant implant sites and deploy the device. This allows the user to study the device tissue interface in an immersive virtual environment. We explore the possibilities of this functionality be recreating multiple cadaver studies of Micra deployments in a fraction of the time within virtual reality.

Introduction

3D modeling has seen increased uses in the fields of medical device development and has also been deemed beneficial when used for preoperative planning and/or clinical education [1]. Much of this is because these models retain all spatial 3D information of the original human anatomies. In addition, the FDA has committed significant resources into further supporting the utilities of computational modeling for medical device innovation; due to their significant cost-saving potentials [2].

When designing medical devices, studies are typically conducted by performing multiple device deployments within unique target anatomies. By deploying devices within varied anatomies, medical device innovators can gain invaluable insights relative to the potential for varied device tissue interactions. Hence, virtual device deployments can yield insights into many crucial details; e.g., relative to next generation devices or how next generation devices would fit within the volume of varied anatomies [3].

With the exponential increased uses of 3D modeling of patient specific anatomies, there exist opportunities to perform computational deployments of devices to better understand optimal and sub-optimal device tissue placements/interfaces. Computational and simulated deployments of devices within unique anatomies has already been performed for a variety of devices, such as pulmonary valve deployments and intracranial aneurysm stenting [4,5]. Previously, our lab has performed computational deployments of a variety of cardiac devices within several unique cardiac specimen models [6]. While these methodologies of computational device deployments that were employed were effective, they can be very time consuming. We often observed that the process of correctly aligning a given device with the target anatomical implant site was often difficult to do correctly using a mouse and keyboard on a computer. In other words, often, numerous adjustments were needed, before the device had been considered to be computationally placed in the correct orientation.

Here, we propose a methodology for performing computational device deployments within the Visible Heart® Laboratories' Virtual Reality platform [7]. Employing both generated 3D model of a given device and detailed anatomical models within a Virtual Reality environment, the user was enabled to pick up the device with their controller and position and reposition it as much as desired. The user positions the device by moving their controller which allows for increased maneuverability of the device compared to a mouse and keyboard. With this increased control, users can more easily perform endless computational device deployments as well as multiple device positionings within generated anatomical models.

For the demonstrations of these VR developments, the device to be computationally deployed was chosen to be the Medtronic Micra™ transcatheter pacing system (TPS) (Medtronic PLC, Minneapolis, MN, USA). Today, the Micra is described as a next generation pacing system that is deployed directly into the right ventricle of the patient; mainly, into the RV apex and/or septal wall: this is a leadless pacing system with an internal battery. Since the system is implanted directly into the heart, there is no way to change the internal battery as is standard with a traditional cardiac pacemaker. In some patients, this may pose challenges, as the Micra battery is expected to only last approximately 10 years; today the average age of a Micra recipient is only 76 years [8].

Thus, it is a possibility that many Micra recipients will hopefully outlive the ~10-year battery life of the device.

When a Micra battery is near the end of its life, the Micra can either be removed from the patient, or an additional Micra can be implanted within the patient's same RV. While both options are possible, extraction procedures can present multiple obstacles such as recapturing the device and tissue encapsulation. In order to implant more than one device in a single RV, it must be determined that multiple Micras can be deployed within RVs of varying size and unique anatomy. While preliminary studies have been done to assess this by deploying multiple Micras within human cadavers, such studies can be costly and time-consuming processes [3]. We aim to continue the work done and demonstrate the time/cost saving possibilities of performing Micra deployments within 10 unique human heart models in VR. These could be important training tools for physicians and well and those for device design innovators.

Methods

10 magnetic resonance imaging (MRI) scans of human hearts, each obtained from the Visible Heart® Laboratories human heart library, were imported to Mimics (Materialise, Leuven, Belgium) for manual segmentation. Two separate segmentation masks were created: a full tissue segmentation of each heart's myocardium, and additional segmentations of each right ventricular blood volume, as shown below. Before the tissue models were used for generating VR scenes, we utilized the blood volume mask to

calculate the relative volumes within each heart's right ventricle. Then, a measurement was made from the tricuspid valve annulus to the right ventricular apex (AV Measurement) in order to determine the approximate height of each heart's right ventricle.

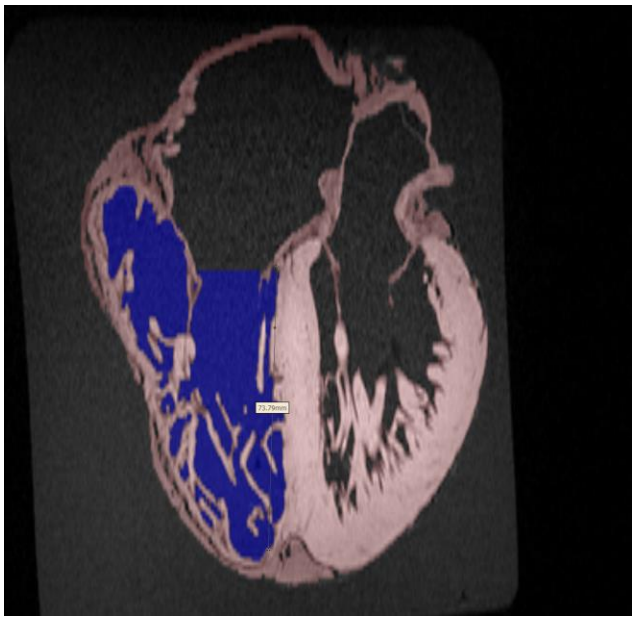

Figure 50. Shown here is a typical screenshot of the Mimics workspace depicting the segmented tissue (red), the segmented right ventricular volume (blue), and the relative measurements from the tricuspid valve annulus to the right ventricular apex.

A detailed 3D model of a Medtronic Micra^{TM} transcatheter pacing system (TPS) (Medtronic) and the generated human heart models (n=10) were next placed within a virtual reality environment via Unity software (Unity Technologies, San Francisco, CA, USA) as previously reported [7]. Further, the third-party asset VRTK (Extended Reality Ltd., Evesham, United Kingdom) was imported into our Unity workspace. VRTK uses abstractions that allow for easier implementations of object interactions within VR. In

order to interact with the Micra within the virtual environment, a VRTK interaction script was added to both the VR controller and the Micra, within Unity.

Next, a custom collider was added to the Micra object in Unity. A collider is a set of coordinates that creates a unique object/device mesh. A collider registers anytime an object is touched by another object in the virtual environment: this was a necessity since a user needs to be able to touch an object in order to pick it up. In our project here, the collider was a capsule shape that surrounds the entirety of the Micra. We then added functionality that changed the rendering color of the Micra to light grey whenever the controller was touching the Micra collider. Feedback such as this was considered important to notify a user when they had appropriately grabbed an object within a virtual environment; since there is no haptic feedback.

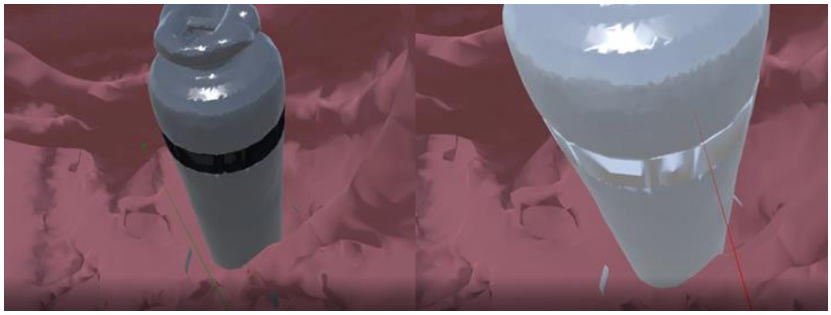

Figure 51. Examples of Micra placed within a virtual environment, when it is not being manipulated (left) and when it is being engaged by the VR user (right, lighter grey).

In the example presented here, functionality was added that allows the user to grab the Micra by pressing the grip buttons on the side of the VR controller. Whenever the user was touching the Micra, pressing the grip buttons allowed them to pick up and hold the

Micra. The Micra was attached to the controller precisely where the controller was touching it when the grip buttons were pressed. Once attached, the Micra's movement within the complex cardiac anatomy will follow the controller wherever it moves within the virtual environment. This allows the user to navigate the Micra to any location within the heart and then deploy it. Whenever the user has the Micra at the desired implant site within the heart, the Micra can be computationally deployed by again pressing the grip buttons on the controller. A custom script was written so that the transform information (position and rotation) of the Micra is recorded whenever the Micra is deployed. One could also to deploy more than one computational device in a given cardiac anatomy.

Results

We have utilized this computational approach to perform computational Micra deployments within multiple detailed human hearts, each with unique anatomies. These have been in a variety of hearts presenting with differing clinical disorders: these are listed in the below table, along with select information about the patient and their heart. Importantly, these developed methodologies allow the user to quickly perform multiple computational device deployments within the virtual environment: an important educational-training opportunity. For example, each deployment was performed in less than one minute, allowing for many implants in multiple hearts to be completed in short periods of time. We estimate that it would take longer to perform each of these same

deployments when using a mouse and keyboard, and even longer to organize a cadaver study to perform deployments in the heart.

Table 3. A typical list of the human heart computational models used in such virtual experiences. Critical information concerning each heart and the corresponding patient information was listed.

Heart	RV Volume (cm^3)	AV Measurement (cm)	Age	Sex	Patient Weight (kg)	Patient Height (cm)	Cardiac History
102	147.074	7.379	14	F	79.8	142	NA
126	82.492	6.14	50	M	102	173	Hypertension, Mild Epicardial CAD, LAD Stenosis
131	97.018	7.982	51	M	109.9	183	Hypertension
145	163.494	8.39	53	M	112	177	NA
148	85.798	6.881	73	M	72.6	173	Atrial Fibrillation
150	180.625	9.017	55	M	90.7	183	Hypertension (35 years)
215	85.203	6.486	57	F	47.3	157	NA
229	146.041	7.231	44	F	83.8	163	Hypertension
248	167.889	7.814	64	F	105.6	178	Hypertension
311	62.541	5.898	20	F	38.6	142	NA

Single Micra Deployments

In the first series of VR applications, a single Micra was virtually deployed at various locations within the right ventricular of each heart. A collage of a few select deployments within these hearts are depicted in the figure below. In all 10 hearts used for this initial study, the Micra occupied at most 1.6% of the RV volume (in the smallest heart) and at the least 0.6% of the RV volume (in the largest heart). Therefore, even in a noticeably small heart, the Micra occupies a negligible portion of the total computationally determined RV volume.

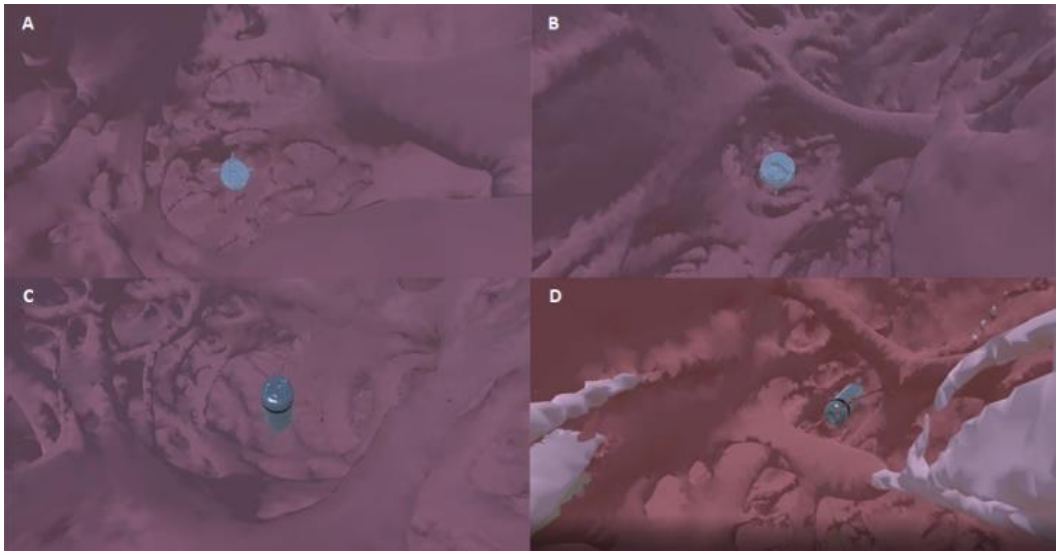

Figure 52. A collage of Micra pacing systems that were computational deployed in VR into the right ventricular apexes of human heart models: (A) Heart 248, (B) Heart 311, (C) Heart 102, AND (D) Heart 229. The VR user was observing the computational deployments while standing in the tricuspid valve annulus of each heart.

Multiple Micra Deployments

As discussed above, it is also possible for a patient to require having multiple Micras implanted in their right ventricle. Thus, it is imperative that these devices only occupy a small volume of the heart, while not physically interacting with each other to ensure that the Micras are able to work properly and restore a more normal heart rhythm. Thus, we virtual deployed up to three Micras into the RV of the 10 human heart models used in this study. For example, shown here 3 Micras were all placed within the hearts in clinically relevant positions; that also ensured enough space between the devices to avoid any physical interaction. With these placements, the Micras occupied at the least 1.6% and at the most 4.8% of the calculated right ventricular volumes. This data shows that three

Micras can be comfortably implanted into the RV, even in small hearts found in young patients: i.e., before doing so clinically.

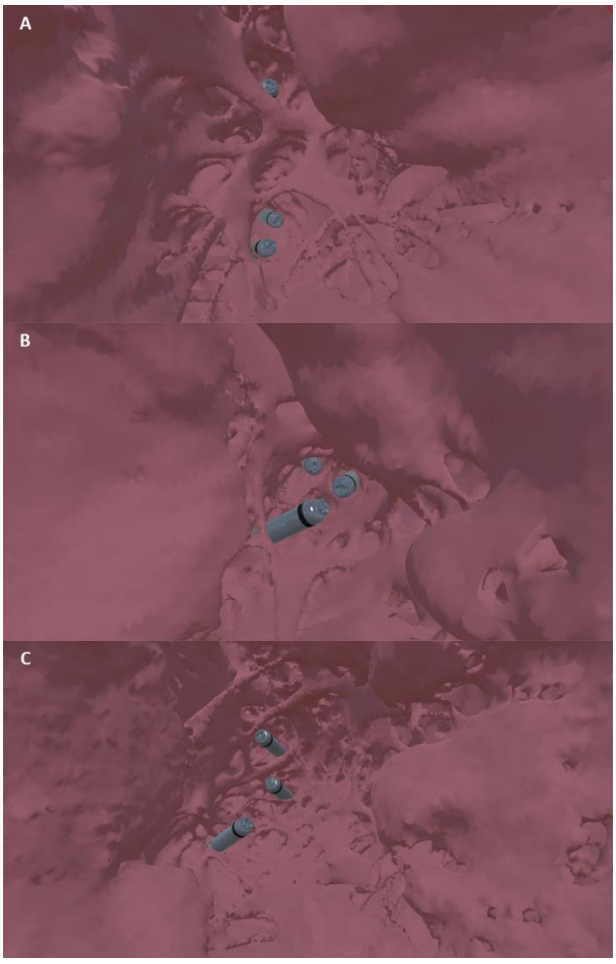

Figure 53. Shown here is a collage of three Micras computationally deployed in human heart models using VR. These devices were deployed in the right ventricle; mainly the right ventricular apex and the septal wall. The heart models depicted here are: (A) Heart 150, (B) Heart 215, and (C) Heart 145.

Discussion

Recently, computational modeling has taken on explosive uses in the medical field broadly. Further, while performing computational device deployments has many benefits,

they have been time-consuming processes until recently; i.e., to correctly align a given device within complex human anatomies, at the desired implant locations. Here, we propose methodologies for performing rapid computational deployments of a leadless pacemaker within human heart models within VR environments. Performing these types of deployments allows the users to gain important insights relative to theses device tissue interfaces at different deployment sites within a variety of human heart anatomies. Additionally, this provides one to learn how the different anatomies will attribute to a viable device deployments within a given heart.

It was also shown that all the hearts used in this study, including smaller sized adult human hearts, could accommodate 1 to 3 Micras without fear of them occupying too large a portion of the RV volume or physically interacting with other devices. Taken together, this yields helpful insights for clinicians who might otherwise be hesitant to implant a second Micra device within the RV of a patient. Further, these can be helpful approaches for device designer to employ in early stage developments.

Limitations

This research approach allows a user to computationally deploy a chosen device into a heart within VR. However, there are certain limitations to these methodologies when compared to actual device deployments in patients or cadavers. One current limitation is that the delivery pathway of the device and its interaction with the delivery catheter were not yet fully modeled or simulated. Thus, it could be possible that one could deploy a

device in an implant location that would be difficult for a clinician to reach using currently available delivery catheters; in a given patient. Note, it is likely that an experienced individual with the procedure, would likely have a good understanding of where the delivery catheter would be able to navigate within the anatomy.

Another limitation of this work is that we are only studying the physical interfaces between the device and the tissue. We have not added simulations of the electrical activities of the heart or the Micra. While these devices could be placed in clinically relevant locations, we are unable to validate the electrical performances of the devices at such locations.

Conclusion

While these described methodologies of computational device deployments using VR was only demonstrated using Micra devices, it should be noted that these immersive approaches could be applied to a wide variety of medical devices. We also consider these VR applications to be valuable tools for performing studies relative to device tissue interfaces; importantly by decreasing the times required to gather such critical data. While these computational approaches would not completely remove the need for cadaver studies, it would allow medical device designers to augment their cadaver studies with VR experiences. These added insights may enable better understandings of the variances in anatomies of a varied patient population which in turn could be acquired with reduced time investments.

Acknowledgements

Thank you to everyone at Medtronic and the Visible Heart® Laboratories that assisted with this project. We also would like to thank the organ donors and their families for providing these critical research specimens for research for the 3D model generations.

Bibliography

Section 1.1 – Virtual Prototyping: Computational Device Placements within Detailed Human Heart Models References

1. Holm, M.S; Iaizzo, P.A. “Importance of Human Cadaver Studies in Education and Medical Device Research: Insights Derived from Various Imaging Studies and Modalities.” In *Engineering in Medicine: Advances and Challenges;* Iaizzo P.A., Ed; Academic Press: Cambridge, MA, USA, 2019; pp. 255-280, ISBN 9780128135143.
2. Zarins, C.K.; Taylor, C.A. “Endovascular Device Design in the Future: Transformation from Trial and Error to Computational Design.” *J Endovasc Ther* 2009***,*** *16:Suppl 1*, 12-21, doi:10.1583/08-2640.1.
3. Goff, R.P.; Spencer, J.H.; Iaizzo, P.I. “MRI Reconstructions of Human Phrenic Nerve Anatomy and Computational Modeling of Cryoballoon Ablative Therapy.” *Ann Biomed Eng* 2016, *44*, 1097-1106, doi:10.1007/s10439-015-1379-3.
4. Morrison, T.M.; Pathmanathan, P.; Adwan, M.; Margerrison, E. “Advancing Regulatory Science with Computational Modeling for Medical Devices at the FDA’s Office of Science and Engineering Laboratories.” *Front Med (Lausanne)* 2018, *5*, 241, doi:10.3389/fmed.2018.00241.

5. Spencer, J.H.; Goff, R.P.; Iaizzo, P.A. “Left Phrenic Nerve Anatomy Relative to the Coronary Venous System: Implications for Phrenic Nerve Stimulation during Cardiac Resynchronization Therapy.*” Clin Anat* 2015, *28*, 621-626, doi:10.1002/ca22537.
6. Warriner, R.K.; Haddad, M.; Hendry, P.J.; Mussivand, T. “Virtual Anatomical Three-Dimensional Fit Trial for Intra-Thoracically Implanted Medical Devices.” *ASAIO J* 2004, *50*, 354-359, doi:10.1097/01.MAT.0000132658.64086.74.
7. Bernhard, J.C.; Isotani, S.; Matsugasumi, T.; Duddalwar, V.; Hung, A.J.; Suer, E.; Baco, E.; Satkunasivam, R.; Djaladat, H.; Metcalfe, C.; et al. “Personalized 3D Printed Model of Kidney and Tumor Anatomy: A Useful Tool for Patient Education.” *World J Urol* 2016, *34*, 337. doi:10.1007/s00345-015-1632-2.
8. Chinchoy, E.; Soule, C.L.; Houlton, A.J.; Gallagher, W.J.; Hjelle, M.A.; Laske, T.G.; Morissette, J.; Iaizzo, P.A. “Isolated Four-chamber Working Swine Heart Model.” *Ann Thorac Surg 2000*, 70, 1607-1614. doi:10.1016/s0003-4975(00)01977-9.
9. Omdahl, P.; Eggen, M.D.; Bonner, M.D.; Iaizzo, P.A.; Wika, K. “Right Ventricular Anatomy Can Accommodate Multiple Micra Transcatheter Pacemakers.” *Pacing Clin Electrophysiol* 2016, 39, 393-397. doi:10.1111/pace.12804.

Section 2.1 – The Importance of Domain Specific Knowledge when Applying Deep Learning to Medical Data: Employing the Unique Dataset of Reanimated and Perfusion Fixed Human Hearts

1. G. Simantiris and G. Tziritas, "Cardiac MRI Segmentation With a Dilated CNN Incorporating Domain-Specific Constraints," in IEEE Journal of Selected Topics in Signal Processing, vol. 14, no. 6, pp. 1235-1243, Oct. 2020, doi: 10.1109/JSTSP.2020.3013351.
2. Krupa K, Bekiesińska-Figatowska M. “Artifacts in Magnetic Resonance Imaging.” Pol J Radiol. 2015;80:93-106. Published 2015 Feb 23. doi:10.12659/PJR.892628
3. Bennett DH. “Comparison of the acute effects of pacing the atrial septum, right atrial appendage, coronary sinus os, and the latter two sites simultaneously on the duration of atrial activation.” Heart 2000;84:193-196.
4. Akiko Ueda, Karen P. McCarthy, Damián Sánchez-Quintana, Siew Yen Ho, “Right atrial appendage and vestibule: further anatomical insights with implications for invasive electrophysiology,” EP Europace, Volume 15, Issue 5, May 2013, Pages 728–734, https://doi.org/10.1093/europace/eus382
5. Visible Heart Laboratories, “Atlas of Human Cardiac Anatomy”, http://www.vhlab.umn.edu/atlas/index.shtml, last accessed 2021/02/24.
6. Perloff, Joseph K., and William C. Roberts. "The mitral apparatus: functional anatomy of mitral regurgitation." Circulation 46.2 (1972): 227-239.

7. Anderson RH. “Clinical anatomy of the aortic root.” Heart 2000;84:670-673.
8. Cleveland Clinic, “Thoracic Aortic Aneurysm Surgery”, https://my.clevelandclinic.org/health/treatments/17527-thoracic-aortic-aneurysm-surgery, last accessed 2021/03/02.
9. Ernst, Calvin B. "Abdominal aortic aneurysm." New England Journal of Medicine 328.16 (1993): 1167-1172.
10. Holm, Mikayle A., and Paul A. Iaizzo. "Importance of Human Cadaver Studies in Education and Medical Device Research: Insights Derived from Various Imaging Studies and Modalities." Engineering in Medicine. Academic Press, 2019. 255-280.

Section 2.2 – Utilizing a Deep Learning Pipeline to Assist in the Segmentation of a Large Anatomical MRI Dataset

1. Maron, Martin S., et al. “Mitral Valve Abnormalities Identified by Cardiovascular Magnetic Resonance Represent a Primary Phenotypic Expression of Hypertrophic Cardiomyopathy.” Circulation, vol. 124, no. 1, 2011, pp. 40–47., doi:10.1161/circulationaha.110.985812.
2. Deakyne, A.J.; Iles, T.L.; Mattson, A.R.; Iaizzo, P.A. Virtual Prototyping: Computational Device Placements within Detailed Human Heart Models. Appl. Sci. 2020, 10, 175. https://doi.org/10.3390/app10010175

3. Morris PD, Narracott A, von Tengg-Kobligk H, et alComputational fluid dynamics modelling in cardiovascular medicineHeart 2016;102:18-28.
4. A. F. Frangi, D. Rueckert, J. A. Schnabel and W. J. Niessen, "Automatic construction of multiple-object three-dimensional statistical shape models: application to cardiac modeling," in IEEE Transactions on Medical Imaging, vol. 21, no. 9, pp. 1151-1166, Sept. 2002, doi: 10.1109/TMI.2002.804426.
5. Eggen MD, Swingen CM, Iaizzo PA: Ex vivo diffusion tensor MRI of human hearts: relative effects of specimen decomposition. Magnetic Resonance in Medicine 67:1703-1709, 2012. DOI: 10.1002/mrm.23194.
6. Gaasedelen, E., Deakyne, AJ., et al. "Virtual Reality and Visualization of 3D Reconstructed Medical Imaging: Learning Variations Within Detailed Human Anatomies." (2020) Proceedings of the Future Technologies Conference (FTC) 2020, Volume 3, Chapter No: 14.
7. Olaf Ronneberger, Philipp Fischer, and Thomas Brox. U-net: Convolutional networks for biomedical image segmentation. Medical Image Computing and Computer-Assisted Intervention – MICCAI 2015, page 234–241, 2015.
8. Kaiming He, Xiangyu Zhang, Shaoqing Ren, and Jian Sun. Deep residual learning for image recognition. 2016 IEEE Conference on Computer Vision and Pattern Recognition (CVPR), Jun 2016.
9. Yoshua Bengio. Deep learning of representations for unsupervised and transfer learning. In ICML Unsupervised and Transfer Learning, 2011.

10. Leslie N. Smith. A disciplined approach to neural network hyper-parameters: Part 1 – learning rate, batch size, momentum, and weight decay, 2018.
11. G. Simantiris and G. Tziritas, "Cardiac MRI Segmentation With a Dilated CNN Incorporating Domain-Specific Constraints," in IEEE Journal of Selected Topics in Signal Processing, vol. 14, no. 6, pp. 1235-1243, Oct. 2020, doi: 10.1109/JSTSP.2020.3013351.

Section 3.1 – Fixed Spline Navigation in Anatomical Virtual Reality Scenes: Applications for Learning Delivery Pathways for Medical Devices

1. Gaasedelen, E.N., Deakyne, A.J. et al. “Virtual reality and visualization of 3d reconstructed medical imaging: Learning variations within detailed human anatomies.” Proceedings of the Future Technologies Conference (FTC) 2020, Volume 3, pages 217–227, Cham, (2021). Springer International Publishing.
2. Oculus for Developers. https://developer.oculus.com/learn/artificial-locomotion/, last accessed 2021/03/13.
3. Ping Hu, Qi Sun, Piotr Didyk, Li-Yi Wei, and Arie E. Kaufman. 2019. Reducing simulator sickness with perceptual camera control. ACM Trans. Graph. 38, 6, Article 210 (2019), 12 pages. DOI:https://doi.org/10.1145/3355089.3356490

4. Latsios, George, Ulrich Gerckens, and Eberhard Grube. "Transaortic transcatheter aortic valve implantation: A novel approach for the truly “no-access option” patients." Catheterization and Cardiovascular Interventions 75.7 (2010): 1129-1136.
5. Généreux, Philippe, et al. "Vascular complications after transcatheter aortic valve replacement: insights from the PARTNER (Placement of AoRTic TraNscathetER Valve) trial." Journal of the American College of Cardiology 60.12 (2012): 1043-1052.
6. Krishnaswamy, A., Parashar, A., Agarwal, S., Modi, D.K., Poddar, K.L., Svensson, L.G., Roselli, E.E., Schoenhagen, P., Tuzcu, E.M. and Kapadia, S.R. (2014), Predicting vascular complications during transfemoral transcatheter aortic valve replacement using computed tomography: A novel area-based index. Cathet. Cardiovasc. Intervent., 84: 844-851. https://doi.org/10.1002/ccd.25488
7. Patel, Jayendrakumar S., et al. "Access options for transcatheter aortic valve replacement in patients with unfavorable aortoiliofemoral anatomy." Current cardiology reports 18.11 (2016): 1-10.
8. Utilities: Unity Asset Store, “Bézier Path Creator”, https://assetstore.unity.com/packages/tools/utilities/b-zier-path-creator-136082, last accessed 2021/03/13

Section 3.2 – A Helpful Relocation Function for Augmenting Teaching in a Multiple User Shared Virtual Environment

1. Gaasedelen, E.N., Deakyne, A.J. et al. “Virtual reality and visualization of 3d reconstructed medical imaging: Learning variations within detailed human anatomies.” Proceedings of the Future Technologies Conference (FTC) 2020, Volume 3, pages 217–227, Cham, (2021). Springer International Publishing.
2. Deakyne, A.J. “Immersive Anatomical Scenes that Enable Multiple Users to Occupy the Same Virtual Space: A Tool for Surgical Planning and Education”. Retrieved from the University of Minnesota Digital Conservancy. (2019). http://hdl.handle.net/11299/202095.
3. Visible Heart Laboratories, “Atlas of Human Cardiac Anatomy”, http://www.vhlab.umn.edu/atlas/index.shtml, last accessed 2021/02/24.
4. Perloff, Joseph K., and Roberts, William C. "The mitral apparatus: functional anatomy of mitral regurgitation." Circulation 46.2 (1972): 227-239.
5. Selle, D., Preim, B., Schenk, A., and Peitgen, H. "Analysis of vasculature for liver surgical planning," in IEEE Transactions on Medical Imaging, vol. 21, no. 11, pp. 1344-1357, Nov. 2002, doi: 10.1109/TMI.2002.801166.

Section 3.3 – Development of Anaglyph 3D Functionality for Cost-Effective Virtual Reality Anatomical Education

1. Kong, X., Nie, L., Zhang, H. et al.: Do 3D Printing Models Improve Anatomical Teaching About Hepatic Segments to Medical Students? A Randomized Controlled Study. World J Surg 40, 1969–1976 (2016).
2. Jurgaitis, J., Paskonis, M., Pivoriunas, J. et al.: The comparison of 2-dimensional with 3-dimensional hepatic visualization in the clinical hepatic anatomy education. Medicina (Kaunas) 44:428 (2008).
3. Chang, P.W., Chen, B.C., Jones, C.E., Bunting, K., Chakraborti, C., Kahn, M.J.: Virtual reality supplemental teaching at low-cost (VRSTL) as a medical education adjunct for increasing early patient exposure. Med. Sci. Educ. 28(1), 3–4 (2018).
4. Gaasedelen, E.N., Deakyne, A.J. et al.: Virtual reality and visualization of 3d reconstructed medical imaging: Learning variations within detailed human anatomies. Proceedings of the Future Technologies Conference (FTC) 2020, Volume 3, pages 217–227, Cham, (2021). Springer International Publishing.
5. Deakyne, A.J.: Immersive Anatomical Scenes that Enable Multiple Users to Occupy the Same Virtual Space: A Tool for Surgical Planning and Education. Retrieved from the University of Minnesota Digital Conservancy. (2019). http://hdl.handle.net/11299/202095.
6. Burzotta, F., Cook, B., Iaizzo, P.A., Singh, J., Louvard, Y., Latib, A.: Coronary bifurcations as you have never seen them: the Visible Heart® Laboratory bifurcation programme. EuroIntervention. (2015);11 Suppl V:V40-3. doi: 10.4244/EIJV11SVA9. PMID: 25983169.

7. Visible Heart Laboratories, Atlas of Human Cardiac Anatomy, http://www.vhlab.umn.edu/atlas/index.shtml, last accessed 2020/04/09.

Section 3.4 – Interactive Computational Medical Device Deployments within Virtual Reality

1. Jurgaitis J, Paskonis M, Pivoriunas J, et al. 2008. “The comparison of 2-dimensional with 3-dimensional hepatic visualization in the clinical hepatic anatomy education”. Medicina (Kaunas) 44:428.
2. Morrison, T. M., Pathmanathan, P., Adwan, M., & Margerrison, E. 2018. “Advancing Regulatory Science with Computational Modeling for Medical Devices at the FDA's Office of Science and Engineering Laboratories”. Frontiers in medicine, 5, 241.
3. Omdahl P., Eggen M.D., Bonner M.D., Iaizzo P.A., Wika K. 2016. “Right ventricular anatomy can accommodate multiple Micra Transcatheter Pacemakers.” Pacing Clin Electrophysiol. 39: 393-397.
4. Capelli C., Taylor A.M., Migliavacca F., Bonhoeffer P., and Schievano S. 2010. “Patient-specific reconstructed anatomies and computer simulations are fundamental for selecting medical device treatment: application to a new percutaneous pulmonary valve”. Phil. Trans. R. Soc. A.3683027–3038.

5. Appanaboyina S., Mut F., Lohner R., Putman C., and Cebral J. 2009. “Simulation of intracranial aneurysm stenting: Techniques and challenges.” Computer Methods in Applied Mechanics and Engineering. 198:3567–3582.
6. Deakyne, A.J.; Iles, T.L.; Mattson, A.R.; Iaizzo, P.A. 2020. “Virtual Prototyping: Computational Device Placements within Detailed Human Heart Models.” Appl. Sci. 10, 175.
7. Gaasedelen, E.N., Deakyne, A.J. et al. 2021. “Virtual reality and visualization of 3d reconstructed medical imaging: Learning variations within detailed human anatomies.” Proceedings of the Future Technologies Conference (FTC) 2020, Volume 3, pages 217–227, Cham. Springer International Publishing.
8. Reynolds, D.; Duray, G.Z.; Omar, R.; Soejima, K.; Neuzil, P.; Zhang, S.; Narasimhan, C.; Steinwender, C.; Brugada, J.; Lloyd, M.; et al. A Leadless Intracardiac Transcatheter Pacing System. *N. Engl. J. Med.* **2016**, *374*, 533–541.